8-2018

The N-terminal methyltransferase homologs NRMT1 and NRMT2 exhibit novel regulation of activity through heterotrimer formation.

Jon David Faughn
University of Louisville

THE N-TERMINAL METHYLTRANSFERASE HOMOLOGS NRMT1 AND NRMT2 EXHIBIT NOVEL REGULATION OF ACTIVITY THROUGH HETEROTRIMER FORMATION

By

Jon David Faughn
B.S. Western Kentucky University, 2006
M.S. Western Kentucky University, 2011
M.S. University of Louisville, 2015

A Dissertation
Submitted to the Faculty of the
School of Medicine of The University of Louisville
in Partial Fulfillment of the Requirements
for the Degree of

Doctor of Philosophy in Biochemistry and Molecular Genetics

Department of Biochemistry and Molecular Genetics
University of Louisville
Louisville, Kentucky

August 2018

THE N-TERMINAL METHYLTRANSFERASE HOMOLOGS NRMT1 AND NRMT2 EXHIBIT NOVEL REGULATION OF ACTIVITY THROUGH HETEROTRIMER FORMATION

By

Jon David Faughn
B.S. Western Kentucky University, 2006
M.S. Western Kentucky University, 2011
M.S. University of Louisville, 2015

A Dissertation Approved on

June 26, 2018

by the following Dissertation Committee:

_____
Christine Schaner Tooley Ph.D.

_____
Alan Cheng Ph.D.

_____
Brian Clem Ph.D.

_____
David Samuelson Ph.D.

_____
Robert Mitchell Ph.D.

ACKNOWLEDGEMENTS

First and foremost, I would like to thank my family for entertaining all of my pursuits, educationally and otherwise, with the utmost support and love. I also have an almost indescribable amount of gratitude towards Dr. Christine Schaner Tooley for her ability to be a mentor and friend for the past few years. Similarly, I appreciate all the guidance, both professionally and personally, I've received from all the current and former members of my lab. The additional guidance I've received from all the members of my committee, as well as Dr. Bill Dean, is also greatly appreciated. Finally, I cannot put into words how grateful I am to my friends, both in Louisville and Buffalo, who have helped make this entire experience pretty fantastic.

ABSTRACT

THE N-TERMINAL METHYLTRANSFERASE HOMOLOGS NRMT1 AND NRMT2 EXHIBIT NOVEL REGULATION OF ACTIVITY THROUGH HETEROTRIMER FORMATION

Jon David Faughn

June 26, 2018

Protein, DNA, and RNA methyltransferases have an ever-expanding list of novel substrates and catalytic activities. Even within families and between homologs, it is becoming clear the intricacies of methyltransferase specificity and regulation are far more diverse than originally thought. In addition to specific substrates and distinct methylation levels, methyltransferase activity can be altered through formation of complexes with close homologs. This work involves the N-terminal methyltransferase homologs NRMT1 and NRMT2. NRMT1 is a ubiquitously expressed distributive trimethylase. NRMT2 is a monomethylase expressed at low levels and in a tissue-specific manner. They are both nuclear methyltransferases with overlapping target consensus sequences but have distinct enzymatic activities and tissue expression patterns. Co-expression of NRMT1 with NRMT2 increases the trimethylation activity of NRMT1, and here I aim to understand how this occurs. I used analytical ultracentrifugation to show that while NRMT1 primarily exists as a dimer and NRMT2 as a monomer, when co-expressed they form a heterotrimer. I used co-immunoprecipitation and molecular modeling to demonstrate *in vivo* binding and map areas of interaction.

While overexpression of NRMT2 increased the half-life of NRMT1, the reciprocal experiment did not produce the same results, indicating that NRMT2 may be increasing NRMT1 activity via increase the stability of the enzyme. Accordingly, the catalytic activity of NRMT2 is not needed to increase NRMT1 activity or increase its affinity for less preferred substrates. Additionally, monomethylation could not rescue phenotypes seen with loss of trimethylation. Taken together, these data support a model where NRMT2 expression activates NRMT1 activity, not through a catalytic change, but by increasing the stability and substrate affinity of NRMT1.

TABLE OF CONTENTS

LIST OF TABLES

LIST OF FIGURES

CHAPTER I

A WORLD OF METHYLATION

Types of Cellular Methylation

As the study of genetics progressed beyond Mendel's classic experiments using plant hybrides, it became clear that the central dogma of molecular biology was not a robust explanation for *who we are*. The knowledge that every cell in an organism shares the same genetic information, though they can become functionally and morphologically distinct, led to the idea that DNA sequence alone cannot control all hereditary traits and gave rise to what would eventually become the field of epigenetics. (Esteller 2007). Initially, epigenetics referred to modifications to DNA that did not involve changes in the DNA sequence. These modifications influenced the association of DNA with various regulatory proteins, with the most well-characterized of these being methylation of CpG-rich regions of DNA. These areas, termed CpG islands, are generally found in upstream regulatory sites of genes, and in their unmethylated state allow the gene to be transcribed after association with the necessary transcription factors (Holliday and Pugh). However, genes that need to be expressed dynamically or in a tissue-specific manner have promoter regions that are heavily methylated. This adds an extra layer of control over DNA sequence for establishing distinct cellular phenotypes.

DNA methylation also allows for modification of gene control over an organism's lifespan. Studies looking at phenotypic differences between monozygotic twins (twins sharing a common genotype) found disease susceptibility and morphological differences between all sets of twins. However, in examining global and locus-specific DNA methylation, twins were found to be epigenetically indistinguishable early in life. Only in examining older twin sets did it become evident that there were vast alterations in the amount and distribution of promoter methylation between genetically identical pairs (Fraga et al. 2005). This was striking evidence that dynamic changes in protein expression can give rise to individual phenotypes that are regulated by mechanisms outside heritable genotype, such as DNA methylation. Furthermore, these mechanisms can change over time and in response to environmental stimuli.

It soon became clear that DNA methylation was not the only type of methylation affecting the epigenetic landscape. In 1964, while using puromycin to inhibit protein translation, it was noted that amino acid incorporation into histone proteins is blocked but the addition of methyl groups is not (Allfrey et al., 1964). This provided evidence of an enzyme responsible for post-translationally methylating histone proteins. The enzyme responsible, Protein Methylase I, was partially purified and found to use S-adenosyl-L-methionine (SAM) as a methyl donor to target the guanidino group of arginine residues. Around 70% of the radio-labeled SAM was found to be incorporated into histones, and it was concluded these were the primary methyl acceptor proteins. Soon after, Protein Methyltransferase II, targeting the carboxyl groups of proteins, and Protein

Methyltransferase III, targeting the ε-amino groups of lysine, were discovered and purified. The discovery of Protein Methyltransferase III also speculated on the existence of multiple enzymes for mono-, di-, and trimethylation (Kim & Paik, 1965; Paik & Kim, 1968; Kim & Paik, 1970; Paik & Kim, 1970).

While the number of post-translational modifications and their associated enzymes continued to grow, it wasn't until the 1990s that genetic and chromatin biology experimental techniques had advanced enough to associate functional roles for protein methylation. The demonstration that arginine methylation, carried out by the yeast homolog of human protein arginine N-methyltransferase 1 (PRMT1), is necessary for the export of nuclear ribonucleoproteins uncovered the first physiological role for post-translational protein methylation (Shen et al., 1998). Soon after, a role for eukaryotic histone lysine methylation was discovered. Methylation of lysine 4 of histone 3 (H3K4) is highly conserved and plays a necessary roll in the facilitation of transcription (Strahl et al., 1999). Within the coming years, the histone-targeting SET domain-containing family of protein methyltransferases would be discovered. As the size of the SET family increased, it became evident that histones were not the only targeted substrates, but non-histones as well, controlling signaling pathways, transcription factors, and tumor suppressors (Herz et al., 2013). The SET classification currently has 56 family members that methylate a variety of targets, and in many of which mutations have been shown to coincide with various diseases and cancer (Albert & Helin, 2010).

The discovery of multiple methyltransferase families, as well as associations with other post-translational modifications (PTMs) such as acetylation, phosphorylation, ADP-ribosylation, ubiquitination, and citrullination of histones gave rise to the concept these chemical marks may encode a kind of "language," eventually termed the histone code (Strahl & Allis, 2000). The histone code specifies the pattern of these PTMs on histones encodes for transcriptional activation or repression, with histone methylation contributing to the heritable nature of the code (Strahl & Allis, 2000). To add a level of complexity, histone methylation can promote transcriptional activation or repression depending on which residue it occurs. Histone H3 lysine 4 trimethylation (H3me3K4) is a classic marker of transcriptional activation, while histone H3 lysine 9 trimethylation (H3me3K9) is a classic marker of transcriptional repression (Bernstein et al., 2002). The level of methylation on each individual residue can also have distinct effects. For example, monomethylated histone 3 lysine 27 (H3meK27) promotes transcriptional activation, while the di- or trimethylated residue (H3me2/3K27) is repressive. Histone 3 lysine 79 mono- and dimethylation (H3me1/2K79) also promote transcriptional activation, while trimethylation can cause either activation or repression dependent upon other PTMs nearby (Rosenfeld et al., 2009; Barski et al., 2007; Steger et al., 2008).

Epigenetic modification of RNA nucleotides is the most recent discovery and includes modification of the four common nucleotide bases to over a hundred chemically distinct modified structures that are present in all eukaryotic

species (Cantara et al., 2011). These modifications allow for intricate control over RNA-specific cellular processes and RNA-mediated structural support. It was long thought that RNA modifications were static, due to the covalent nature of the bonds (He, 2010). However, within the last 5-10 years, the most common epigenetic mark among mammalian RNA, N^6-methyladenosine, has been demonstrated to be dynamic and reversible (Jia et al., 2011; Zheng et al., 2013).

N^6-methyladenosine has ubiquitous tissue distribution and broad implications in post-transcriptional gene regulation. Using m^6A RNA immunoprecipitation, followed by high-throughput sequencing, m^6A has been identified in more than 7,000 human mRNAs and 300 non-coding RNA transcripts. It has also been found in micro-RNAs and long non-coding RNA transcripts (Dominissini et al., 2012; Meyer et al., 2012, Fu et al., 2014). m^6A methylation is ubiquitously involved across the life cycle of RNA, as well as different tissues and cell lines. m^6A methylation directly modifies RNA structure, subsequently improving accessibility for a number of RNA-binding proteins (Lue, et al., 2015). It is also involved in pre-mRNA splicing, pri-miRNA processing, nuclear export, modulation of translation, and RNA degradation (Pan et al., 2018). The misregulation of m^6A RNA methylation is implicated in both solid and hematopoietic tumor development, continued oncogenesis, and tumor metastasis (Vu et al., 2017; Cai et al., 2018; Cui et al., 2017; Yuan et al., 2014; Chen et al 2017). Recently, m^6A RNA methylation has been also linked to pluripotency of cancer stem cells; small subsets of neoplastic cells within tumors with stem-like capacity of self-renewal, survival, and the ability to reemerge as drivers of

tumorigenesis even years after detection of a primary tumor (Vu et al., 2017; Kreso & Dick, 2014).

Methyltransferase families

The addition of a methyl group can be accomplished by a variety of reactions onto hundreds of different substrates. However, the enzymes that catalyze these reactions are found in a relatively small number of structural arrangements and with conserved primary structures that allow for their separation into similar groups (Petrossian & Clarke, 2011). As of 2017, structural alignment and clustering of the catalytic domains of known methyltransferases result in the classification of eleven SAM-dependent and four SAM-independent families (Fenwick & Ealick, 2018). SAM-dependent methyltransferases employ SAM as the methyl group donor to methylate target substrates, leaving the product S-adenosyl-homocysteine (SAH) (Cheng & Blumenthal, 1999). SAM-independent methyltransferases employ a variety of methyl donors, including tetrahydrofolate (THF), betaine, methylamine, and O6-methylguanine-DNA (Doukov et al., 2000; Evans et al., 2002; Moore et al., 1994; Niedzialkowska et al., 2016).

Structurally, the majority of the SAM-dependent methyltransferases fall into the *Class I* (7-beta-strand) methyltransferase family. *Class I* methyltransferases are composed of alternating beta strands and alpha helices, typically forming a seven-stranded beta sheet with three alpha helices on each side (Fenwick & Ealick, 2018). The evolutionarily-conserved N-terminal side of the beta sheet forms the Rossman fold SAM-binding motif of each enzyme, while

the dynamic C-terminal side of the sheet binds the substrate. Given the number of possible substrates for SAM-dependent methyltransferases (nucleic acids, proteins, small molecules), the vast shape and structure of the C-terminal region isn't surprising. (Martin & McMillan, 2002). While many of the SAM-dependent methyltransferases are monomers, they can also be expressed as homodimers and tetramers (Huang et al., 2000).

The DNA methyltransferases (DNMT1, DNMT3A, and DNMT3B) are part of the *Class I* family and are each comprised of a large, multi-domain N-terminus with regulatory functions, and a catalytic C-terminus (Cheng & Blumenthal, 2008). Each catalytic domain is comprised of a common structure consisting of a mixed seven-stranded beta sheet, formed by six parallel and one antiparallel beta strands (Cheng & Blumenthal, 2008). Additionally, six helices are folded around the central beta sheet. This conserved domain is implicated in both catalysis and cofactor binding, with a nearby nonconserved region that recognizes specific DNA targets (Cheng et al., 1995; Jeltsch et al., 2002; Cheng et al., 2008; Jurkowska, 2011). While DNMT1, DNMT3A, and DNMT3B have catalytic activity alone, there is a fourth DNMT, DNMT3L, that is unable to bind SAM and is catalytically inactive, despite sharing homology to its other family members (Gowher et al., 2002; Gowher et al., 2005; Kareta et al., 2006). DNMT3A and DNMT3L form a heterotetramer consisting of two DNMT3A and two DNMT3L homologs. Both enzymes contain hydrophobic interfaces characterized by the stacking of two phenylalanine residues, facilitating protein-protein interactions as well as contact between DNMT3A and DNMT3L. This

region of contact affects the position of alpha helices in DNMT3A and is likely responsible for the increased interaction of the complex with target DNA, even though DNMT3L has no catalytic activity of its own (Jia et al., 2007; Jurkowska et al., 2008; Jurkowska et al., 2011).

The first identified "writer" of m^6A methylation was found to be a highly-conserved methyltransferase enzyme, METTL3, which is also in the *Class I* family (Bokar et al., 1997). After its identification as an RNA methyltransferase, it was shown that its catalytic activity was also dependent on interaction with an inactive homolog, METTL14 (Bokar et al., 1997; Bujnicki, 2002; Wang et al., 2014; Ping et al., 2014). Both METTL3 and METTL14 are SAM-dependent enzymes, and subsequent investigation has shown that this heterodimer complex and its associated interaction with Wilms' tumor 1-associating protein (WTAP) are implicated in increased substrate selectivity and tighter control of levels of target methylation (Ping et al., 2014). Knocking down the METTL3-METTL14-WTAP complex results in longer half-lives and more abundant distribution of their target RNAs (Ping et al., 2014). This is indicative that m^6A methylation is functioning to repress the transcription of target genes (Alexandrov et al., 2002; Ozanick et al., 2005; Leulliot et al., 2008). Additionally, knockdown of WTAP results in mislocalization of METTL3 and METTL14 to their associated mRNAs, indicating an interaction among each of the components is crucial for proper substrate targeting (Ping et al., 2014).

The methylation activity of the METTL3-METTL14-WTAP complex is greater than that METTL3 and METTL14 individually (note: WTAP does not have

methyltransferase activity itself) (Liu et al., 2014). Crystallization of the complex revealed METTL3-METTL14 methyltransferase domains that are highly similar to other Rossman fold-containing methyltransferases, with each comprising a central, curved, eight-stranded beta sheet flanked by four alpha helices. Dimerization of the complex was found to be governed by extensive hydrogen bonding interactions and hydrophobic contacts. Interestingly, though both METTL3 and METTL14 have low catalytic activity individually, steric hindrance and occlusion by METTL3 side chains prevented the binding of SAM to the catalytic site of METTL14 when in complex (Sledz & Jinek, 2016; Wang et al., 2016). Knockout of METTL3 or METTL14, individually, has been demonstrated to abrogate all substrate binding and subsequent m^6A mRNA methylation in mouse embryonic stem cells (Geula et al., 2015). This is indicative that METTL14 is likely facilitating an increase in integrity and substrate targeting of the complex, though not playing a role in catalysis.

The SPOUT family of methyltransferases comprises the second most abundant SAM-dependent class of methyltransferases and is characterized by a six-stranded parallel beta sheet surrounded by seven alpha helices, with the first three strands forming the classic Rossman fold (Anantharaman, 2002; Fenwick & Ealick, 2018). As a homodimer, the C-terminus comprises several conserved catalytic residues, and the active site is located near the surface and comprises residues of both monomers (Anantharaman et al., 2002; Shubert 2003; Michel et al., 2003). SPOUT family members share a common topological feature of a deep trefoil knot in the catalytic domain, responsible for binding S-adenosyl-

methionine (Lim, et al., 2003). SPOUT-family methyltransferases target tRNA for methylation, which is associated with a number of molecular functions, including promotion of secondary structure and thermodynamic stability of tRNA, protection from degradation, and a variety of effects on translation (Voigts-Hoffman et al., 2007; Edmonds et al., 1991; Alexandrov et al., 2006, Björk et al., 2001).

The other major SAM-dependent family of methyltransferases is the Su(var), Enhancer of zeste, Trithorax (SET) family. SET-domain methyltransferases function primarily in large macromoleculer complexes. Each SET-domain methylatransferase contains eight curved beta strands that form three small sheets, with the C-terminus forming a knot-like structure below the surface loop. Unique to the SET family, a set of highly conserved residues form a triangular zinc cluster that is necessary for cofactor binding and transfer of the methyl group (Schultz et al, 1998; Zhang et al., 2002). Substrate recognition by the SET domain is governed by the N- and C-termini, which are near the active site, and by recognition of regions far from the active site during incorporation with other large macromolecular complexes (Trieval et al., 2002). Species of SET proteins can mono-, di-, or trimethylate, and are generally classified by the lysine residues they target on histones (Lachner & Jenuwein, 2002; Santos-Rosa et al., 2002).

Methylation readers

Chemical modifications to nucleotides or proteins are only as effective as their ability to be recognized. Methylation "readers" encompass a number of proteins whose actions are dependent on the recognition of this methylation state. The inability or aberrant recognition of this epigenetic state is implicated in developmental defects and various cancers, implicating methyl-readers as critical factors in health and disease (Wang & Allis, 2009; Chi et al., 2010).

A number of methylation readers have been described (Taverna et al., 2007; Musselman et al., 2012; Patel et al., 2013), with the largest family of readers making up the plant homeodomain (PHD) finger-containing proteins. The PHD finger is a globular protein consisting of two beta-sheets and an alpha helix, featuring conserved cysteine and histidine residues that function to coordinate two Zn^{2+} ions (Pascual et al., 2000). The PHD finger family of readers recognizes multiple levels of methylated lysine and unmodified lysine residues on histone tails (Musselman & Kutateladze, 2011; Sanchez & Zhou, 2011). As with many readers of methylation, the recognition of the substrate is governed by a structurally-conserved region of the PHD finger consisting of two to four aromatic residues, forming an aromatic cage. The aromatic rings are positioned in such a way as to cation-pi, hydrophobic, and van der Waals contacts with the trimethylated lysine residue (Mussleman 2009, 2011).

The so-called "Royal Family" methylation readers include the three beta-strand core regions of chromodomains, Tudor, malignant brain tumor (MBT) repeats, and conserved proline and tryptophan (PWWP) domains. Each of these

share significant sequence similarities and have evolved from a larger homologous superfamily (Maurer-Stroh et al., 2003). The Tudor and chromodomains also share equivalent recognition regions, with both binding methylated peptides using equivalent amino acid positions and structure (Maurer-Stroh, et al., 2003). The PWWP domain contains a five beta-stranded structure and likely is a result of divergent evolution from the same superfamily from which the Tudor and chromodomains evolved (Maurer-Stroh et al., 2003). DNMT3B contains a PWWP domain that contains a basic surface region and is responsible for DNA binding, although these basic residues are not evolutionarily conserved (Maurer-Stroh et al., 2003. As such, it remains unclear if all PWWP-containing proteins exclusively bind DNA. Interestingly, though the PWWP domain of DNMT3B binds DNA, it has not been demonstrated as a necessary requirement for CpG methylation (Qui, et al., 2002).

The MBP family of methyl readers have a general preference for binding mono- or dimethylated peptides over trimethylated peptides (Kim et al., 2006). This is a result of steric clashes within the aromatic cage of MPB repeats with trimethylated (and unmodified) peptides. This is due to hydrogen bond formation between the methylammonium proton and carboxylate acid residue of an aspartic acid residue lining the aromatic cage pocket (Li et al., 2007). Additionally, the other methylammonium proton of the substrate is hydrogen bonded to a water molecule that is held in place by the nearby main-chain residues (Li et al., 2007). This aromatic cage recognition motif is shared among all members of the “royal family” readers. The multiple binding pockets of MBP

domains give precise control over which level of methyl mark is bound, furthering the evidence that tight control of chromatin regulation by histone PTMs isn't only controlled by whether or not a methyl group is present, but to the level at which it is present.

Functions for different levels of methylation

In 1971, it was noted that mono- and dimethylated arginine had distinctly different levels of resistance to tryptic attack, and as such, proposed that specific levels of methylation could govern association with nearby proteins via an increasing hydrophobic characteristic of the guanidine group that is promoted by increasing methylation (Brostoff & Eylar, 1971). However, it wasn't until the discovery of the histone code that distinct functions for distinct levels of methylation became clear.

The emergence of the concept of the histone code described the idea that the sequence of PTMs on histone proteins could form a language governing the recruitment of chromatin remodelers and subsequent expression and repression of genes (Strahl & Allis, 2000). As reader proteins were discovered and characterized, this "language" evolved and control of gene expression by PTMs was found to be increasingly complex (Patel & Wang, 2013). An additional layer of complexity was illuminated when it was found that reader proteins not only recognize if lysine and arginine residues in histones are methylated but also to

what degree the methyl marks are deposited (mono-, di-, or trimethylation for lysine and mono- or dimethylation for arginine) (Kim et al., 2006).

Proteome diversity is not only governed by the presence or absence of a methyl group, but also to what extent a residue is methylated. Different methylation states will recruit different reader proteins, ultimately facilitating different protein-protein interactions, or in the case of histone proteins, differential gene expression (Li et al., 2006). A number of factors are involved in the recognition of different methyl states, though the majority involve the aromatic cage present in all methyllysine reader complexes (Beaver & Waters, 2016). The shape, depth, and composition of the binding pocket, number of cation-pi interactions among the aromatic rings and polarized methyl groups, and presence of negatively charged side chains and hydrogen bond acceptors all contribute to the selectivity of distinct levels of methylation (Hughes et al., 2007; Ma & Dougherty 1997; Guo et al., 2009; Botuyan et al., 2006; Jacobs & Khorasaniz 2002; Llin et al., 2006; Taverna et al., 2007). Additionally, single amino acid substitutions within these chromodomains facilitate enough alteration of the binding pocket to differentiate between di-, and trimethylysine residues (Eisert & Waters, 2011).

Demethylases

The ability to read PTMs at the level of methylation led to the idea that not only is methylation deposition tightly regulated, but its removal may be as well. It

was long suspected that histone methylation was an irreversible mark, because the half-lives of histones and the methylated lysine residues associated with them had been shown to be the same (Byvoet, 1972). However, rapid activation and repression of gene expression isn't compatible with the idea that the methylated residues must degrade at the same rate as the histone itself (Chinenov, 2002), and it was thought that a histone demethylase must exist. A number of demethylating enzymes, with various catalytic methodologies had been described, but their characterization was limited by the inability to pinpoint their activity to a specific target or show direct activity against amino acid side chains within proteins (Kim et al., 1964; Paik & Kim 1973; Paik & Kim, 1974; Khanna & Jorns, 2001; Chinenov 2002).

The first protein lysine-specific demethylase (or "eraser" protein) was characterized in 2004 (Shi et al., 2004). Lysine-specific demethylase-1 (LSD1) is an evolutionarily conserved amine oxidase that preferentially targets methylated H3K4 for demethylation via an oxidation reaction (Shi et al., 2004). Similar to the substrate specificity of its methyltransferase counterparts, LSD1 is able to distinguish between methylated lysine on H3K4 and H3K9 (Shi et al., 2004). Additionally, it is able to discriminate between di- and trimethylation of H3K4, as trimethylated variants of the same residue are unable to be demethylated (Shi et al., 2004; Metzger et al., 2005). Soon after the discovery of LSD1, a second demethylase was discovered, JmjC domain-containing histone demethylase 1 (JHDM1). JHDM1 specifically targets dimethylated H3K36 for demethylation via a hydroxylation-mediated mechanism (Tsukada et al., 2006).

Whether it was steric hindrance between the demethylase binding pocket and lysine trimethylation (as the case for JHDM1) or the requirement of a protonated nitrogen (as in the case for LSD1), the discovery of a demethylase capable of removing a trimethylation mark remained elusive. The first family of demethylases capable of removing trimethylation, JMJD2, was found using a candidate gene screen (Tsukada et al., 2006). Twenty-eight members of the JmjC family were assayed for the ability to use a hydroxylation-mediated mechanism to demethylate trimethylated histone lysines (Cho et al., 2012). JMJD2A and JMJD2C were shown to catalyze demethylation of trimethylated H3K9 and trimethylated H3K36. However, while they could both convert trimethylation to dimethylation, neither could convert dimethylation to monomethylation (Whetstine et al., 2006). The only JMJD2 family member capable of converting H3me3K9 to H3me1K9 was JMJD2D (Toyokawa et al, 2011). While the JMJD2 family members all were specific for methylated lysine residues, they differed in the degree of methylation they could remove, indicating an additional level of demethylation regulation and reinforcing the notion that different levels of methylation encode different functional readouts (Whetstine, et al., 2006, Vakoc et al., 2005; Krogan et al., 2006).

Physiological impact of aberrant protein & DNA methylation

As described above, the dynamics of protein methylation are incredibly precise and tightly controlled. Perturbing this system, whether it be through mis-writing, mis-reading, or mis-erasing of methylation marks has been shown to

facilitate oncogenesis and the progression of a variety of other diseases. The overall misregulation of DNA methylation has emerged as a fundamental part of chromosomal stability, proper gene expression, genome imprinting, and transcriptional silencing of foreign DNA fragments (Levin & Moran, 2011; Peters 2014; Jaenisch & Bird; 2003). Inappropriately methylated DNA can interact with other genomic elements, such as histone modifications, and can similarly be involved in the incorrect positioning of histones during tumor initiation and oncogenesis (Esteller, 2007; Feinberg et al; 2006). Oftentimes, this misregulation of DNA methylation is found in common patterns among tumor- and stage-specific variants cancers and can serve as a useful biomarker for clinical diagnostics (Cancer Genome Atlas Network, 2008).

Cancer-related inhibition of DNA methylation has become a common target of chemotherapeutic development over the last 15 years. Small-molecule inhibitors like azacitidine target DNA methyltransferases by functioning as a nucleoside cytidine and incorporating into RNA to lead to inhibition of the production of the protein (Cihak, 1974). Azacitidine has shown efficacy in treating myelodysplastic syndrome and cutaneous T-cell lymphoma, as well as moderate success in acute myelogenous leukemia (Cowan et al., 2010). In addition to a cancer therapeutic, azacytidine has been in successful in the treatment of HIV and human T-lymphotropic virus (Dapp et al., 2009; Diamantopoulous et al., 2012).

More recently, combinatorial therapies using monoclonal antibodies targeting immune checkpoint factors such as programmed cell death protein-1/2

(PD-1, PD-2) or cytotoxic T lymphocyte antigen-4 (CTLA-4) receptors and DNA methyltransferase inhibitors have been explored in order to increase immunotherapy responses and decrease the ability for malignancies to evade the host immune system (Mazzone et al., 2017). Increased H3K27 trimethylation (H3K27me3), facilitated by Enhancer of Zeste-2 (EZH2) can lead to differentiation and increased plasticity of $CD4^+$ T-cells, decreasing immunosurveillance and the ability to distinguish tumor cells from non-tumor cells (Tumes et al., 2013). Pre-clinical studies have shown combinatorial therapy with anti-PD-1 and anti-CTL-4 antibodies and azacytidine to be more efficacious in eradicating metastatic tumors from melanoma in mice versus treatment with both immunotherapies alone (Kim et al., 2014).

Mutations of the highly conserved H3K27 methyltransferase, (EZH2), the catalytic component of the polycomb repressor complex (PRC2), are among the most common driver mutations found in the progression of solid tumors (Varambally et al., 2002). Overexpression of EZH2 has been shown to be a prognostic marker for prostate cancer progression, with the lowest expression being associated with localized disease and highest found in metastatic tumors (Varambally et al., 2002; Rhodes et al., 2003, Saramaki et al., 2006; Yu et al., 2003). A correlation between increased EZH2 expression is also found in invasive breast metastases versus primary and local tumors (Kleer et al., 2003).

Additionally, recent work has found mutations in EZH2 to be associated with hematological disease progression (Yap et al., 2011). A subset of B-cell lymphoma patients feature mutations of Y641 in SET domain of the EZH2

complex, with the EZH2(Y641) phenotype being associated with increased levels of H3K27 trimethylation levels and acting as a gain-of-function mutation to increase histone methylation (Ciferri et al., 2012; Yap et al., 2011). Around 30% of germinal center B-cell type diffuse large B-cell lymphoma (DLBCL) and around 10% of follicular lymphoma (FL) harbor this mutation (Morin et al., 2010). EZH2(Y641) mutants are shown to favor trimethylation over mono- or dimethylation, and thus accumulate an abnormal amount of trimethylated histone marks versus wild type (WT). This is likely associated with a structurally larger substrate-binding pocket formed by a mutation of the Tyr 641 residue to a smaller residue such as His, Asn, or Phe (Yap, 2011). Mutations in DLBCL and FL repress genes associated with cellular proliferation checkpoints and terminal differentiation (Yap et al., 2011). Normally, the expression of WT EZH2 decreases and the expression of genes involved in terminal differentiation increases, as the B-cell moves away from the germ center phenotype (Yap et al., 2011). However, mutant EZH2 mitigates these checkpoints and results in B-cell hyperplasia (Yap et al., 2011). Similar to that of prostate cancer (Saramaki et al., 2006), these epigenetic mutations are reversible in lymphoma, with suppression of EZH2 correlating with the reexpression of tumor suppressor genes (Beguelin, 2013).

In addition to misregulated histone methylation, aberrant expression of methyltransferases can also result in sweeping changes in the function of non-histone oncogenes and tumor suppressors. Lysine residues on cancer-associated transcription factors, including p53, NFkappaB, and STAT3, are

targeted for methylation by some of the same enzymes associated with histone methylation (Stark et al., 2011). The functional consequences of this methylation are dependent on the particular residue and degree to which it is methylated (Stark et al., 2011). SMYD2, an H3K4 methyltransferase, also monomethylates K370 on p53, leading to transcriptional repression of certain p53 target genes (Huang, 2006). K370 is also a target for dimethylation, which stimulates interaction with the p53 coactivator 53BP1 and strongly increases p53 expression (Huang et al., 2007). Both mono- and dimethylation are removed from p53 K370 by the H3K4 demethylase LSD1 (Huang, 2007). Additionally, lysine residues in the regulatory C-terminus of p53 are targets for the histone methyltransferase, Set9 (Chuikov et al., 2004) Methylation of these residues is associated with p53 stability and association with target genes, and a reduction in Set9 decreases both these phenotypes (Chuikov et al., 2004).

Interestingly, SET9 also targets lysine residues on the p65 subunit of the NFκB transcription factor. Increased NFκB-associated inflammatory response was noted with increased SET9-dependent lysine methylation (Ea et al., 2009; Lu 2010). In an opposing manner, monomethylation of the RelA subunit of NFκB by SETD6 attenuated RelA-dependent transcription pathways, including inflammatory responses of immune cells (Levy et al., 2011). In addition to its role as an H3K27 trimethylase, a novel role for EZH2-dependent methylation of the STAT3 transcription factor has been elucidated. Increased tyrosine phosphorylation of STAT3 is associated with increased proliferation of glioblastoma stem-like cells, and this phosphorylation is dependent on EZH2

methylation. Inhibition of EZH2 reverses this phenomenon and decreases expression of pro-oncogenic proteins (Kim et al., 2013).

To further illustrate the role methyltransferases play on transcription factors, tumor-associated proteins, and downstream cell proliferation, SMYD2-mediated methylation of estrogen receptor alpha (ERα) attenuates recruitment to chromatin and prevents active transcription of target genes under an estrogen-depleted condition (Zhang et al., 2013; Hamamoto et al., 2014). This methylation is diminished upon estrogen stimulation and allows for acetylation of ERα, increasing target gene transcription and demonstrating the crosstalk between PTMs and related transcriptional changes (Zhang et al., 2013). Increased SMYD2 expression is also found to correlate with human bladder carcinomas compared to non-neoplastic bladder tissue. This is due to the increased methylation of Rb by SMYD2, in which the methylation also accelerated phosphorylation of Rb, promoting cell cycle progression of cancer cells (Cho, 2011; Carr 2011).

Besides transcription factors, various other non-histone substrates are also targets for modification by methyltransferases. and the over or under-expression of these associated enzymes can facilitate pro-tumorigenic outcomes. Heat-shock protein 70 (HSP70) is a highly evolutionarily conserved molecular chaperone, found to be non- or minimally-methylated in non-neoplastic tissues, with highly dimethylated variants found in a number of cancerous tissues (Cho et al., 2012). This is due to increased expression of the SET1D1A methyltransferase, which increases lysine dimethylation of HSP70 and promotes

a methyl-dependent association with Aurora kinase B and subsequent growth of cancer cells (Cho et al., 2012). In a similar manner, HSP90 is methylated in much higher amounts in cancerous tissues due to increased SMYD2-dependent methylation, facilitating increased chaperone complex formation and accelerated proliferation (Hamamoto, et al., 2014).

Elevated expression of SMYD3 is associated with colorectal, hepatocellular, and breast carcinomas (Hamamoto et al., 2004; Hamamoto et al., 2006; Saddic et al., 2010; Mazur et al., 2014). SMYD3-dependent methylation of vascular endothelial growth factor receptor 1 (VEGFR1) on a lysine residue in its kinase domain increases its kinase activity and accelerates proliferation of carcinoma cells (Kunizaki et al., 2007). In a similar study, increased SMYD3 expression increases methylation of MAP3K2, which promotes increased MAP kinase signaling and promotes the formation of Ras-driven carcinomas (Mazur et al., 2014). Additionally, highly methylated arginine and lysine residues of VEGFR2 have been shown to play a critical role in the tyrosine phosphorylation and activation of VEGFR2-mediated angiogenesis pathways (Hartsough et al., 2013). Thus, alteration in histone methyltransferase expression not only affects transcriptional dynamics directly through chromatin architecture but also indirectly through regulating the function of non-histone protein targets. It can also be associated with changes in additional PTMs, dramatically altering the PTM landscape of proteins.

N-terminal methylation

Most of the literature focusing on the functional roles of protein methylation centers on methylation of lysine and arginine side chains. However, an additional type of protein methylation, α-amino methylation of the N-terminal amino acid (N-terminal methylation), has also been identified. The initial reports of N-terminal methylation on the bacterial ribosomal proteins L16 and L33 were first published in 1976, and the list of N-terminally methylated substrates slowly expanded for the next three decades (Brosius & Chen, 1976; Chang et al., 1976; Wittman-Liebold et al., 1976; Stock et al., 1987). A common consensus sequence of Xxx-Pro-Lys (X-P-K) emerged as the number of mono-, di-, and trimethylated substrates grew, and it was hypothesized that an enzyme or group of enzymes were responsible for the recognition of this sequence and subsequent methylation (Stock et al., 1987).

N-terminal RCC1 methyltransferase-1 (NRMT1), formally notated as METTL11A, was identified as the first N-terminal methyltransferase enzyme in both yeast and humans (Webb et al., 2010; Tooley et al., 2010). As predicted, it is able to methylate an X-P-K consensus sequence, and database searches for proteins beginning with this consensus identified at least 100 putative target substrates (Tooley et al., 2010). NRMT1 is a 25 kDa protein from the *Class I* family of methytransferases. *In vitro* peptide methylation assays and substrate immunoprecipitations have recently expanded the X-P-K consensus sequence of NRMT1 (Petkowski, 2012). After initiating methionine cleavage, position 1 can be alanine, proline, serine, glycine, or methionine. Position 2 can encompass

most uncharged polar or nonpolar amino acids, and position three can be either Lys or Arg (Petkowski, 2012). This expanded consensus sequence increases the number of potential NRMT1 targets to over 300, making α-N-terminal methylation a much more abundant modification than initially hypothesized (Petkowski, 2012). Specificity was further characterized by showing the affinity of NRMT1 for its substrates is dictated by the substrate's consensus sequence (Petkowski, 2012). Of those already tested, NRMT1 exhibits the strongest affinity for substrates beginning with a P-P-K consensus or substrates that have been previously mono- or dimethylated (Petkowski, 2012).

This preference for ringed prolines or pre-methylated substrates is predicted to result from a favorable interaction between these substrates and a conserved triad of aromatic residues making up the "aromatic cage" domain of NRMT1 (Petkowski et al., 2012). Of note, this aromatic cage is similar to those seen in chromodomains that bind methylated lysine residues (Nielson et al., 2002). Kinetic studies using an N-terminal RCC1 peptide as substrate and/or specific chemical inhibitors have determined that NRMT1 works through a random sequential bi-bi kinetic mechanism with distributive processivity (Richardson et al., 2015). Either SAM or the protein substrate can be the first to bind NRMT1, and methyl groups are distributed one at a time versus *en masse* (Richardson et al., 2015). Similarly, *in vitro* methylation assays using an N-terminal peptide of the NRMT1 substrate CENP-A, confirmed that NRMT1 has a greater affinity for di- versus monomethylated and mono- versus unmethylated

substrates, further explaining the observed processivity of the enzyme (Wu, 2015).

Crystal structures of NRMT1 along with SAH (a reaction product and methyltransferase inhibitor) and a variety of X-P-K substrates (with X varying among six residues) revealed a unique β-hairpin insert between β-strand 5 and α-helix 7 and an N-terminal extension consisting of two α-helices are both involved in substrate binding and likely to contribute to the substrate specificity of the enzyme (Wu et al., 2015; Dong et al., 2015). Substrate binding is found deep within a negatively charged channel connecting to the cofactor binding pocket, though the free and peptide-bound structures show little conformational change, indicating the likelihood that this pocket it preformed (Wu et al., 2015). An inserted peptide is oriented in such a way to point the α-N-terminal toward the cofactor, likely facilitating the methyl transfer. This stereochemistry is unique to this enzyme compared to other protein methyltransferases and likely contributes to the specificity of N-terminal methylation (Dong et al., 2015).

Sequence analysis of NRMT1 has yielded one predicted homolog, METTL11B (later renamed NRMT2). Primary structure identity between NRMT1 and NRMT2 is approximately 50%, with key catalytic residues sharing 100% sequence identity and spatial location within the catalytic site (Tooley et al., 2010; Petkowski et al., 2013). Crystallization of NRMT2 to 2 Å has recently been deposited in the protein data bank (PDB: 5UBB), but NRMT2 also has an additional 60 amino acid N-terminal domain has yet to be crystalized (Petkowski, 2013). NRMT1 and NRMT2 similarly localize to the nucleus, though NRMT1 is

ubiquitously expressed, and NRMT2 expression is highly tissue-specific (Petkowski, 2013). NRMT2 is found predominately in the liver and skeletal muscle (Petkowski, 2013).

While sequentially and structurally similar and capable of methylating the same consensus sequences, NRMT1 and NRMT2 differ in their catalytic specificities (Petkowski, 2013). *In vitro* methylation assays with recombinant NRMT1 or NRMT2, reveal NRMT2 to be exclusively capable of monomethylation (Petkowski, 2013). This is in striking contrast to the mono-, di-, or trimethylase activity found in its homologous counterpart (Petkowski, 2013). Interestingly, the rate at which substrates achieved trimethylation was increased when NRMT1 and NRMT2 were combined, indicating NRMT2 may be serving a priming function for NRMT1 by adding the initial methyl group and reducing the substrate burden on NRMT1 (Petkowski et al., 2013). This model is further supported by the fact that NRMT1 is a distributive methyltransferase with increasing affinity for substrates with higher levels of methylation (Wu et al., 2015). Increasing the amount of monomethylated substrates available could increase the affinity for subsequent di- and trimethylation by NRMT1, which would be useful in times of high substrate concentration (Petkowski, 2013).

Functions of N-terminal methylation

The very first proposed functional role for N-terminal methylation was increasing protein stability, as dimethylation of the N-terminal proline of *Crithidia* cytochrome *c-557* protected it from tryptic digestion (Smith and Pettigrew, 1980).

However, to date, this is the only known substrate where N-terminal methylation has been proven to increase protein stability. More recently, it has been shown that N-terminal methylation also promotes protein-DNA interactions (Chen, 2007). The binding of RCC1 to chromatin is absolutely necessary for proper mitosis, nuclear-cytoplasmic transport, and nuclear envelope assembly (Nemurgut et al., 2001; Hetzer et al., 2002). NRMT1 uniquely methlyates the α-amino group of RCC1, and mutants of RCC1 that can't be methylated (lysine 4 of the consensus sequence is mutated to a glutamine - K4Q) fail to localize to chromatin during mitosis (Chen et al., 2007). *In vitro* binding assays have shown that N-terminal methylation of RCC1 directly promotes its interaction with DNA and not the histone proteins (Chen, 2007). It is hypothesized that the permanent positive charge on the α -N terminus of RCC1, resulting from N-terminal trimethylation, facilitates electrostatic binding to the phosphate backbone of DNA (Stock et al, 1987; Chen et al., 2007). The diffuse distribution and decreased association with DNA of the K4Q-RCC1 mutants results in an increased frequency of multipolar spindles and an eventual disruption of mitosis, providing one example of the biological importance of N-terminal methylation (Chen et al., 2007).

Another proven target for N-terminal methylation is damaged DNA binding protein-2 (DDB2) (Cai et al., 2014). DDB2 exhibits high affinity for UV light-induced cyclobutane pyrimidine dimers (CPD) and other bulky DNA adducts produced by a number of carcinogens (de Laat et al., 1999). UV-DDB (a heterodimer complex of DDB1 and DDB2) functions as a global genome

nucleotide excision repair (NER) factor, where DDB2 acts to detect UV-damaged chromatin and recruit xeroderma pigmentosum complementation group C (XPC) (Moser et al., 2005). DDB2 features an N-terminal Ala-Pro-Lys (A-P-K) consensus sequence, and is mono-, di-, and trimethylated on the N-terminal alanine residue by NRMT1 (Cai et al., 2014). NRMT1-induced N-terminal methylation promotes nuclear localization of DDB2, facilitated recruitment of DDB2 to CPD foci, increased CPD repair efficiency, induced proper cell-fate decisions via ATM activation, and increased resistance of cells to UV damage (Cai et al., 2014). Methylation-defective mutants of DDB2 are defective in nuclear localization and recruitment to CPD foci (Cai et al., 2014). This is predicted to be through a mechanism similar to RCC1, whereby N-terminal methylation enhances the binding of DDB2 to DNA though electrostatic interaction (Cai et al., 2014).

NRMT1 has also been implicated in double-stranded break repair (DSB), and as such, to function as a tumor suppressor (Bonsignore (1) et al., 2015). Loss of NRMT1 results in increased sensitivity of human breast cancer cell lines to both etoposide and ɣ-irradiation, agents that cause double strand DNA breaks (Bonsignore (1) et al., 2015). Loss of NRMT1 also increases the proliferation rate, invasive potential, anchorage-independent growth, xenograft tumor size, and sensitivity to tamoxifen of these breast cancer cell lines (Bonsignore (1) et al., 2015). The exact mechanism of how NRMT1 depletion sensitizes cancer cells to double stand breaks remains to be determined, but both BRCA-associated protein-1 (BAP1) and poly [ADP-ribose] polymerase-3 (PARP3) are

predicted NRMT1 targets involved in homologous recombination and non-homologous end-joining, respectively. As with DDB2, N-terminal methylation may also regulate their recruitment to damaged-DNA (Bonsignore (1) et al., 2015).

In accordance with the phenotypes seen with NRMT1 knockdown in cell culture, global knockout of NRMT1 in mice ($NRMT1^{-/-}$ mice) gives rise to phenotypes similar to that seen in other mouse models defective in DNA damage repair (Bonsignore (2) et al., 2015; de Boer, et al., 2002). $NRMT1^{-/-}$ mice typically die before three weeks of age, are smaller than their wildtype counterparts, exhibit female-specific sterility, have marked kyphosis, decreased mitochondrial function, and increased liver pathogenesis (Bonsignore (2) et al., 2015). $NRMT1^{-/-}$ livers show altered expression of genes related to apoptosis, oxidative phosphorylation, fatty acid metabolism, and steroid biosynthesis (Bonsignore (2) et al., 2015). Given the number of NRMT targets, it is likely these mice aren't merely deficient in DNA damage repair (as demonstrated by Chen et al., 2007 and Bonsignore (1) et al., 2010), but are likely deficient in a number of protein-protein and protein-DNA interactions as well.

As NRMT1 has now been shown to have significant biological relevance, we are interested in determining more about its regulation. We have previously seen that co-expression with NRMT2 activates NRMT1 trimethylase activity and are especially interested in how this is occurring. Recent studies with other homologous methyltransferases have identified a new pattern of regulation through heterodimer formation (Liu et al., 2014; Wang et al., 2016). The major

type I arginine methyltransferase in *Trypanosoma brucei*, PRMT1, is activated through binding of its inactive homologous prozyme, PRMT3 (Kafkova, 2017). Though PRMT3 has no activity itself, through binding, it stabilizes and activates PRMT1 (Kafkova, 2017).

Similarly, the N^6-methyadenosine (m^6A) RNA methyltransferase METTL14 was recently reported to form a heterodimer complex with its homolog METTL3. Both METTL14 and METTL3 have methyltransferase activity individually, though the METTL14-METTL3 complex shows dramatically enhanced methyltransferase activity compared to either enzyme alone (Liu et al., 2014). Both enzymes contain catalytic domains, though phylogenetic analysis shows a much more conserved DPPW domain in METTL3 compared to the variable motif of METTL14 (Bujnicki et al., 2002; Iyer et al., 2016). The crystal structure of the METTL3-METTL14 complex, along with its bound cofactor SAM, has been solved to 1.70 Å and 1.65 Å, respectively. There are steric clashes in the METTL14 when SAM is bound that aren't present in METTL3, indicating that METTL3 is the catalytic subunit of the complex. However, as METTL3 has minimal activity alone, its interaction with METTL14 is structurally necessary to lead to catalytic action (Wang et al., 2016). A similar mechanism of synergistic complex formation is found in DNA methylation, with the binding of catalytically inactive DNMT3L with active DNMT3a or DNMT3b (Jia, et al., 2007). The following chapter will explore the hypothesis that NRMT1 and NRMT2 also complex in a heterodimer, with the less active NRMT2 stabilizing and activating NRMT1 (Figure 1).

Figure 1

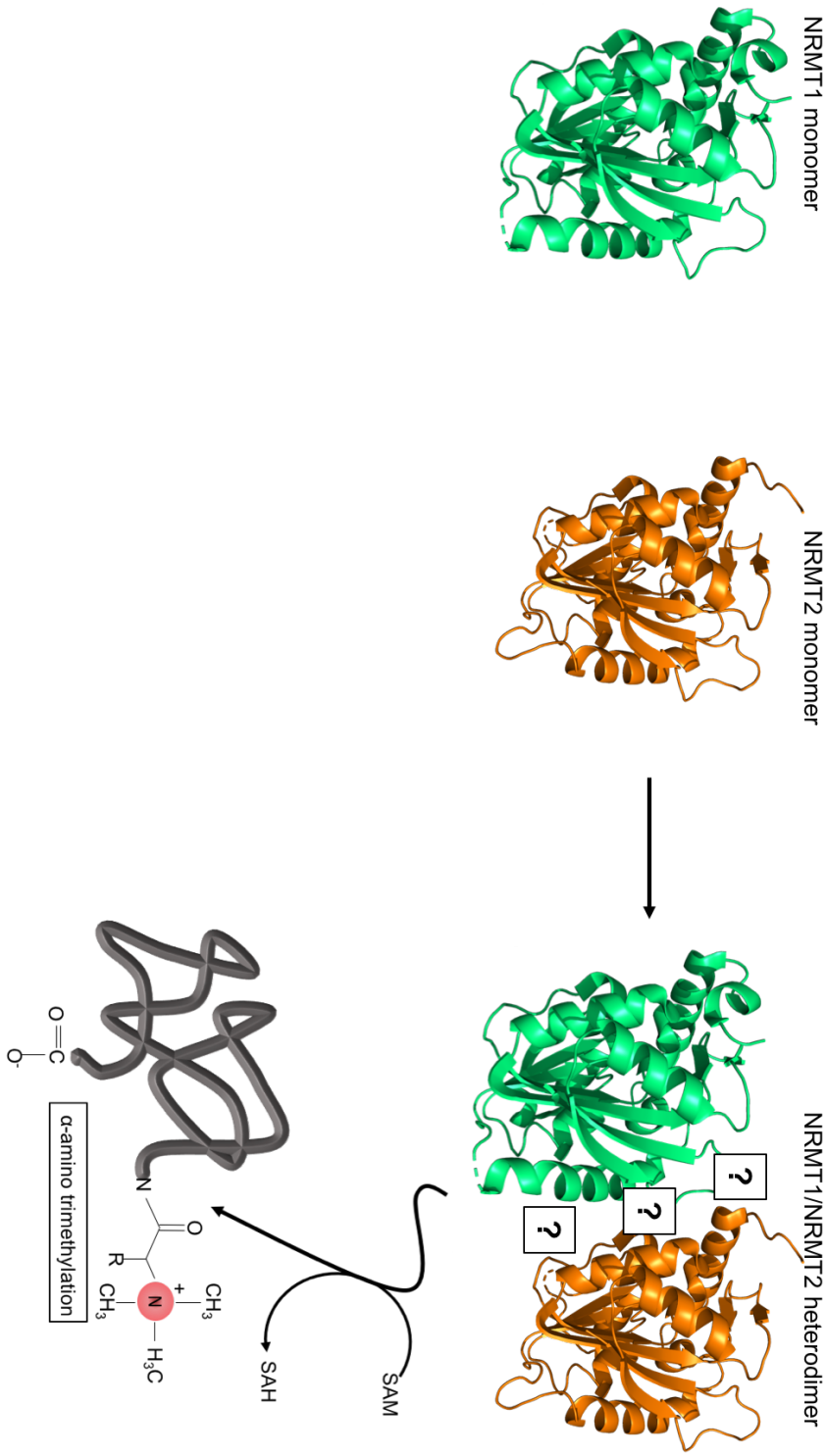
NRMT1 monomer
NRMT2 monomer
NRMT1/NRMT2 heterodimer
?
?
?
SAM
SAH
α-amino trimethylation

Figure 1. Model of predicted NRMT1 and NRMT2 heterodimer complex, with the less catalytically active NRMT2 stabilizing NRMT1 to promote trimethylation.

CHAPTER II

THE N-TERMINAL METHYLTRANSFERASE HOMOLOGS NRMT1 AND NRMT2 EXHIBIT NOVEL REGULATION OF ACTIVITY THROUGH HETEROTRIMER FORMATION

Introduction

The initial defining feature of methyltransferase enzymes was onto which type of substrate they catalyzed the transfer of methyl groups from S-adenosyl-methionine (SAM). DNA methyltransferases have been further characterized into those that place 5'methylcytosine *de novo* or maintain it at hemimethylated CpG sites (Holliday and Pugh 1975). Protein methyltransferases have been further characterized by the amino acid they methylate and the level (mono, di, or tri) of methylation they catalyze (Boriack-Sjodin and Swinger 2016). Likewise, the RNA methyltransferases have been divided into four superfamilies based on their structure and the nucleotide they methylate (Motorin and Helm 2011). It is becoming clear, however, that in addition to these intrinsic methyltransferase qualities, there is an additional layer of functional regulation in their expression patterns and complex formation.

A common theme emerging is complex formation between methyltransferase homologs. In *Trypanosoma brucei*, the major type I arginine methyltransferase, PRMT1, has a very narrow substrate specificity and weak

activity *in vitro* (Kafkova et al. 2017). However, co-expression with its close paralog PRMT3 increases PRMT1 stability, and subsequently, its activity (Kafkova et al. 2017). PRMT3 is missing key catalytic residues and does not exhibit *in vitro* enzymatic activity and has been characterized as a prozyme (Kafkova et al. 2017). Activation of a catalytically weak enzyme by an inactive prozyme paralog has also been seen in *T. brucei* polyamine biosynthesis and described as the prozyme paradigm (Willert, Fitzpatrick, and Phillips 2007). On average, the enzyme/prozyme complex typically exceeds the activity of the active enzyme alone by 2000 fold (Willert, Fitzpatrick, and Phillips 2007; Nguyen et al. 2013).

Similarly, the recently discovered N^6-methyladenosine (m^6A) RNA methyltransferase METTL3 forms a heterodimer with its close homolog METTL14 (Liu et al. 2014). Unlike *T. Brucei* PRMT1 and PRMT3, METTL3 and METTL14 each show weak methyltransferase activity *in vitro* (Liu et al. 2014; Wang et al. 2016). However, m^6A methylation activity is significantly increased upon heterodimer formation, and this binding also promotes reciprocal stability of the homologs (Liu et al. 2014; Wang et al. 2014). Though these data suggest METTL14 is not strictly an inactive prozyme, it appears its catalytic activity is not required for *in vivo* activity of the complex (Wang, Doxtader, and Nam 2016). The crystal structure of the heterodimer catalytic domains also indicates the METTL14 catalytic site is relatively occluded and does not bind SAM (Wang, Doxtader, and Nam 2016). The current model is that the primary role of

METTL14 is to provide structural support to METTL3 and interact with RNA substrate (Wang, Doxtader, and Nam 2016; Wang et al. 2016).

The mammalian methyltransferase EZH2 is part of the PRC2 complex that represses transcription by di- and trimethylating histone H3 on lysine 27 (H3K27me2/3) (Schuettengruber et al. 2007). EZH2 has one close homolog, EZH1, which also interacts with members of the PRC2 complex (Margueron et al. 2008). PRC2-EZH1 can also repress transcription, but EZH1 has weak H3K27me2/3 activity (Margueron et al. 2008). In contrast to PRC2-EZH2, PRC2-EZH1 represses transcription by binding and compacting nucleosomes (Margueron et al. 2008). The PRC2-EZH2 and PRC2-EZH1 complexes are thought to be primarily mutually exclusive, but data indicate EZH1 and EZH2 can interact with each other both *in vitro* and *in vivo* (Margueron et al. 2008; Oliviero et al. 2016). It is still functionally unclear why a PRC2 complex that contains EZH2 would also contain EZH1 (Oliviero et al. 2016), but as they accomplish the same goal by different mechanisms, there may be certain circumstances when synergistic activity would be beneficial. Unlike T. brucei PRMT1 and PRMT3 and mammalian METTL14 and METTL3, Ezh1 and Ezh2 have very different expression patterns (Margueron et al. 2008), and the need for complexed EZH1 and EZH2 may be specific to the tissues and developmental times where their expression patterns overlap.

We work on the N-terminal methyltransferase homologs NRMT1 (N-terminal RCC1 methyltransferase 1) and NRMT2 (N-terminal RCC1 methyltransferase 2), which, following cleavage of the initiating methionine,

methylate the α-amine of the first N-terminal residue of their substrates. NRMT1 and NRMT2 are 50% identical and 75% similar and share an N-terminal X-P-K consensus sequence (Petkowski et al. 2013; Petkowski et al. 2012). Though structurally similar, they differ in their catalytic activities. *In vitro*, NRMT1 exhibits distributive trimethylase activity, and *in vivo*, complete knockout of NRMT1 via homologous recombination or CRISPR/Cas9 abolishes N-terminal trimethylation (Petkowski et al. 2013; Shields et al. 2017; Bonsignore, Tooley, et al. 2015). NRMT2 exhibits monomethylase activity *in vitro* (Petkowski et al. 2013), but its knockout phenotypes remain to be characterized due to lack of an antibody that successfully detects it endogenously.

There are over 300 predicted NRMT targets (Petkowski et al. 2012) and over a dozen verified targets, including RCC1, the tumor suppressor Retinoblastoma protein (Rb), the histone chaperone SET, the centromere proteins CENP-A and CENP-B, Poly(ADP-Ribose) Polymerase 3 (PARP3), Damaged DNA-binding protein 2 (DDB2), and a variety of myosin light chains and ribosomal proteins (Bailey et al. 2013; Dai et al. 2013; Dai et al. 2015; Cai et al. 2014; Tooley et al. 2010). For the verified targets, N-terminal methylation seems to predominantly regulate protein-DNA interactions. Loss of N-terminal methylation of RCC1 disrupts its binding to DNA, its localization to chromatin, and its ability to properly establish mitotic spindles (Chen et al. 2007). N-terminal trimethylation of CENP-B enhances its binding to α-satellite DNA (Dai et al. 2013), and N-terminal trimethylation of CENP-A is also required for its recruitment to the centromere (Sathyan, Fachinetti, and Foltz 2017). DDB2 that

cannot get N-terminally methylated cannot be as efficiently recruited to UV-induced cyclobutane dimers and these dimers cannot be as effectively repaired (Cai et al. 2014).

NRMT1 and NRMT2 have distinct mRNA expression patterns. NRMT1 is expressed ubiquitously in all tissues, while NRMT2 has much lower, tissue-specific expression, with its highest expression found in the skeletal muscle and the liver (Petkowski et al. 2013). This indicates NRMT1 can function independently without NRMT2. In addition, NRMT1 knockout does not significantly affect monomethylation levels (Shields et al. 2017), indicating that even at low levels, NRMT2 can function without NRMT1 present. Taken together these data indicate both NRMT1 and NRMT2 can function independently without the other present. However, it is unknown if N-terminal mono- and trimethylation are functionally redundant, and *in vitro* co-expression of NRMT2 with NRMT1 is able to increase the trimethylation activity of NRMT1 (Petkowski et al. 2013), indicating the two may also work synergistically under certain conditions.

Here I aimed to better understand the interdependence of NRMT1 and NRMT2 and determine if they function in a complex. First, I used analytical ultracentrifugation to show that purified recombinant NRMT1 and NRMT2 interact and determined the stoichiometry of interaction as 2:1 NRMT1 to NRMT2. Next, I used co-immunoprecipitation (co-IP) to show NRMT1 and NRMT2 can be found complexed together *in vivo* and molecular modeling to map their areas of interaction. I also used cycloheximide experiments to determine that while the half-life of NRMT1 increases in the presence of overexpressed NRMT2, the

converse is not true. I used kinetic assays to quantitatively determine the effect of NRMT2 expression on NRMT1 activity and site directed mutagenesis to determine that NRMT2 enzymatic activity is not needed for an increase in NRMT1 trimethylase activity or substrate affinity. Finally, to determine if N-terminal mono- and trimethylation are functionally redundant, I tagged the NRMT substrate SETα with Dendra2 photoswitchable protein and showed its half-life is significantly decreased in NRMT1 CRISPR/Cas9 knockout cells. This decrease in half-life can be rescued by NRMT1 overexpression but not by overexpression of NRMT2. From these data, I conclude that NRMT1 and NRMT2 are most similar to their family members METTL3 and METTL14, which both exhibit methyltransferase activity *in vitro* but the activity of METTL3 predominates *in vivo*. Stability and substrate affinity are increased by complex formation and monomethylase priming activity is not required. These data do not rule out an additional unique function of N-terminal monomethylation by NRMT2, but show one of its functions when expressed is to promote N-terminal trimethylation.

Materials and methods

Constructs and antibodies

For recombinant protein production, full-length human NRMT1, NRMT2, and NRMT2 V224L were cloned into pet15b (Merck Millipore, Burlington, MA) and purified as described previously (Petkowski et al. 2013; Chen, Brownawell, and Macara 2004; Shields et al. 2017). The full-length human NRMT1-FLAG,

NRMT1-GFP, NRMT2-FLAG, and NRMT2-GFP used in the co-IPs were cloned into pKH3 (FLAG constructs) or pKGFP2 (GFP constructs), as previously described (Petkowski et al. 2013). All truncated constructs were sub-cloned from these full-length ORFs using primer sets that combined the primers used for full-length cloning and the following unique primers:

$NRMT1_{1\text{-}59}$ Reverse: 5'-GGGAATTCTTGTTCGGGCCTTCCCTCA-3',

$NRMT1_{52\text{-}172}$ Forward: 5'-GGTCTAGAATGTTTTTGAGGGAAGGCCCGAAC-3'

$NRMT1_{52\text{-}172}$ Reverse: 5'-GGGAATTCTCCTGGGCCATGTTGTCTTTGATGAC-3'

$NRMT1_{178\text{-}223}$ Forward: 5'-GGTCTAGAATGGACGTGGACAGCAGCGTGTGC-3

$NRMT2_{1\text{-}112}$ Reverse: 5'-GGGGATCCCCAGGCCCCCCAACAAATTT-3'

$NRMT2_{77\text{-}223}$ Forward: 5'-GGTCTAGAATGCAAGAAGTACCAGCCACAGAA-3'

$NRMT2_{77\text{-}223}$ Reverse: 5'- GGGGATCCGTCCTTCAATATGATGATGCC-3'

To make SETα-Dendra2-pCDH, human SETα was amplified from our previously published SETα-FLAG construct (Tooley et al. 2010) to introduce 5' Xho1 and 3' HindIII restriction sites and sub-cloned into the pDendra2-N vector (Clontech, Mountain View, CA). The SETα-Dendra2 construct was then amplified to introduce 5' Xba1 and 3' Swa1 restriction sites and sub-cloned into the lentiviral vector pCDH-CMV-EF1-Puro (pCDH, Addgene, Cambridge, MA). Lentivirally expressed NRMT2-GFP, NRMT1-FLAG, and NRMT2-FLAG were first amplified from the corresponding mammalian expression vectors to introduce 5' Xba1 and 3' Swa1 restriction sites and sub-cloned into pCDH. Primary antibodies for

western blots were used at the following dilutions: rabbit anti-FLAG-HRP (1:1000, Sigma-Aldrich, St. Louis, MO), rabbit anti-GFP (1:1000, Cell Signaling Technologies, Danvers, MA), rabbit anti-NRMT1 (1:1000) (Tooley et al. 2010), rabbit anti-me3-RCC1 (1:10,000) (Tooley et al. 2010), rabbit anti-me1/2-RCC1 (1:5000) (Tooley et al. 2010), rabbit anti-GAPDH (1:2000, Trevigen, Gaithersburg, MD), and mouse anti-Dendra2 (1:500, Origene, Rockville, MD).

Cell culture and lentivirus production

Human embryonic kidney cells (HEK293, ATCC, Manassas, VA) cells were maintained in Dulbecco's Modified Eagle Medium (DMEM, Life Technologies, Carlsbad, CA) supplemented with 10% fetal bovine serum (FBS, Atlanta Biologicals) and 1% penicillin-streptomycin (P/S; Life Technologies). HCT116 human colorectal carcinoma cell lines (generous gift from Dr. Ian Macara) were maintained in McCoy's 5a Modified Medium (Life Technologies) supplemented with 10% FBS and 1% P/S. Lentivirus expressing empty pCDH vector, NRMT2-GFP-pCDH, SETα-Dendra2-pCDH, NRMT1-FLAG-pCDH, or NRMT2-FLAG pCDH was made by co-transfecting HEK293 cells with 50 µg pCDH containing the appropriate cDNA, 37.5 µg psPAX2 packaging vector, and 15 µg pMD2.G viral envelope plasmid using calcium phosphate transfection (McCaffrey and Macara 2009). Forty-eight hours post-transfection, supernatant was collected and virus concentrated using 100 kD ultrafilters (EMD Millipore). Virus concentration was determined by titration in HEK293 cells and HCT116 cells

were transduced by addition of a volume of virus equal to a multiplicity of infection (MOI) of 1. Three days post-transduction, transduced cells were selected for by addition of 2 μg/ml puromycin. For Dendra2 experiments, cells were first transduced with overexpression virus. Transduced cells were selected for with puromycin after three days, and then retransduced with SETα-Dendra2 expressing virus.

Co-Immunoprecipitations (co-IPs)

For co-IP experiments, $1x10^6$ HEK293 cells were seeded in 60 mm tissue culture dishes 24 hours prior to calcium phosphate transfection with 2 μg each of appropriate constructs. 24 hours post-transfection, cells were scraped directly into 100 μl lysis buffer (50mM Tris pH 7.5, 300 mM NaCl, 5 mM $MgCl_2$, 1% NP-40, 7mM BME) plus protease inhibitors for protein isolation. 20 μl of cell lysate was retained for input control, and the remainder mixed with 20 μl M2 agarose beads (Sigma-Aldrich). The bead/protein mixture was rotated 1-2 hours at 4^oC and washed 3x with PBS + 0.1% NP-40. The immunoprecipitated proteins were eluted from the beads in 5X Laemmli buffer and boiled for 5 minutes at 95^o C. The bead-free supernatant from IP and 15ug total protein input samples were run on 12% SDS-PAGE gels. Western blotting was performed using the above antibodies.

Analytical Ultracentrifugation

Sedimentation velocity experiments were carried out in a Beckman Coulter ProteomeLab XL-A analytical ultracentrifuge (Beckman Coulter Inc., Brea, CA) at 20°C and 40,000 rpm in standard 2 sector cells. Buffer density and viscosity (50 mM Tris, 50 mM KCl at pH 8.0) were calculated using Sednterp (free software: Biomolecular Interaction Technologies Center at the University of New Hampshire, http://jphilo.com/sdtr0601.exe). Data were analyzed with the program Ultrascan 3.0 (free software: www.ultrascan.uthscsa.edu/) using the "combine pseudo-3D distributions" operation. The partial specific volumes of NRMT1 and NRMT2 were calculated from the amino acid compositions (0.734 ml/g for NRMT1 and 0.737 ml/g for NRMT2) using the Protparam tool in ExPASy (free software: web.expasy.org). Dr. Bill Dean is greatly appreciated for performing the analytical ultracentrifugation and subsequent analysis.

Cycloheximide experiments

$1x10^6$ HCT116 cells, HCT116 cells transduced with lentivirus expressing NRMT2-GFP, HCT116 cells with CRISPR/Cas9-mediated knockout of NRMT1 (HCT116 $NRMT1^{-/-}$) (Shields et al. 2017), or HCT116 $NRMT1^{-/-}$ cells transduced with lentivirus expressing NRMT2-GFP were plated 24 hours prior to the start of the cycloheximide chase experiment. At the start of each time point, the McCoy's 5a Modified Medium was replaced with fresh media containing 100 µg/ml cycloheximide (Sigma-Aldrich). Cells were harvested in 100 µl cell lysis buffer (see above) and protein was quantified using the Pierce 660 nM Protein Assay (Thermo-Fisher Scientific, Waltham, MA). 20 µg total protein per time point was

separated on 12% SDS-PAGE gels and subjected to Western blotting using antibodies against NRMT1, GFP, and GAPDH as a loading control. Pixel density and normalization for each band was quantified using Image Lab software (Bio-Rad, Hercules, CA).

Dendra2 experiments

As described above, HCT116 or HCT116 NRMT1$^{-/-}$ cells were transduced with control (empty pCDH vector), NRMT1-FLAG, or NRMT2-FLAG expressing lentivirus at an MOI of 1. Three days post-transduction cells were selected with puromycin treatment. Three days post-puromycin treatment, cells were retransduced with lentivirus expressing SETα-Dendra2 at an MOI of 1. 72 hours post-transduction, 2000 cells per well of each experimental condition were plated at an N=6 on a 96-well plate and allowed to adhere and grow for 48-72 hours. Kinetic fluorescent analysis using the Cytation5 Imaging System (BioTek, Winooski, VT) was started by taking pre-conversion images in the GFP and RFP channel for each well. Each well was then exposed to the DAPI channel (UV) at maximum intensity for 16 seconds for photoconversion of the Dendra2. Post-conversion RFP kinetic imaging was performed once per hour for 24 hours, with cells maintained at 5% CO_2 and 37°C. Imaging settings remained constant throughout. The raw fluorescence value of the RFP channel for each well was then normalized to the 0-hour time point and fluorescent decay between cell types was measured.

In vitro methylation assays

Methyltransferase assays were conducted using the MTase-Glo Methyltransferase Assay (Promega, Madison, WI) and following the given protocol. Briefly, after optimization for protein concentration, all assays used 0.4 μM recombinant enzyme, 20 μM S-adenosyl methionine (SAM), and varied concentrations of SPK-RCC1 (SPKRIAKRRSPPADA) or SSK-MYL9 (SSKRAKAKTTKKRPK) peptides as substrate. Substrates were serially diluted in a 96-well plate and reactions were started with the addition of the appropriate recombinant enzyme. All reactions were carried out at room temperature and stopped after 20 minutes with the addition of 0.5% trifluoroacetic acid. The MTase-Glo detection reagents were then added and luminescence was quantified using the Cytation5 Imaging System (BioTek).

Protein modeling and statistical analysis

Molecular modeling and the associated images were produced using the PyMOL Molecular Graphics System, Version 2.0.6 (Schrödinger, LLC). PDB accession numbers are 2EX4 (NRMT1) and 5UBB (NRMT2). Modeling was performed by molecular alignment of monomeric species of NRMT2 (5UBB) and dimeric NRMT1 (2EX4). Each species was rotated to minimal root-mean-square deviation (RMSD) scores (adapted from Coutsias et al., 2004) and potential interacting residues were measured using the “measurement wizard,” natively

incorporated into the PyMOL user interface. All measured residues of interaction had a distance >4Å, satisfying the maximum Van der Waals radius between atoms involved. All statistical analyses were performed using GraphPad Prism Software for Mac Version 7.0d (La Jolla, California). The specific statistical test is noted in the respective figure captions and results are presented as mean ± standard error, n = 3 unless specifically stated.

Results

NRMT1 and NRMT2 form heterotrimers

Like METTL3 and METTL14, NRMT1 (METTL11A) and NRMT2 (METTL11B) are part of the Methyltransferase like (METTL) family of class I methyltransferases containing seven-beta-strand methyltransferase motifs and Rossman folds for binding SAM (Iyer, Zhang, and Aravind 2016; Schapira and Ferreira de Freitas 2014). Though the enzymes in the METTL family have a wide range of substrates, including protein, RNA, and small molecules, they are structurally similar (Richon et al. 2011). Given that METTL3 and METTL14 must form a heterodimer for optimal m^6A methylation activity (Liu et al. 2014), and NRMT1 has been shown to have increased N-terminal trimethylation activity when co-expressed with NRMT2 (Petkowski et al. 2013), I wanted to determine if NRMT1 and NRMT2 also heterodimerize.

His-tagged recombinant human NRMT1 and NRMT2 were expressed and purified from *E. coli* and analyzed individually and combined by analytical

ultracentrifugation. Ultrascan 3 analysis identified a pool of NRMT1, that when analyzed alone, sediments as a monomer of approximately 33 kD (Figure 2A). This is slightly larger than the predicted molecular mass of 25 kD for a NRMT1 monomer. The majority of NRMT1, however, sedimented as a 52 kD dimer (Figure 2A). NRMT2 showed an opposite pattern when run alone. There was a pool of NRMT2 that sedimented as a 52.6 kD dimer, but the majority sedimented as a 35.7 kD monomer, which is close to its predicted molecular mass of 32 kD (Figure 2B). When run in combination at equimolar concentrations, monomers of each NRMT1 and NRMT2 were still present, but a new species of 83.8 kD was now visible, representing a heterotrimer formed from a NRMT1 dimer and a NRMT2 monomer (Figure 2C). The pool of NRMT1 dimer was completely depleted, suggesting that if NRMT2 monomer is present the NRMT1 dimer will bind it. In addition, as there was excess monomeric NRMT1 and NRMT2 present and no indication of a NRMT1 and NRMT2 heterodimer, these data also suggest NRMT1 cannot bind NRMT2 unless it is already homodimerized and a pool of NRMT2 monomer can exist independent of the heterotrimer.

Figure 2

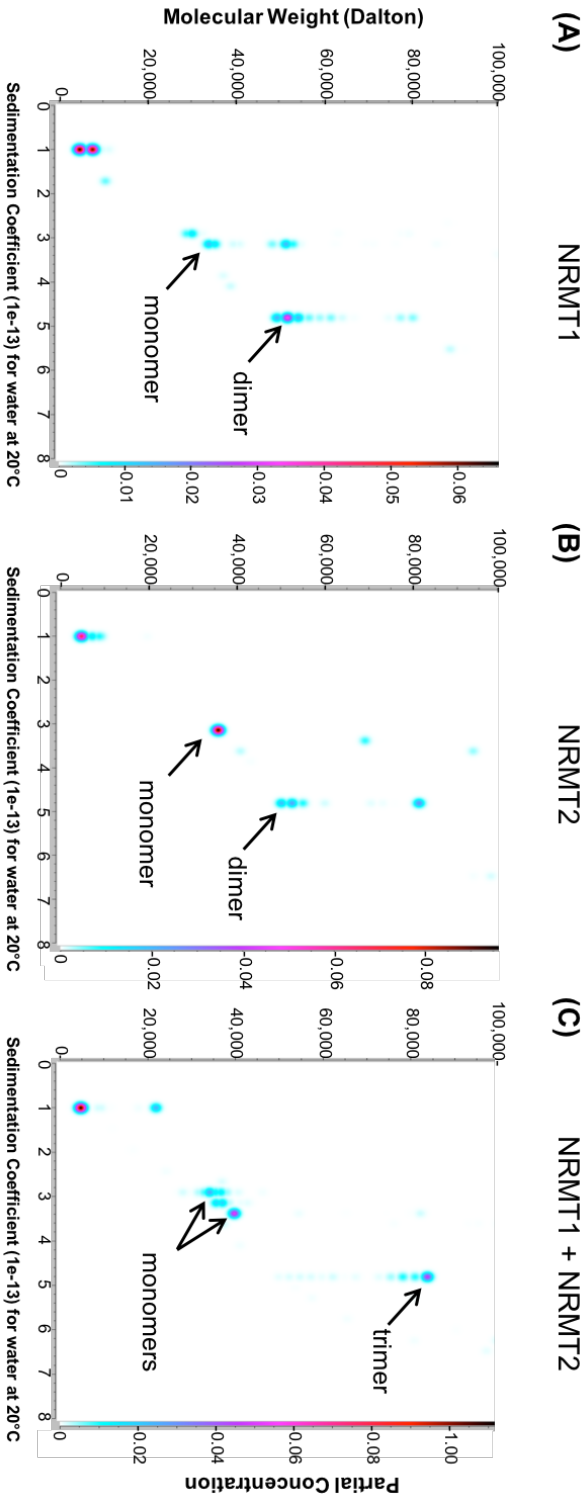
(A)
NRMT1
(B)
NRMT2
(C)
NRMT1 + NRMT2
Molecular Weight (Dalton)
Sedimentation Coefficient (1e-13) for water at 20°C
Partial Concentration
monomer
dimer
monomers
trimer

Figure 2. NRMT1 and NRMT2 form heterotrimers. (A) Ultrascan 3 analysis shows a minor pool of His-tagged NRMT1 sediments as a monomer of approximately 33 kD and a major pool sediments as a homodimer of approximately 52 kD. (B) The majority of His-tagged NRMT2 sediments as a monomer of approximately 35.7 kD, with a minor pool sedimenting as a homodimer of approximately 52.7 kD. (C) An equimolar mixture of NRMT1 and NRMT2 shows the formation of an 83.8 kD heterotrimeric species, representing a NRMT1 dimer and NRMT2 monomer. NRMT1 dimers are no longer present, but monomers of both NRMT1 and NRMT2 can still be seen. Dr. Bill Dean is greatly thanked for the running and interpretation of the analytical ultracentrifugation experiment.

NRMT1 and NRMT2 interact *in vivo*

Now knowing that NRMT1 and NRMT2 can interact *in vitro*, I wanted to next determine if the homologs also interact *in vivo*. Full length C-terminally-tagged human NRMT1-FLAG and NRMT2-GFP were co-expressed in human embryonic kidney cells (HEK293) by transient transfection. Twenty-four hours post-transfection, NRMT1-FLAG was immunoprecipitated (IP) out of the cell lysate and western blots were used to determine if NRMT2-GFP co-immunoprecipitated. As expected, full length NRMT1-FLAG was able to co-IP NRMT2-GFP (Figure 3A). To test if the reciprocal was true, full length human NRMT2-FLAG and human NRMT1-GFP were also co-expressed in HEK293 cells by transient transfection. While NRMT1-GFP did show some non-specific binding to beads alone, it was enriched in the co-IP lane, indicating full length NRMT2-FLAG is able to co-IP NRMT1-GFP (Figure 3B).

As both these co-IPs were done with overexpressed tagged proteins, I next wanted to determine if endogenous NRMT1 and NRMT2 interact. We have previously developed a rabbit antibody against human NRMT1 that successfully works for western blot but not for IP (Tooley et al. 2010). Though NRMT1 and NRMT2 are 50% identical, the fourteen amino acid peptide antigen used to produce the NRMT1 antibody only had three amino acids in common and does not appear to detect NRMT2 (Tooley et al. 2010). As we have yet to find a NRMT2 antibody that consistently works for either western blot or IP from cell lysate, I expressed full length NRMT2-FLAG in HEK cells, immunoprecipitated it with anti-FLAG agarose and assayed for the presence of endogenous NRMT1 by

western blot. As a control, I also expressed VRK2-FLAG, which has been shown to interact with endogenous NRMT1 (Petkowski et al. 2012). I found that endogenous NRMT1 did co-IP with both VRK2-FLAG and NRMT2-FLAG (Figure 3C). Taken together, these data indicate that NRMT1 and NRMT2 can interact both *in vitro* and *in vivo*.

Figure 3

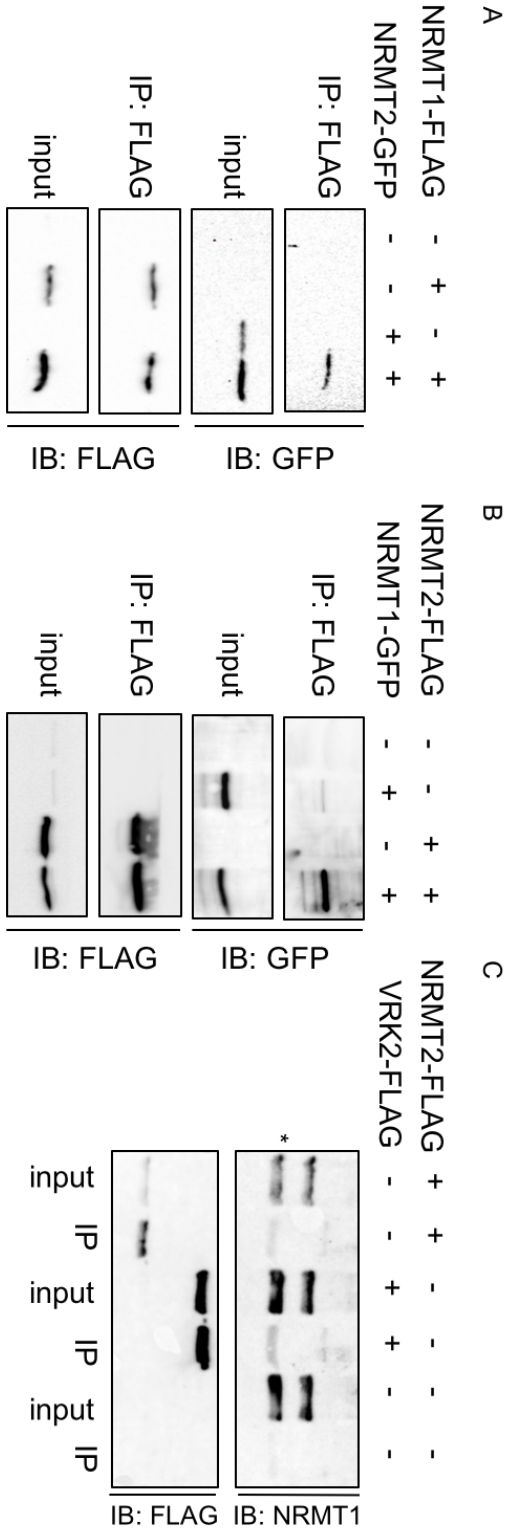
A
NRMT1-FLAG - + - +
NRMT2-GFP - - + +
input
IP: FLAG
input
IP: FLAG
IB: FLAG
IB: GFP
B
NRMT2-FLAG - - + +
NRMT1-GFP - + - +
input
IP: FLAG
input
IP: FLAG
IB: FLAG
IB: GFP
C
NRMT2-FLAG + + - - -
VRK2-FLAG - - + - -
*
input
IP
input
IP
input
IP
IB: FLAG
IB: NRMT1

Figure 3. NRMT1 and NRMT 2 interact *in vivo* (A) Western blots showing NRMT2-GFP co-immunoprecipitates with NRMT1-FLAG after co-transfection into HEK293 cells. (B) Reciprocally, NRMT1-GFP co-immunoprecipitates with NRMT2-FLAG. (C) Endogenous NRMT1 co-immunoprecipitates with both NRMT2-FLAG and VRK2-FLAG (a known binding partner of NRMT1, used as a positive control) (Petkowski et al. 2012). * denotes NRMT1 band. Upper band is a non-specific band detected by NRMT1 antibody (Tooley et al. 2010).

Modeling of NRMT1 and NRMT2 interactions

I next wanted to determine which domains on NRMT1 and NRMT2 are responsible for heterotrimer formation. The crystal structures of NRMT1 and NRMT2 (PDB codes 2EX4 and 5UBB) have been determined to 1.75 and 2 Å, respectively (Min 2005; Dong 2017), and as predicted by homology modeling (Petkowski et al. 2013) are almost identical barring the additional N-terminal domain on NRMT2, which was not included in the structure (Dong 2017). The core of both enzymes is a seven-stranded β sheet (β1-7) flanked by five α-helices (α1-5) (Wu et al. 2015). In addition, there are several other structural elements including three N-terminal helices and a pair of β hairpins (β_{AB}) inserted between β5 and α6 (Wu et al. 2015).

To help predict which domains of NRMT1 and NRMT2 interact, I first used PyMOL molecular visualization software to model the NRMT1 dimer. The space-filling model (Figure 4A) and ribbon diagram (Figure 4B) indicate NRMT1 homodimerization is facilitated by α5 of one monomer and the loop between α1/β1 on the second monomer (Figure 4B). Neither of these regions are involved in either the substrate or SAM-binding motifs (Wu et al. 2015) but are exposed on the outside of the protein and would be available for interaction (Figure 4A). The model specifically predicts interactions between Ser157 and Gly156 of the α5 helix with Ser64 and Arg68 of the α1/β1 loop, which are 4.2 and 3.9 Å apart, respectively (Figure 4C).

Though our analytical ultracentrifugation results suggest NRMT2 is predominantly found as a monomer, it can also be found as a homodimer (Figure 2B), and these dimerization interactions could provide insights into how it heterotrimerizes with NRMT1. The NRMT2 crystal structure (PDB code 5UBB) and our PyMOL models of NRMT2 dimerization (Figure 4D, E), indicate its homodimerization is facilitated by the unstructured N-termini (minus the 59 amino acid region unique to NRMT2, which is not included in the crystal structure) and the β_{AB} hairpins of each monomer. Our model specifically predicts Gln60, Val61, and Ile62 of the N-terminus interact with Cys229, Ile230, and Leu231 of the β_{AB} hairpin, respectively (Figure 4F). The extreme N-terminus is not currently predicted to contribute to substrate or SAM binding (Wu, 2015), but it is hard to predict how the additional 59 amino acid NRMT2 N-terminal tail could affect the overall structure. The β_{AB} hairpins are predicted to contribute to the substrate-binding pocket (Wu et al. 2015), which indicates binding of NRMT2 to NRMT1 could alter the ability of NRMT2 to bind substrate.

Figure 4

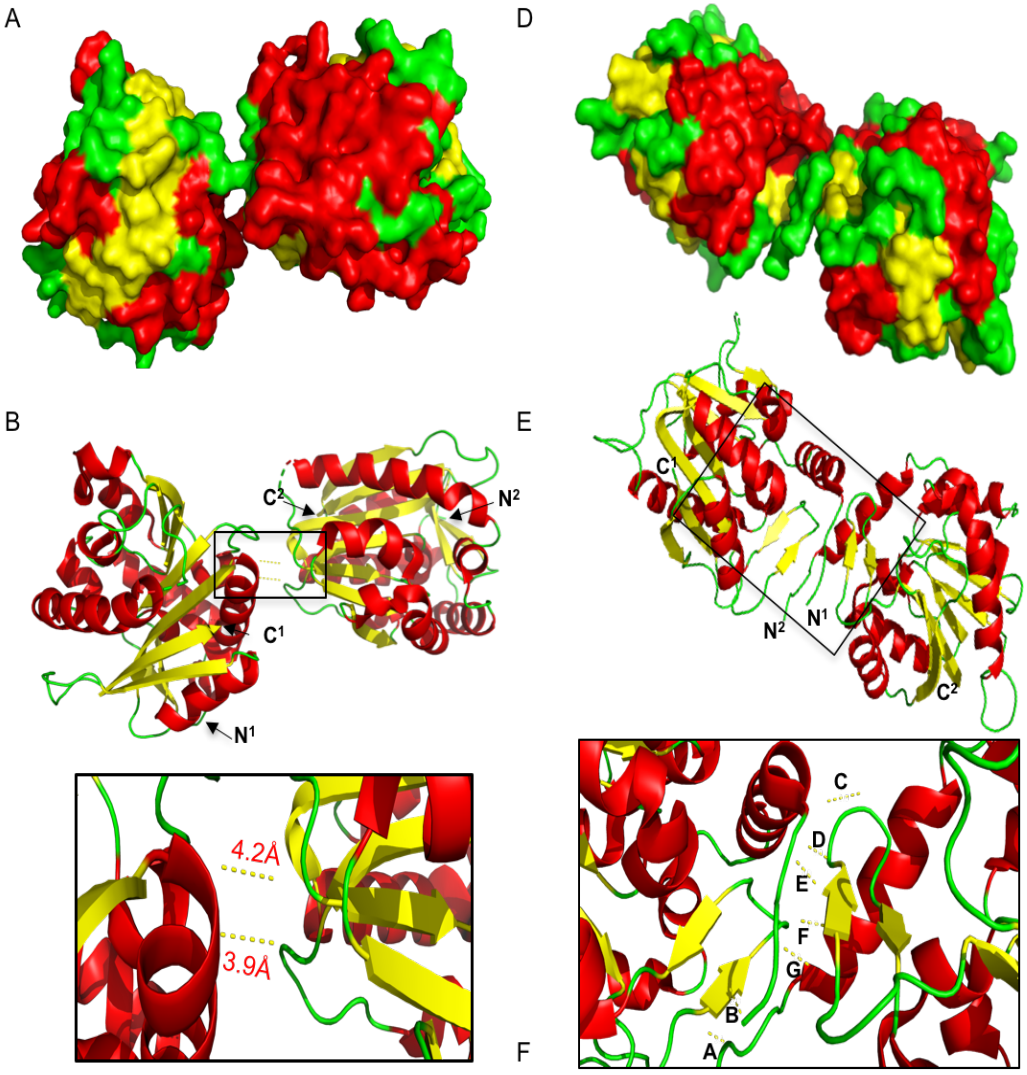

C

NRMT1 A	NRMT1 B	Å
Ser_{157}	Ser_{64}	4.2
Gly_{156}	Arg_{68}	3.9

NRMT2 A	NRMT2 B	Å
A. Cys_{229}	Val_{61}	3.1
B. Leu_{231}	Ile_{62}	2.8
C. Arg_{71}	Gln_{67}	3.6
D. Asn_{63}	Leu_{233}	3.0
E. Ile_{62}	Leu_{231}	2.8
F. Val_{61}	Ile_{230}	2.8
G. Gln_{60}	Cys_{229}	3.1

Figure 4. Modeling of NRMT1 and NRMT2 dimers**.** Space-filling model of (A) NRMT1 and (D) NRMT2 homodimers showing regions of dimerization (green overlap, middle). Ribbon diagrams of (B) NRMT1 and (E) NRMT2 homodimers and detail of regions of interaction between monomers. All measurements between residues fall within accepted Van der Waals distances for interaction. Boxed regions are enlarged below each model. Measured distances between interacting residues from monomers of (C) NRMT1 and (F) NRMT2. All interactions were modeled with PyMOL using PDB accessions codes 2EX4 and 5UBB.

I next used PyMOL to model the possible interactions between a NRMT1 dimer and a NRMT2 monomer (Figure 5A). I found that if the previously modeled interactions between NRMT1 monomers are maintained, the NRMT2 monomer primarily interacts within the first 50 amino acids of NRMT1, with a secondary set of interactions between Arg79, Pro83, andTyr104 of NRMT1 and Leu231, Asp232, and Gln60 of NRMT2 (Figure 5A-C). The NRMT2 residues involved are almost identical to those involved in homodimerization (Figure 5C). As predicted, the model suggests that NRMT2 interacts with the NRMT1 dimer as it would with another NRMT2 monomer. As the N-terminus of NRMT1 is not needed for its dimerization, both NRMT1 monomers would theoretically be available for binding to NRMT2. However, NRMT1 dimerization places both N-termini in the same plane, so steric hindrance may preclude binding of more than one NRMT2 monomer to the NRMT1 dimer (Figure 5D).

Figure 5

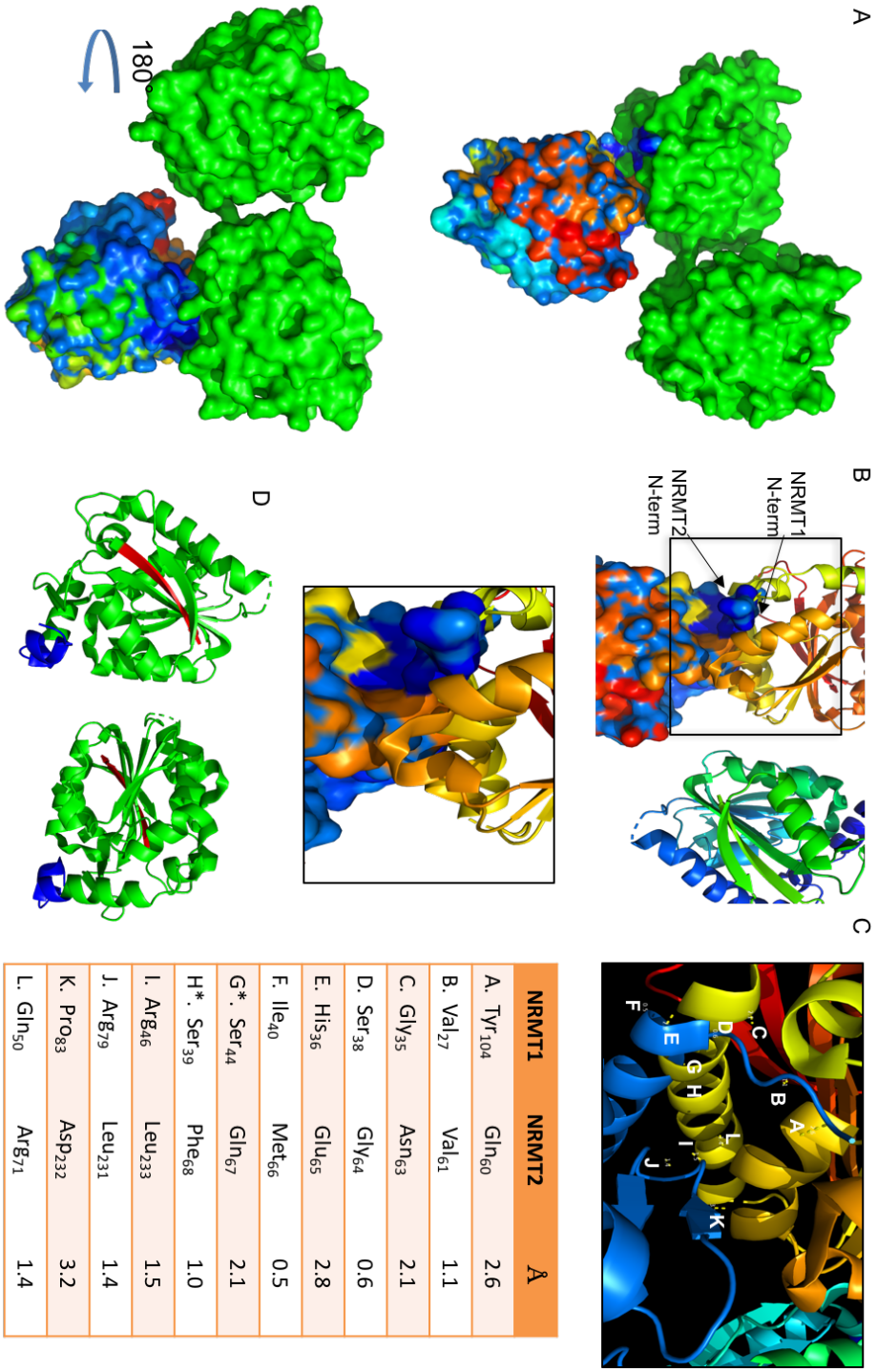

NRMT1	NRMT2	Å
A. Tyr_{104}	Gln_{60}	2.6
B. Val_{27}	Val_{61}	1.1
C. Gly_{35}	Asn_{63}	2.1
D. Ser_{38}	Gly_{64}	0.6
E. His_{36}	Glu_{65}	2.8
F. Ile_{40}	Met_{66}	0.5
G*. Ser_{44}	Gln_{67}	2.1
H*. Ser_{39}	Phe_{68}	1.0
I. Arg_{46}	Leu_{233}	1.5
J. Arg_{79}	Leu_{231}	1.4
K. Pro_{83}	Asp_{232}	3.2
L. Gln_{50}	Arg_{71}	1.4

Figure 5. Modeling of NRMT1 and NRMT2 heterotrimer. (A) *Top* - Space-filling model showing area of interaction between the NRMT1 dimer (green) and NRMT2 monomer (multicolored). *Bottom* - 180^{o} rotation of the heterotrimer model. The NRMT2 monomer is shaded with a blue-to-red gradient, representing the N-terminal to C-terminal orientation of the amino acid sequence. The majority of interactions between the NRMT1 dimer and NRMT2 monomer are predicted to involve the blue (N-terminus) shaded region of NRMT2. (B) Ribbon diagram of the NRMT1 dimer interacting with the space-filling model of the NRMT2 monomer. Boxed region is enlarged below and shows the majority of residues of interaction are found in the N-terminus of both enzymes. (C) Diagram of and measured distances between interacting residues of NRMT1 and NRMT2. (D) Ribbon diagram of NRMT1 homodimer, indicating N-termini of each monomer (purple) are oriented in the same plane. All interactions were modeled with PyMOL using PDB accessions codes 2EX4 and 5UBB.

To test these models, I performed co-IPs with N- and C-terminal fragments of NRMT1 and NRMT2 (Figure 6A). To determine if it is primarily the unstructured N-terminal tail of NRMT2 that interacts with full-length NRMT1-FLAG, I made constructs consisting of the first 112 amino acids of NRMT2 (containing important predicted residues) or amino acids 77-223 of NRMT2 (directly succeeding the important predicted residues) fused to GFP. An additional C-terminal fragment of NRMT2 (amino acids 207-283) was attempted but did not express. NRMT1-FLAG and $NRMT2_{1-112}$-GFP or $NRMT2_{77-223}$-GFP were co-expressed in HEK293 cells, and NRMT1-FLAG was immunoprecipitated using anti-FLAG antibody conjugated to agarose beads. Contrary to the model, the first 112 amino acids of NRMT2 did not strongly interact with NRMT1, though amino acids 77-223 did (Figure 6B,C). The main difference between the co-IPs and the models was that the first 112 amino acids in the co-IPs contained the extra 59 amino acid N-terminal tail that was not included in the crystal structure or subsequent model. These data indicate that the presence of the additional N-terminal amino acids of NRMT2 affect its binding to NRMT1.

To determine if it is primarily the first 50 amino acids of NRMT1 that interact with full-length NRMT2-FLAG, I made constructs consisting of the first 59 amino acids, amino acids 52-172, or amino acids 178-223 of NRMT1 fused to GFP (Figure 6A). NRMT2-FLAG and $NRMT1_{1-59}$-GFP, $NRMT2_{52-172}$-GFP, or $NRMT2_{178-223}$-GFP were co-expressed in HEK293 cells, and NRMT2-FLAG was immunoprecipitated out as previously described. Supporting the model, the first

59 amino acids of NRMT1 did strongly interact with NRMT2 (Figure 6D). However, amino acids 52-172 also interacted with NRMT2 (Figure 6E), as did amino acids 178-223, though to a lesser degree than the first two constructs (Figure 6F). These data indicate that the first 50 amino acids of NRMT1 are sufficient to promote interaction with NRMT2, though the predicted interactions of Arg79, Pro83, and Tyr104 may also be playing a role.

Figure 6

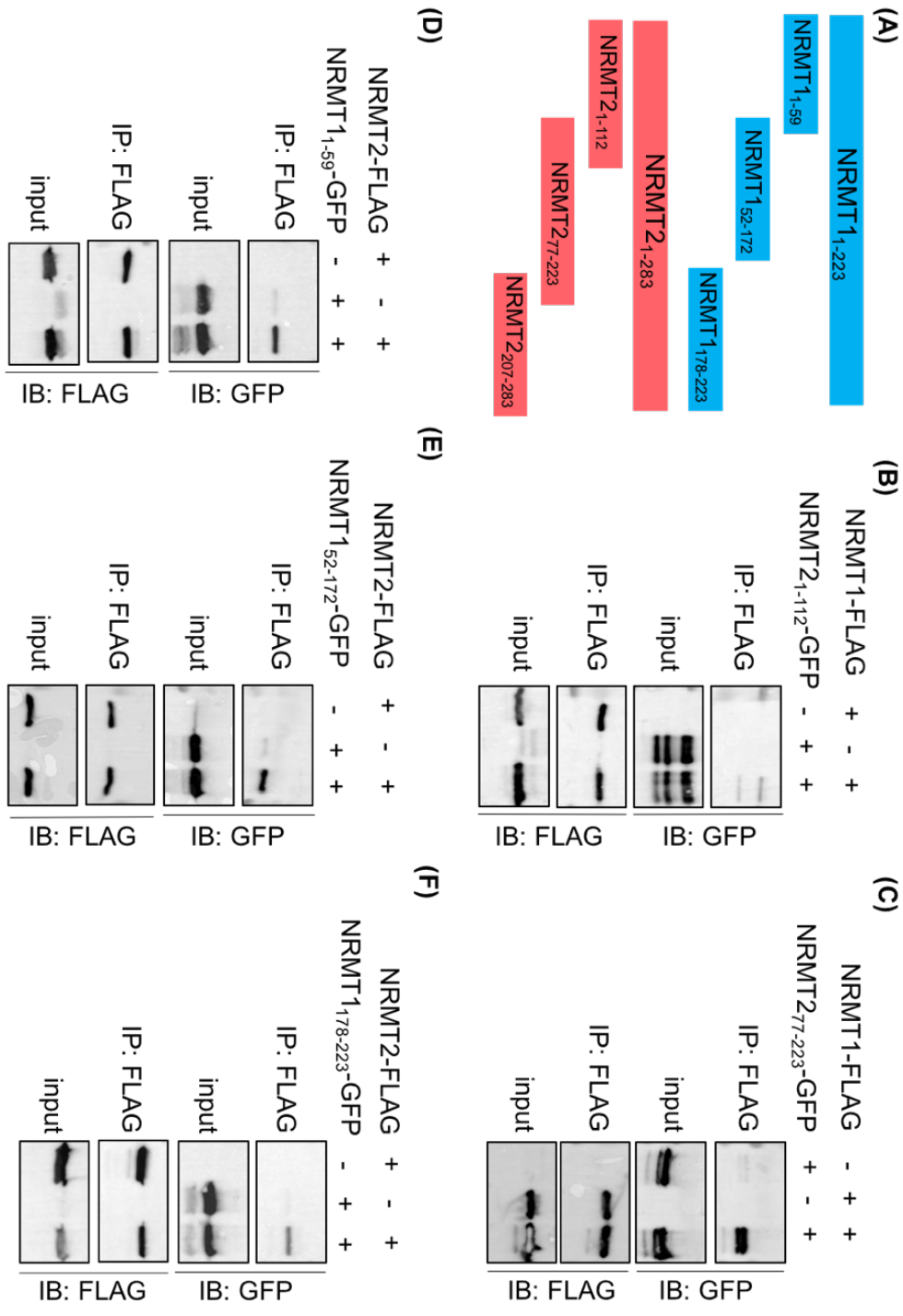
(A)
NRMT1 1-223
NRMT1 1-59
NRMT1 52-172
NRMT1 178-223
NRMT2 1-283
NRMT2 1-112
NRMT2 77-223
NRMT2 207-283
(B)
NRMT1-FLAG + - +
NRMT2 1-112-GFP - + +
IP: FLAG
input
IP: FLAG
input
IB: FLAG
IB: GFP
(C)
NRMT1-FLAG - + +
NRMT2 77-223-GFP + - +
IP: FLAG
input
IP: FLAG
input
IB: FLAG
IB: GFP
(D)
NRMT2-FLAG + - +
NRMT1 1-59-GFP - + +
IP: FLAG
input
IP: FLAG
input
IB: FLAG
IB: GFP
(E)
NRMT2-FLAG + - +
NRMT1 52-172-GFP - + +
IP: FLAG
input
IP: FLAG
input
IB: FLAG
IB: GFP
(F)
NRMT2-FLAG + - +
NRMT1 178-223-GFP - + +
IP: FLAG
input
IP: FLAG
input
IB: FLAG
IB: GFP

Figure 6. NRMT1 and NRMT2 truncation mutants. (A) Diagram showing full-length and truncation constructs of NRMT1 and NRMT2. Subscript indicates the amino acid (aa) sequence from N- to C-terminus of each construct. (B) Full-length NRMT1-FLAG only weakly interacts with the first 112 aa of NRMT2, (C) though strongly interacts with a NRMT2-GFP fragment (amino acids 77-223) that is missing the 59 aa tail that is also lacking from the crystal structure and subsequent model. (D) Full-length NRMT2-FLAG strongly interacts with the first 59 aa of NRMT1, as well as, (E) amino acids 52-172. (F) There is a decreased interaction of NRMT2-FLAG with the C-terminal fragment of NRMT1 (amino acids 178-223). N =3 for each truncation experiment.

NRMT2 expression stabilizes NRMT1

As both PRMT1 and METTL3 stability is enhanced by binding to its homolog partner (Kafkova et al. 2017; Liu et al. 2014; Wang et al. 2014), I wanted to next determine if the half-life of NRMT1 is enhanced by the expression of NRMT2 or vice versa. To first measure the half-life of endogenous NRMT1 under basal conditions (i.e. low levels of NRMT2 as determined by qRT-PCR (unpublished data)), I treated HCT116 human colorectal carcinoma cells with 100 μg/ml cycloheximide and harvested cell lysates at six time points, up to twelve hours after treatment. Western blots of the lysates were probed with our anti-NRMT1 antibody (Tooley et al. 2010) and anti-GAPDH as a loading control. NRMT1 levels were normalized to GAPDH and calculated using Image Lab software. The experimentally calculated half-life for endogenous NRMT1 was approximately 8.8 hours (Figure 7A).

Due to the lack of an antibody that specifically detects endogenous NRMT2 in cell lysate, I used NRMT2-GFP to determine the half-life of NRMT2 under basal conditions. HCT116 cells were transduced with lentivirus expressing NRMT2-GFP at an MOI of 1. 48 hours post-transduction, successfully transduced cells were selected for by puromycin treatment. This was to ensure all cells in the experiment were expressing a homogenously low level of NRMT2-GFP. Again, cells were treated with 100 μg/ml cycloheximide and harvested at six time points, up to twelve hours after treatment. Western blots of the lysates were probed with anti-GFP and anti-GAPDH and analyzed as above. The

experimentally calculated half-life for NRMT2 under basal conditions (i.e. with NRMT1 present) was approximately 5.3 hours (Figure 7B).

To determine if NRMT2 expression is altered in the absence of NRMT1, I first transduced CRISPR/Cas9-mediated NRMT1 knockout HCT116 cells (Shields et al. 2017) with lentivirus expressing NRMT2-GFP at an MOI of 1. After puromycin selection, cells were treated with 100 μg/ml cycloheximide and harvested as previously described. The experimentally calculated half-life for NRMT2 in cells lacking NRMT1 expression was approximately 3.3 hours (Figure 7C). This was not statistically significant from the half-life of NRMT2-GFP in control cells (Figure 7E), indicating the stability of NRMT2 is not dependent on NRMT1 expression. This also highlights the short half-life of NRMT2, and indicates its expression may be tightly regulated and confined to times of specific need.

Next, I aimed to measure if NRMT2 overexpression affects the stability of endogenous NRMT1. As previously, HCT116 cells were transduced with lentivirus expressing NRMT2-GFP at an MOI of 1. They were then treated with 100 μg/ml cycloheximide and harvested as previously. Interestingly, in the presence of overexpressed NRMT2, the half-life of NRMT1 increases to approximately 14.8 hours (Figure 7D). This is a significant increase in NRMT1 half-life as compared to its half-life of 8.8 hours under basal NRMT2 conditions (Figure 7E). These data fit with a model of NRMT1 providing basal housekeeping N-terminal methyltransferase activity, and NRMT2 being induced

to enhance NRMT1 activity when needed during times of stress of increased substrate burden.

Figure 7

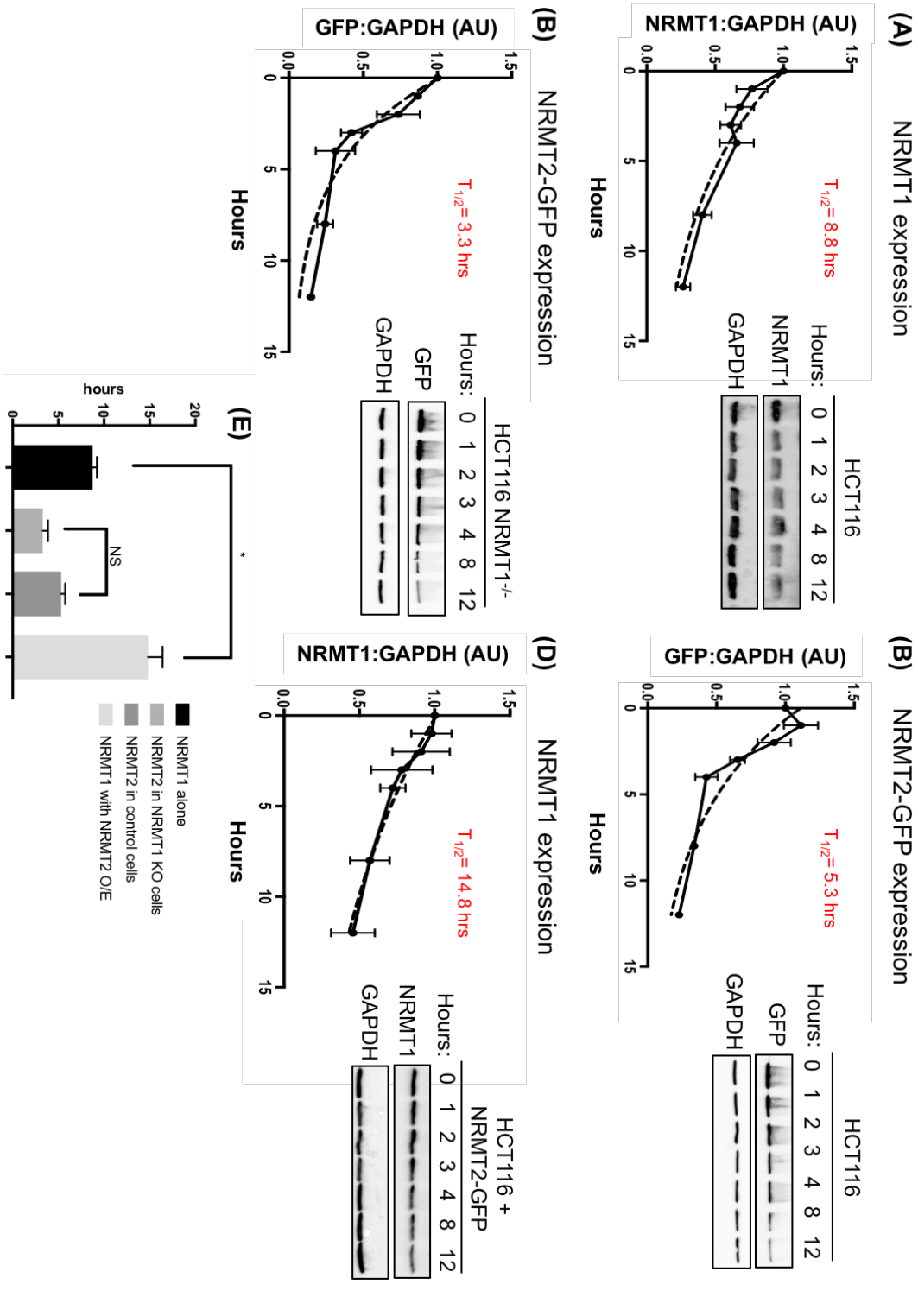
(A)
NRMT1 expression
NRMT1:GAPDH (AU)
T1/2= 8.8 hrs
Hours
HCT116
Hours: 0 1 2 3 4 8 12
NRMT1
GAPDH
(B)
NRMT2-GFP expression
GFP:GAPDH (AU)
T1/2= 5.3 hrs
Hours
HCT116
Hours: 0 1 2 3 4 8 12
GFP
GAPDH
(B)
NRMT2-GFP expression
GFP:GAPDH (AU)
T1/2= 3.3 hrs
Hours
HCT116 NRMT1-/-
Hours: 0 1 2 3 4 8 12
GFP
GAPDH
(D)
NRMT1 expression
NRMT1:GAPDH (AU)
T1/2= 14.8 hrs
Hours
HCT116 + NRMT2-GFP
Hours: 0 1 2 3 4 8 12
NRMT1
GAPDH
(E)
hours
NS
*
NRMT1 alone
NRMT2 in NRMT1 KO cells
NRMT2 in control cells
NRMT1 with NRMT2 O/E

Figure 7. NRMT2 expression stabilizes NRMT1**.** HCT116 cells were treated for 0 -12 hours with 100 μg/ml cycloheximide to inhibit protein synthesis. (A) Half-life of endogenous NRMT1 protein was calculated to be 8.8 hours. (B) Half-life of NRMT2-GFP protein was calculated to be 5.3 hours. (C) HCT116 cells with CRISPR/Cas9-mediated knockout of NRMT1 (HCT116 NRMT1$^{-/-}$) were also treated for 0 -12 hours with 100 μg/ml cycloheximide. The half-life of NRMT2-GFP in the absence of NRMT1 was slightly lower at 3.3 hours (D) Finally, HCT116 cells overexpressing NRMT2-GFP were treated for 0 -12 hours with 100 μg/ml cycloheximide. The half-life of endogenous NRMT1 in the presence of overexpressed NRMT2 was found to be a significantly longer 14.8 hours. (E) Comparison of the half-lives of each group. Blots are representative images of three independent experiments. Pixel densitometry was quantified using Bio-Rad Image Lab software, with GAPDH serving as the loading control for each lane. NRMT1 and/or GFP bands were internally normalized to T=0 lane and set to 1. Half-life was calculated using a one-phase decay non-linear regression and constraining Y_0 to 1 and the plateau to 0 (dashed lines). * denotes $p<0.05$ as determined by ANOVA followed by Tukey's multiple comparison test to compare groups using GraphPad Prism.

Catalytic activity of NRMT2 is not necessary for increased trimethylation by NRMT1

To determine if NRMT2 enhances NRMT1 activity through a priming activity as previously hypothesized (Petkowski et al. 2013), or if it is simply providing enhanced stability, I performed *in vitro* methylation assays with different combinations of wild type (WT) NRMT1, WT NRMT2, and NRMT2 V224L, a mutant initially identified in human breast cancer that is almost completely devoid of methyltransferase activity (Shields et al. 2017). When using as substrate a peptide consisting of the first fifteen amino acids of RCC1 (SPKRIAKRRSPPADA), NRMT1 recombinant enzyme alone exhibited a K_m of 1.1 μM (Figure 8A), WT NRMT2 recombinant enzyme alone exhibited a K_m of 55.6 μM (Figure 8B), and NRMT2 V224L had no activity (Figure 8C). In combination with WT NRMT2, the K_m of NRMT1 decreased to 0.9 μM (Figure 8D), and in combination with NRMT2 V224L, the K_m of NRMT1 decreased to 0.1 μM (Figure 8E), indicating the increased activity of NRMT1 is not dependent on the catalytic activity of NRMT2.

However, only the decrease in K_m with NRMT2 V224L was statistically significant from the K_m of NRMT1 alone (Figure 8F). As the Ser-Pro-Lys consensus sequence of the RCC1 peptide is a preferred substrate for NRMT1 (Petkowski et al. 2012), I wanted to test if I could see a greater decrease in K_m with NRMT2 addition when using a less preferred substrate. We have previously seen that the K_m of NRMT1 is considerably higher when using the Ser-Ser-Lys consensus sequence of myosin regulatory light chain 9 (MYL9) (unpublished

data), so I repeated the experiments above using a peptide of the first fourteen amino acids of MYL9 (SSKRAKAKTTKKRP) as substrate. NRMT1 recombinant enzyme alone exhibited a K_m of 15.6 μM (Figure 8G). Neither WT NRMT2 nor NRMT2 V224L had any activity on the MYL9 peptide (Figure 8H,I). In combination with WT NRMT2, the K_m of NRMT1 decreased to 6.6 μM (Figure 8J), and in combination with NRMT2 V224L, the K_m of NRMT1 decreased to 4.4 μM (Figure 8K). Using this Ser-Ser-Lys substrate, both WT NRMT2 and NRMT2 V224L were able to significantly lower the K_m of NRMT1 (Figure 8L), further verifying the catalytic activity of NRMT2 is not needed, and indicating NRMT2 is not increasing NRMT1 activity via a substrate priming role, but by providing stability and altering substrate affinity.

Figure 8

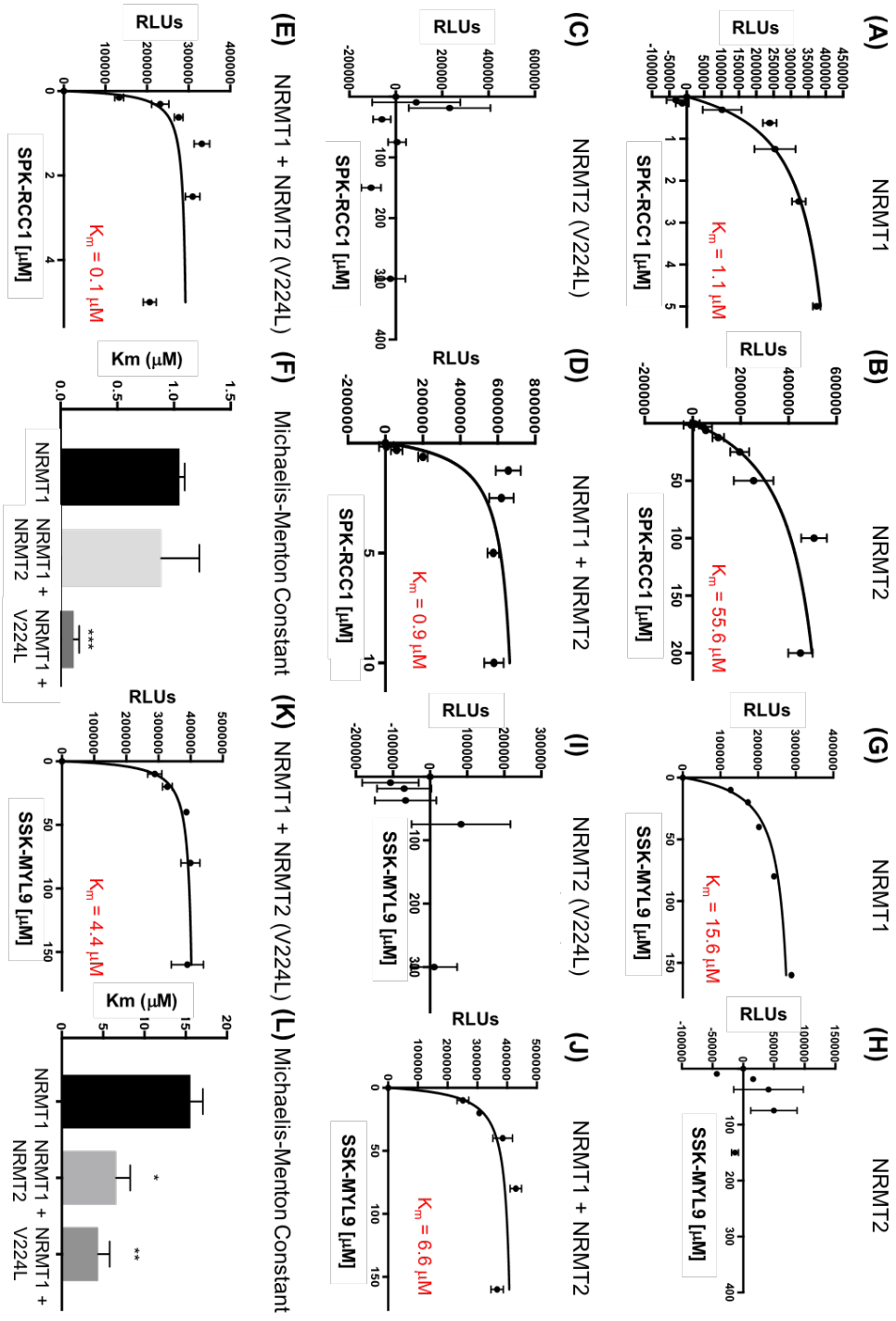
(A) NRMT1
(B) NRMT2
(C) NRMT2 (V224L)
(D) NRMT1 + NRMT2
(E) NRMT1 + NRMT2 (V224L)
(F) Michaelis-Menton Constant
(G) NRMT1
(H) NRMT2
(I) NRMT2 (V224L)
(J) NRMT1 + NRMT2
(K) NRMT1 + NRMT2 (V224L)
(L) Michaelis-Menton Constant
RLUs
SPK-RCC1 [μM]
SSK-MYL9 [μM]
Km = 1.1 μM
Km = 55.6 μM
Km = 0.1 μM
Km = 0.9 μM
Km = 15.6 μM
Km = 6.6 μM
Km = 4.4 μM
Km (μM)
NRMT1
NRMT1 + NRMT2
NRMT1 + V224L
***
*
**

Figure 8. Catalytic activity of NRMT2 is not necessary for increased trimethylation by NRMT1. (A) Wildtype NRMT1 shows a K_m of 1.1 μM when trimethylating the SPK-RCC1 peptide substrate, (B) while the K_m of NRMT2 is 55.6 μM. (C) The catalytically inactive NRMT2 V224L mutant is unable to methylate the same substrate. (D) Combing NRMT1 and NRMT2 lowers the K_m of NRMT1 to 0.9 μM, while (E) the combination of NRMT1 and catalytically inactive NRMT2 V224L further lowers the K_m of NRMT1 to 0.1 μM. (F) Comparison of Michaelis-Menton constants for NRMT1 alone, NRMT2 alone, or NRMT1 in combination with NRMT2 or NRMT2 V224L with SPK-RCC1 peptide as substrate. Only the combination of NRMT1 with NRMT2 V224L was significantly different from NRMT1 alone. Calculated constants are the mean of three independent experiments ± SEM. *** denotes $p< 0.001$ as determined by unpaired Student's t-test. Using a less preferred, but still enzymatically-favorable substrate SSK-MYL9, (G) increases the K_m of NRMT1 to 15.6 μM but shows no enzymatic activity with (H) NRMT2 or (I) NRMT2 V224L. (J) Combining NRMT1 and NRMT2 decreases the K_m of NRMT1 to 6.6 μM, and (K) the combination of NRMT1 and NRMT2 V224L further lowers the K_m of NRMT1 to 4.4 μM. (L) Comparison of Michaelis-Menton constants for NRMT1 alone, NRMT2 alone, or NRMT1 in combination with NRMT2 or NRMT2 V224L with SSK-MYL9 peptide as substrate. The constants for both the combinations of NRMT1 with NRMT2 and NRMT1 with NRMT2 V224L were significantly different from NRMT1 alone. Calculated constants are the mean of three independent experiments ± SEM. *

and ** denote *p<0.05 and 0.01,* respectively, as determined by unpaired Student's t-test.

To understand why NRMT2 V224L was able to significantly decrease the NRMT1 K_m with the RCC1 peptide, and not WT NRMT2, I performed molecular modeling of the NRMT2 V224L mutant (Figure 9). It is easy to see how V224L might disrupt NRMT2 catalytic activity, as Val224 is in the substrate binding pocket and is directly adjacent to Asn223, which forms critical hydrogen bonds and electrostatic interactions with substrate (Petkowski et al. 2013; Shields et al. 2017). When mutated to Leu, this residue extends much further into the pocket, potentially disrupting nearby interactions with substrate (Figure 9B). Interestingly, another residue critical for NRMT2 catalytic activity, Asp232 (Petkowski et al. 2013), is also nearby in this pocket, and is one of the predicted secondary sites of interaction with NRMT1 (Figure 5C, Figure 9C). Though they are not directly adjacent to each other they are connected by a short, unstructured loop, and it is possible to envision how a change in the position of residue 224 could indirectly affect the position of Asp232 (Figure 9C). Mutation of Val224 to Leu could impact NRMT2 function via two different mechanisms, first by disrupting substrate binding and subsequent catalytic activity, and second by promoting Asp232 accessibility and subsequent complex formation with NRMT1.

Figure 9

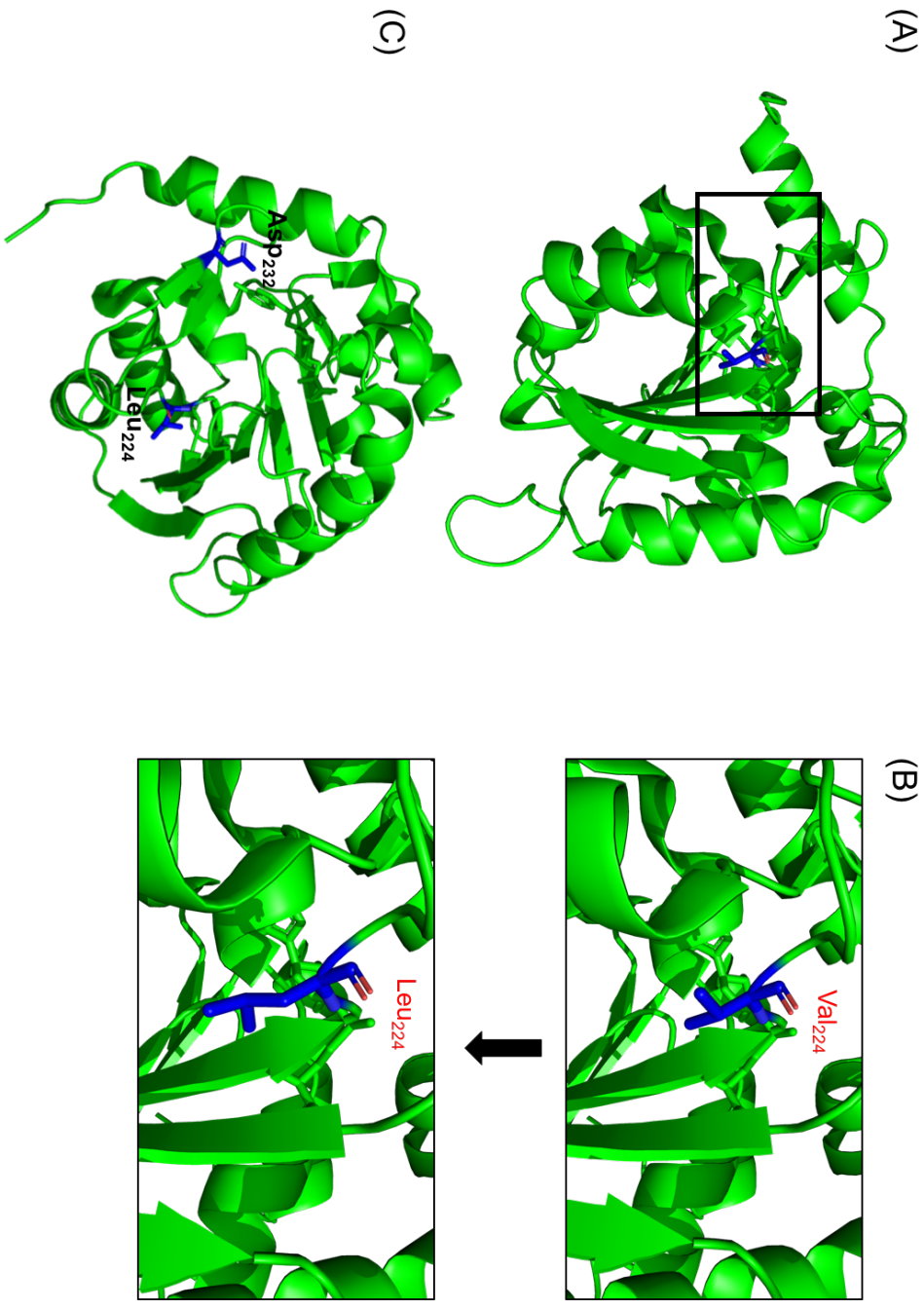

Figure 9. A valine → leucine mutation at position 224 renders NRMT2 catalytically inactive. (A) Cartoon rendering of NRMT2 monomer showing WT valine at position 224 (B, top) mutated to leucine (B, bottom) that eliminates methyltransferase activity. (C) Leu224 and Asp232 are connected by a short, unstructured loop. Images were produced in PyMOL.

NRMT2 overexpression cannot rescue NRMT1 knockout phenotypes

The above data lead to a model where the NRMT1 homodimer normally functions alone as the primary N-terminal methyltransferase in cells, but can act synergistically with NRMT2 to increase N-terminal trimethylation levels at times of high need. This model implies that NRMT2 is not simply a functionally redundant homolog of NRMT1 but an important activator. To further confirm NRMT1 and NRMT2 are not functionally redundant, I wanted to test if NRMT2 expression could rescue NRMT1 knockout phenotypes. It has been shown that N-terminal dimethylation protects the N-terminus of cytochrome c_{557} from digestion in *Crithidia oncopelti* (Smith and Pettigrew 1980). I wanted to see if N-terminal mono- or trimethylation differentially affected this protection and affect the rate of decay, using a mammalian substrate with a known consensus sequence for both NRMT1 and NRMT2, the α isoform of SET (SETα) (Petkowski et al. 2012; Tooley et al. 2010).

Human SETα was C-terminally tagged with Dendra2 photoswitchable protein and lentivirally expressed in HCT116 human colorectal carcinoma cells at an MOI of 1 (Figure 10B). Before excitation, Dendra2 fluoresces green, but when activated by UV-violet or blue light, fluoresces red (Figure 10A) (Zhang et al. 2007). The red form is highly stable independently, but when fused to a protein of interest, its signal can be followed to determine the rate of decay of the protein (Zhang et al. 2007). I first measured the rate of decay of SETα-Dendra2 in control HCT116 cells (Figure 10C, blue). I then showed the rate of decay of

SETα-Dendra2 in HCT116 NRMT1$^{-/-}$ cells was significantly quicker (Figure 10C, red). Overexpression of NRMT1 in the HCT116 NRMT1$^{-/-}$ cells restored the original rate of decay of SETα-Dendra2 (Figure 10C, green). However, overexpression of NRMT2 in the HCT116 NRMT1$^{-/-}$ cells was not able to rescue the SETα-Dendra2 rate of decay, and it remained significantly different from the HCT116 control (Figure 10C, purple). These data indicate N-terminal mono- and trimethylation are not functionally redundant and suggest that, unlike EZH1 and EZH2 (Shields et al., 2017), NRMT1 and NRMT2 are not serving the same function through different mechanisms. Our data point to the stabilization of NRMT1 and an increase in substrate binding as important functions of NRMT2 but do not rule out other specific roles for N-terminal monomethylation that are distinct from those regulated by N-terminal trimethylation.

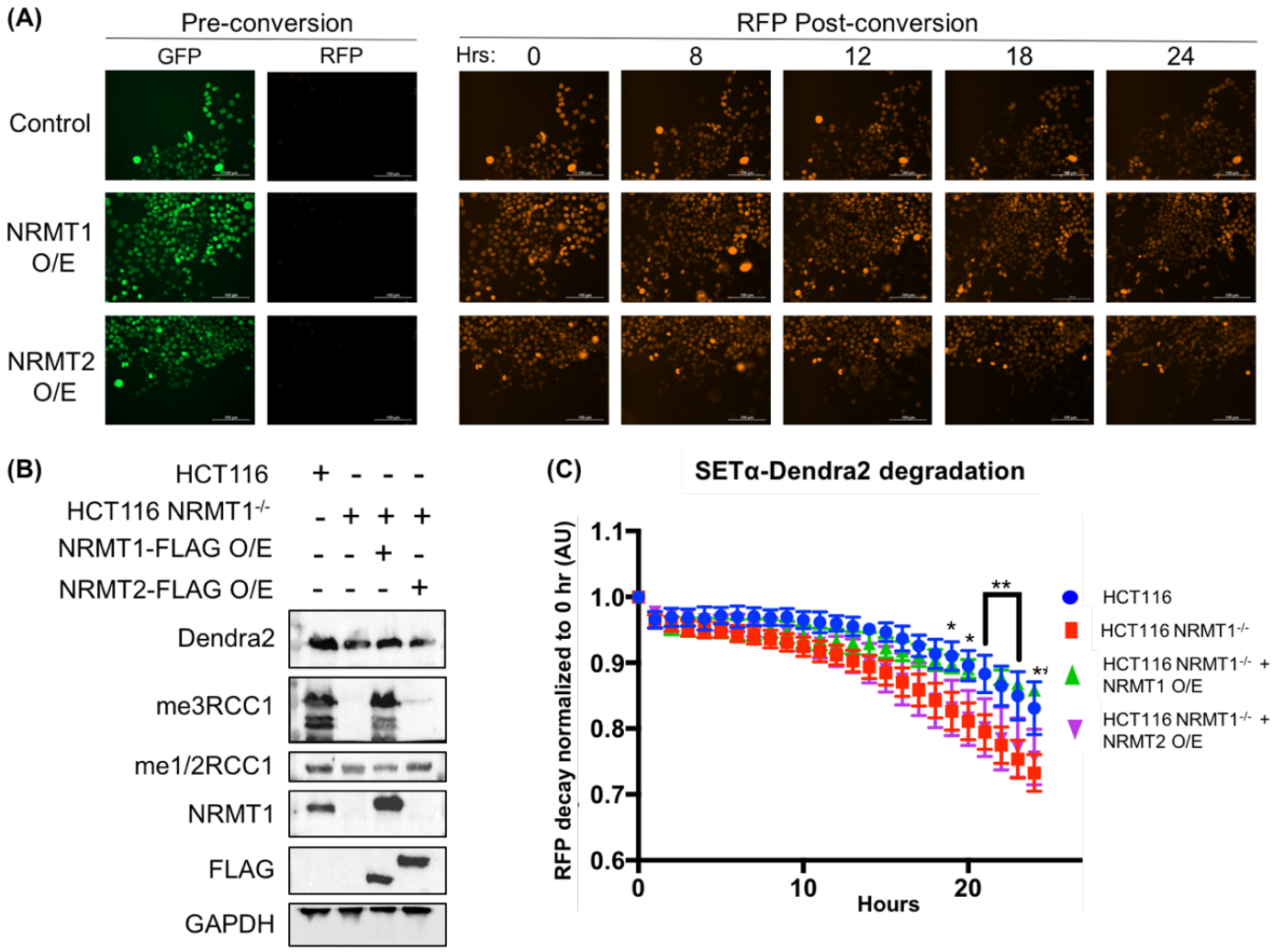
(A)
Pre-conversion
RFP Post-conversion
GFP
RFP
Hrs: 0
8
12
18
24
Control
NRMT1 O/E
NRMT2 O/E
(B)
HCT116 + - - -
HCT116 NRMT1-/- - + + +
NRMT1-FLAG O/E - - + -
NRMT2-FLAG O/E - - - +
Dendra2
me3RCC1
me1/2RCC1
NRMT1
FLAG
GAPDH
(C)
SETα-Dendra2 degradation
RFP decay normalized to 0 hr (AU)
1.1
1.0
0.9
0.8
0.7
0.6
0
10
20
Hours
*
*
**
*
HCT116
HCT116 NRMT1-/-
HCT116 NRMT1-/- + NRMT1 O/E
HCT116 NRMT1-/- + NRMT2 O/E

Figure 10

Figure 10. NRMT2 overexpression cannot rescue NRMT1 knockout phenotypes (A) HCT116 NRMT1$^{-/-}$ cells transduced with empty pCDH virus (control), virus overexpressing NRMT1 (NRMT1 O/E), or virus overexpressing NRMT2 (NRMT2 O/E) were also transduced with virus expressing SETα-Dendra2. Pre conversion SETα-Dendra2 expresses in the GFP channel, post-conversion it expresses in the RFP channel. The RFP signal then decreases over time and a rate of decay can be calculated. (B) Western blots showing HCT116 cells express endogenous NRMT1 and were fully mono/dimethylated (me1/2RCC1) and trimethylated (me3RCC1) (lane 1). In contrast, HCT116 NRMT1$^{-/-}$ cells do not express NRMT1 or exhibit N-terminal trimethylation, but retain mono/dimethylation (lane 2). In HCT116 NRMT1$^{-/-}$ cells overexpressing NRMT1-FLAG, both NRMT1 protein and trimethylation were restored (lane 3). In HCT116 NRMT1$^{-/-}$ cells overexpressing NRMT2-FLAG, a slight increase in mono/dimethylation can be seen, with no restoration of NRMT1 or trimethylation (lane 4). FLAG blot shows both NRMT1-FLAG and NRMT2-FLAG are expressing. Dendra2 blot shows SETα-Dendra2 expression levels are similar between lines. GAPDH was used as a loading control. (C) First, the rate of decay of SETα-Dendra2 was measured in control HCT116 cells (blue). This rate of decay significantly increased in HCT116 NRMT1$^{-/-}$ cells (red). Overexpressing NRMT1-FLAG in HCT116 NRMT1$^{-/-}$ cells restores the original rate of decay (green), and there was no statistically significant difference between control and NRMT1 overexpression cell lines. Overexpressing NRMT2-FLAG in HCT116 NRMT1$^{-/-}$ cells cannot rescue the decay (purple), which remains significantly faster than control. Curves were

constructed by comparing loss of RFP signal over time as compared to time 0 and are the mean of three independent experiments ± SEM. *, **, *** denotes *p<0.05, 0.01, and 0.001,* respectively, as determined by 2-way ANOVA.

Discussion

Our work is the first to demonstrate a physical interaction between the N-terminal methyltransferase homologs, NRMT1 and NRMT2. Here I show that NRMT1 homodimers interact with NRMT2 monomers to form heterotrimers. Heterotrimer formation increases the stability of NRMT1 but has no significant effect on the stability of NRMT2. Though we have previously seen that co-expression with NRMT2 increases NRMT1 activity (Petkowski et al. 2013), I now show that NRMT2 catalytic activity is not necessary for this increase in NRMT1 activity and propose that NRMT2 is not priming for NRMT1, but instead increasing its stability. I also show that N-terminal mono- and trimethylation are not functionally redundant, at least in regards to promoting protein stability, indicating that NRMT1 and NRMT2 are also not functionally redundant. The sole role of NRMT2 may be to stabilize and activate NRMT1, or it may have other distinct functions.

In addition to stabilizing METTL3, METTL14 has been proposed to enhance interaction with RNA substrates (Wang, Doxtader, and Nam 2016; Wang et al. 2016). We have seen that NRMT1 has varying affinities for the different NRMT N-terminal consensus sequences (Petkowski et al. 2012), and it may be that binding of NRMT2 to the NRMT1 homodimer, strengthens its affinity for certain less favored consensus sequences. Our *in vitro* methyltransferase data support this model, as NRMT2 binding had little effect on the K_m of NRMT1 when methylating a Ser-Pro-Lys peptide, but significantly decreased the K_m of NRMT1 when methylating the less preferred Ser-Ser-Lys peptide. We had

originally proposed that NRMT2 was a primer for NRMT1 that was expressed at times of high substrate burden (Petkowski et al. 2013), but it may be that NRMT2 is expressed at times when less preferred substrates require methylation. In this way, it is both providing stability to NRMT1 and altering its substrate preference.

These data indicate that, while overall unique, the interaction between NRMT1 and NRMT2 has the most in common with the interactions of PRMT1/3 and METTL3/14. Like PRMT1/3 and METTL3/14, binding of the homologs increases the stability of the active enzyme (Kafkova et al. 2017; Liu et al. 2014; Wang et al. 2014). Similar to METTL14, but unlike PRMT3, NRMT2 has weak catalytic activity *in vitro* (Wang et al. 2014; Liu et al. 2014; Kafkova et al. 2017). However, SAM was visualized in the active site of the NRMT2 crystal, and I have seen that CRISPR-mediated knockout of NRMT1 results in a complete loss of N-terminal trimethylation, but N-terminal monomethylation remains the same (Figure 8B) (Shields et al. 2017). This indicates that, unlike METTL14, NRMT2 also has some activity *in vivo*. What the function of this *in vivo* N-terminal monomethylation is remains to be determined.

If charge or bulk of the N-terminus are the main regulatory aspects of N-terminal PTMs, it seems intuitive that N-terminal monomethylation could not functionally replace trimethylation, as it is much smaller and does not produce a pH-independent positive charge (Stock et al. 1987). However, similar to lysine monomethylation, N-terminal monomethylation could still have its own distinct function. RNA polymerase II (Pol II) pausing is regulated by the switch between mono- and trimethylation of histone H4 lysine 20 (H4K20me1 and H4K20me3,

respectively) (Kapoor-Vazirani and Vertino 2014). While H4K20me3 promotes pausing by inhibiting the recruitment of the male-specific lethal (MSL) complex, H4K20me1 recruits MSL and promotes the release of Pol II into elongation (Kapoor-Vazirani and Vertino 2014). One way subtle changes in the degree of methylation can affect protein function so dramatically, is that each can be recognized by different methyl-reading chromodomains. H4K20me1 can efficiently recruit the MSL complex to chromatin due to the chromo-barrel domain of MSL3 (Moore et al. 2010; Kim et al. 2010), whereas H4K20me3 is preferentially bound by the double tudor domain of the histone demethylase jumonji domain containing 2A (JMJD2A) (Garske, Craciun, and Denu 2008). Therefore, it is possible that N-terminal mono- and trimethylation could similarly recruit distinct proteins with different binding domains, and in doing so, differentially affect many cellular processes. It will be interesting to determine if families of such N-terminal methylation “readers” exist.

Though the interactions between NRMT1 and NRMT2 seem the most distinct from the interactions between EZH1 and EZH2, there are also some similarities. Most striking is the tissue distribution of the homologs. NRMT1, like EZH1, is ubiquitously expressed in most adult tissue types (Petkowski et al. 2013; Margueron et al. 2008). While NRMT2 has very low basal expression in adult mice, we do see enrichment in both skeletal muscle and the liver (Petkowski et al. 2013). EZH2 also has very low basal expression in adult tissue, with some enrichment in the spleen, but seems to be highly expressed in the proliferative tissue of the kidney during development (Margueron et al. 2008). It

has been hypothesized that these disparate expression patterns represent an evolutionary sub-functionalization of the homologs (Margueron et al. 2008). EZH1 is the general methyltransferase directly involved in transcriptional repression, while EZH2 is dedicated to placing repressive marks during replication (Margueron et al. 2008). Though EZH1 and EZH2 are catalytically distinct, they are functionally redundant in regards to transcriptional repression, and their differential expression patterns could allow for a tighter regulation of this repression (Margueron et al. 2008). The function of PRC2 complexes expressing both EZH1 and EZH2 remains to be determined (Margueron et al. 2008; Oliviero et al. 2016), but like PRMT1/3, METTL3/14, and NRMT1/2, co-expression might result in a more active complex, useful in times of high demand.

Unlike EZH1/2, NRMT1 and NRMT2 do not seem to be functionally redundant. Their evolution may have led to neo-functionalization instead of sub-functionalization (Prince and Pickett 2002). I propose a model where each has a distinct function, but at times when they are co-expressed, can form heterotrimers with increased N-terminal trimethylation activity. In this way, regulated NRMT2 expression would serve to promote its developmental or cell type-specific role and increase N-terminal methylation when needed. It will be interesting to see if NRMT2 expression is regulated during development or in proliferating tissues and continue to explore potential unique roles for N-terminal monomethylation. Also of note is the V224L NRMT2 mutation found in human breast cancer (Shields et al. 2017). While NRMT1 has been shown to have cancer type-specific roles as a tumor suppressor or oncogene (Bonsignore,

Butler, et al. 2015; Shields et al. 2017), there is as yet no data demonstrating NRMT2 misregulation in any cancer type. Therefore, extensive characterization of this mutation has not occurred. However, these data demonstrating it not only abolishes NRMT2 activity but also promotes NRMT1 activity make it an interesting candidate for a driver mutation in cancers that overexpress NRMT1 or a protective mutation in cancers that downregulate NRMT1. Future studies will determine how expression of this mutant affects oncogenic phenotypes in such cancer cell lines.

CHAPTER III

FUTURE DIRECTIONS AND IMPLICATIONS ON HUMAN HEALTH AND DISEASE

Introduction

The work presented in Chapter II illustrates the physical interaction between the α-amino methyltransferase homologs, NRMT1 and NRMT2. I have demonstrated the formation of a heterotrimeric species, consisting of a homodimer of NRMT1 and monomer of NRMT2, which increases the stability of NRMT1 but does not impart a change of stability on NRMT2. Additionally, I have used *in silico* modeling to identify likely residues of interaction among the NRMT1 homodimer, as well as the NRMT1-NRMT2 heterotrimer. Functionally, I have shown that N-terminal trimethylation and monomethylation do not serve redundant purposes, with NRMT2 overexpression being unable to rescue the SETα stability phenotype associated with loss of NRMT1-associated trimethylation. Previous work indicated an increase in NRMT1-associated trimethylation when co-expressed with NRMT2 (Petkowski, 2013). It was originally hypothesized that NRMT2 monomethylation was priming for NRMT1 trimethylation. However, I now show that NRMT2 catalytic activity is not needed for its promotion of NRMT1 activity, and propose NRMT2 increases NRMT1 activity by stabilizing the enzyme.

Though NRMT2 activity is not needed for its activation of NRMT1, it does demonstrate weak *in vitro* and *in vivo* catalytic activity on its own (Petkowski et al.,2013). Also, CRISPR-mediated loss of NRMT1, *in vitro*, abrogates the N-terminal trimethylation of substrates but monomethylation of these same substrates is retained (Shields, 2017). This indicates that providing stability to NRMT1 may not be the sole purpose of NRMT2. The following chapter will discuss potential unique roles of N-terminal monomethylation, how they could be experimentally determined, and how currently unstudied mutations in NRMT2 could actually be important on their own right or through their impact on NRMT1.

Monomethylation vs. Trimethylation

Yeast Set1 is a member of the COMPASS complex and was the first identified methylase capable of mono-, di-, and trimethylation of lysine 4 of histone 3 (H3K4) (Briggs et al., 2001; Krogan et al., 2001; Schneider et al., 2005). *Drosophila* contain three H3K4 methyltransferases related to Set1 and found in COMPASS complexes- dSet1, Trx, and Trithorax-related (Trr), whereas mammals possess two representatives for each of the H3K4 methyltransferases found in *drosophila* (Mohan et al., 2011; Silatifard 2012). The Set1 orthologues in both *drosophila* and mammals are responsible for the bulk of all levels of methylation of H3K4, and these levels are tightly controlled during different stages of development (Mohan et al., 2011; Sedkov et al., 2003; Chauhan et al., 2012). Active promoter regions are marked by H3K4 trimethylation (H3K4me3),

whereas promotor-distant enhancer regions are specifically marked by H3K4 monomethylation (H3K4me1) (Heintzman et al., 2007). These methylation states of enhancers are also noted to distinguish active (noted by H3K4me1 and H3K27 acetylation) versus inactive states (noted by H3K4me1 and H3K4me3) (Heintzman et al., 2009).

The COMPASS complex localizes to both promoters and enhancers, and the Trr methyltransferase (mammalian homolog: MII3) is required for the maintenance of H3K4me1, with significant loss of H3K4me1 and increase in H3K27me3 noted upon knockdown of this Trr or MII3. The loss of H3K4me1 and increase in H3K27me3 switches the enhancer from an inactive to active state (Herz, 2012). Should this switch from an inactive to active state occur in oncogenes, it's possible the misregulation of monomethylation could have pathological consequences. In a similar manner, the deposition of H3K4me1 by mammalian MLL3/4 at enhancers is shown to correlate with increased levels of chromatin interaction and gene activity during differentiation. Loss of H3K4me1 reduces these long-range interactions between promoters and enhancers and subsequently causes defects during development (Yan et al., 2018).

Similar to the enzymatic action catalyzed by NRMT2, protein arginine methyltransferase-7 (PRMT7) is unique in that it is only capable of monomethylating its target proteins (Cáceres et al., 2018). Each level of methylation on arginine residues of histones can have distinct functional consequences. For example, dimethylation of arginine 2 on histone H3 (H3R2me2) inhibits the Set1-mediated trimethylation of H3K4, maintaining

transcriptional silencing. However, monomethylation of this same residue (H3R2me1) does not induce Set1 inhibition and its associated H3K4 trimethylation and is associated with active transcription (Kirmizis et al., 2009). PRMT7, like NRMT2, is also found less broadly expressed than other PRMT family members, and its highest expression is in skeletal muscle (Jeong et al., 2016). It is also notably found in mouse embryonic stem cells and is thought to regulate pluripotency and differentiation. (Buhr et al., 2008).

PRMT7-null mice show reduced oxidative metabolism and increased age-related obesity, indicating a distinct functional role of monomethylation in skeletal muscle metabolism (Jeong et al., 2016). In another function, similar to that of the NRMT family, PRMT7 and its associated monomethylation activity are associated with genes associated with DNA damage repair (Karkhanis et al., 2012). PRMT7 contains an arginine binding pocket featuring larger residues than those found in other PRMT family members capable of dimethylation. The steric hindrance conveyed by these bulkier residues contributes to the monomethylation-only catalytic activity of PRMT7 (Jain et al., 2016; Cáceres et al., 2018). Interestingly, mutation of one particular active site residue, Glu181 to aspartate increases the size of the active site and corresponding affinity for monomethylated substrates, ultimately changing PRMT7 from a methyltransferase only capable of monomethylation to one capable of mono-, and dimethylating substrates (Debler et al., 2016).

Sequence alignment of PRMT7 and its PRMT homologs capable of dimethylation yield fewer regions of conservation compared to NRMT1 and

NRMT2, which share a 50% sequence identity and 75% sequence similarity, with all the catalytic residues being fully conserved (Cáceres et al., 2018; Petkowski et al., 2013). The distinct feature of NRMT2, setting it apart from NRMT1, is the additional 60 amino acid N-terminal tail, comprised of two alpha helices. This tail is unstructured and floats freely from the N-terminal region of the enzyme, and it was initially thought that this bulky region was likely responsible for the detection of previously methylated substrates, thus restricting NRMT2 to monomethylation only (Petkowski et al., 2013). Additionally, while the catalytic regions of NRMT1 and NRMT2 are similar in structure, they differ in residues. It was hypothesized that switching the catalytic residues of NRMT2 to those of NRMT1 could yield di- and trimethylating capability for NRMT2 (Petkowski et al., 2013). We have conducted these experiments and found the removal of the N-terminal tail does not change the monomethylation capacity of NRMT2 to one of di- or trimethylation, but abolishes activity of NRMT2 altogether (Shields et al., 2017). Addition of the tail to NRMT1, failed to yield soluble recombinant protein (Shields et al., 2017). Furthermore, mutation of the catalytic residues of NRMT2 to those of NRMT1 also yielded no change in catalytic ability or altered substrate specificity (Shields et al., 2017).

I have now shown that while NRMT2 does have enzymatic function on its own, one of its major roles is contributing to the structural stability of NRMT1. It is likely the additional 60 amino acid tail is playing a structurally supportive versus catalytic role in the heterotrimer complex. A number of studies have demonstrated disruptions to unstructured regions of proteins distant from the

active site can have functional consequences and/or affect protein stability (Bromberg & Rost, 2009; Teng et al., 2010; Yang et al., 2013). At high concentrations, proteins with intrinsically disordered regions often bind to multiple partners with modest affinity, as the mass action caused by this high concentration overcomes the specificity of interaction (Vavouri et al., 2009). These unfavorable interactions explain the toxicity found by the overexpression of these proteins in some disease states. It is possible the highly flexible and dynamically plastic N-terminal tail of NRMT2 is cause for its tightly controlled, and thus overall low expression throughout tissues. Many proteins that contain intrinsically disordered regions are able to bind a broad range of partners, including other proteins, nucleic acid structures, or even themselves (He et al., 2009). I have shown that removal of the unstructured tail of NRMT2 abolishes its ability to monomethylate target peptides *in vitro*, and this loss of specificity could be attributed to the decreased protein-protein interaction previously conveyed by the N-terminal tail (discussed in Shields et al., 2017).

Potential Roles for N-terminal Monomethylation

I have shown here that stability of the NRMT1 target SETα is significantly decreased upon knockout of NRMT1 compared to control cells (Figure 10 A & C). This phenotype can be rescued by overexpression of NRMT1 alone, but not NRMT2 (Figure 10 A & C). These data indicate that, in regards to regulating protein stability, N-terminal methylation is not functionally redundant with N-terminal trimethylation. This could be due to its smaller size or its inability to

produce a positively charged N-terminus. However, in addition to regulating protein stability, N-terminal trimethylation also regulates protein-DNA interactions and is predicted to regulate protein-protein interactions (Tooley et al., 2010; Chen et al., 2007). N-terminal monomethylation could function redundantly in either of these roles.

We have previously seen that loss of NRMT1 leads to increased migration of MCF-7 cells (Bonsignore, 2015). To test if this migration phenotype, can be rescued by restoration of just N-terminal monomethylation, I repeated the cell migration assay using control MCF-7 cells, NRMT1-knockdown MCF-7 cells (transduced with an shRNA against NRMT1), and NRMT1-knockdown MCF-7 cells rescued with flag-tagged NRMT1 or NRMT2, respectfully. (Figure 11A). Cells were grown to ~70% confluency and scratched with a pipette tip and images were taken at 0, 24, 48, and 72 hours (Figure 11B). As expected, NRMT1 knockdown in MCF-7 cells increased the migratory ability of the cells over that of control. Interestingly, at the 48 and 72-hour time-points, rescue of this migration phenotype is accomplished by both NRMT1 and NRMT2 (Figure 11C). This indicates that while N-terminal monomethylation is not functionally redundant in regards to regulating protein stability, it can functionally replace N-terminal trimethylation when promoting migration. I propose that in this particular phenotype, N-terminal methylation is regulating protein-protein interactions.

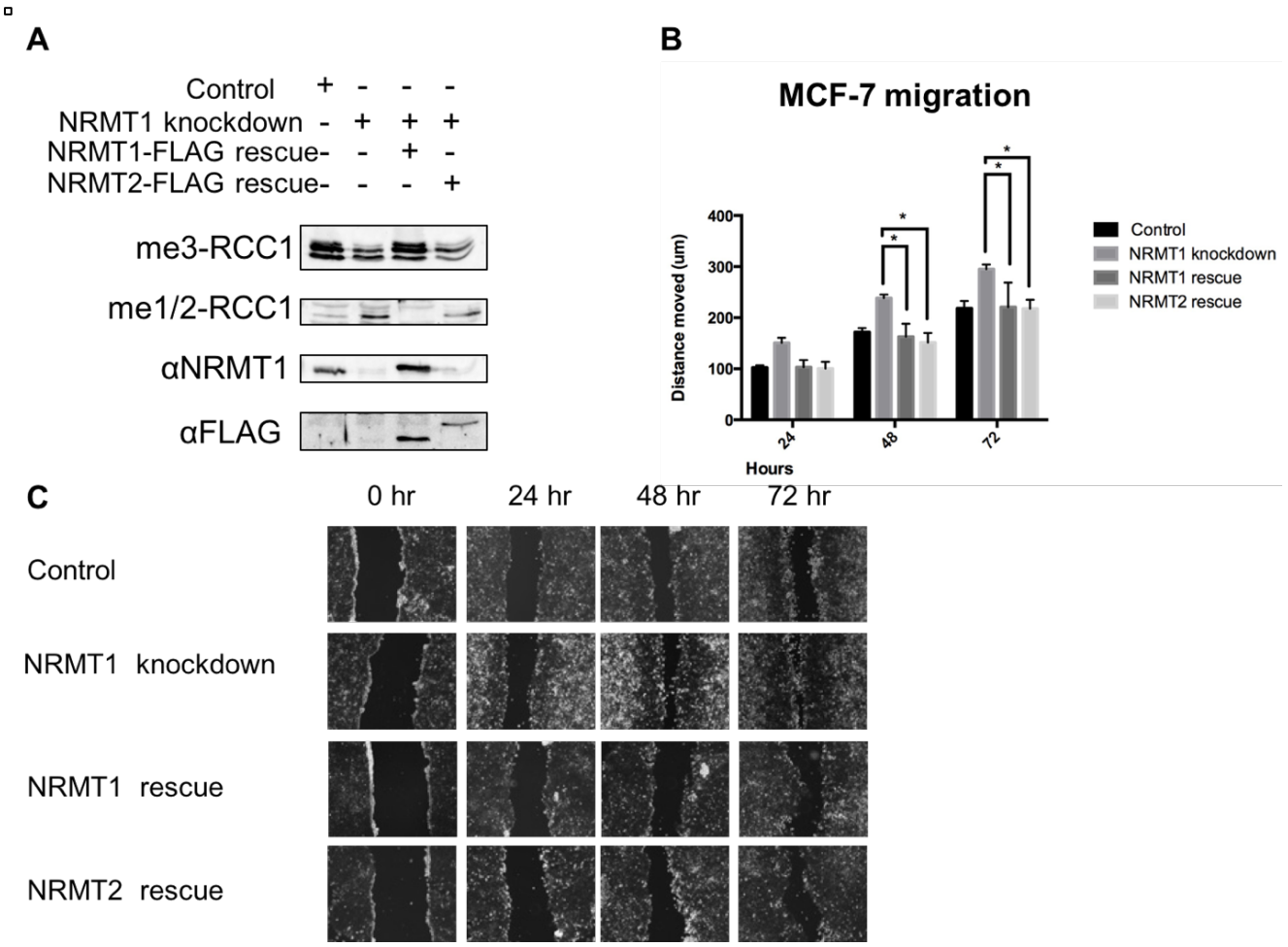
A
Control + - - -
NRMT1 knockdown - + + +
NRMT1-FLAG rescue- - + -
NRMT2-FLAG rescue- - - +
me3-RCC1
me1/2-RCC1
αNRMT1
αFLAG
B
MCF-7 migration
Distance moved (um)
400
300
200
100
0
24
48
72
Hours
Control
NRMT1 knockdown
NRMT1 rescue
NRMT2 rescue
C
0 hr
24 hr
48 hr
72 hr
Control
NRMT1 knockdown
NRMT1 rescue
NRMT2 rescue

Figure 11

Figure 11. NRMT1 knockdown increases migratory potential of MCF-7 breast adenocarcinoma cells. (A) Representative immunoblots showing control MCF-7 lysate (lane 1), NRMT1 knockdown (lane 2), NRMT1 knockdown + flagged-tagged NRMT1 rescue construct (lane3), NRMT1 knockdown + flagged-tagged NRMT2 rescue construct (lane 4). (B) 24, 48, 72-hour time points measuring distanced moved relative to 0 hour. (C) Representative images from each cell line at each time point. Distance moved was determined by measuring total area of no cell invasion in three wells per experiment per day. Values are a combination of three independent experiments and error bars represent SEM. GraphPad Prism was used to determine statistical significance via two-way ANOVA between groups followed by a multiple comparisons test via Tukey's post-hoc analysis. * denotes $p<0.05$

One NRMT1 target, myosin light chain-9 (MYL9), plays a regulatory role in the actin-myosin II complex and is promotes cytoskeletal dynamics and motion in both muscle and non-muscle cells (Ouderkirk & Krendal, 2014). MYL9 has also been implicated in cytoskeletal rearrangement and both overexpression and aberrant activation of MYL9 can promote invasion of cancer-associated fibroblasts and increased metastatic potential of primary carcinoma cells (Calvo et al., 2013; Cermák et al., 2010). We have seen that loss of N-terminal methylation of MYL9 promotes both cell spreading and cell migration (Nevitt, unpublished data), and I attribute the increased migration of MCF7 cells seen with NRMT1 knockdown, at least in part, to altered action of MYL9.

Our lab has recent SILAC mass spectrometry data showing that mono-, and trimethylation of MYL9 both block a significant portion of its protein-protein interactions (Nevitt, unpublished data), and I propose that N-terminal methylation of MYL9 disrupts protein-protein interactions that inhibit the migratory functions of MYL9. Rescue by NRMT2 allows only monomethylation to occur, but this is adequate to block aberrant protein-protein interactions and return cells to a less migratory phenotype.

The third function of N-terminal trimethylation is to regulate protein-DNA interactions (Chen et al., 2007). I predict that N-terminal monomethylation will not be able to rescue this function, as only trimethylation produces a pH-independent charge on the N-terminal residue, facilitating interaction with the negatively charged phosphate backbone of DNA. However, to test this

hypothesis, one could look at the DNA binding ability of mono- vs trimethylated MYL9. We have previously used chromatin immunoprecipitation (ChIP) to show loss of N-terminal methylation reduces the occupancy of MYL9 at the ICAM1 promoter (Nevitt, unpublished data). To see if the level of methylation is important for this promoter occupancy, these experiments can be performed in the HCT116 CRISPR/Cas9 NRMT1 knockout strain rescued with NRMT1 or NRMT2. I hypothesis that restored binding capacity of MYL9 to the ICAM1 promoter will only be seen after NRMT1 rescue, due to the potential for trimethylation and a pH-independent positive charge on the N-terminus of MYL9.

NRMT2 mutations in human cancers

In testing whether NRMT2 catalytic activity was needed to activate NRMT1, I discovered that the V224L NRMT2-null mutant found in human breast cancer actually activated NRMT1 better than wild type NRMT2 (Figure 7E & K). Molecular modeling showed that mutation of Val224 to Leu could impact NRMT2 function via two different mechanisms, first by disrupting substrate binding and subsequent catalytic activity, and second by promoting Asp232 accessibility and subsequent complex formation with NRMT1 (Figure 9). To date, ninety-one NRMT2 missense mutations have been identified in human cancers (Cosmic Catalogue of Somatic Mutations in Cancer), and I decided to see if any additional mutations could predictably alter NRMT1/NRMT2 interactions.

Of the 91 mutations, a number affect residues I have found to be implicated in formation of the NRMT1-NRMT2 heterotrimer (bold, Table I), while

others are found in the active site of NRMT2 near conserved aromatic residues (Petkowski et al., 2013). As noted in Chapter II, modeling predicts that heterotrimer formation of the NRMT1 dimer and NRMT2 monomer is governed, in part, by non-covalent interactions between proximally located resides (Figure 4). Of the seven missense mutations found in human cancers listed in Table I, four affect specific residues deemed important for heterotrimer formation (Figure 5F), and modeling predicts each one of these increases the distance between the wildtype NRMT1 and NRMT2 residues (Figures 12A,C-15A,C) and mutated residues (Figures 12B,D-15B,D). This increase in distance will likely disrupt these non-covalent forces associated with heterotrimer formation, possibly destabilizing the structure.

Table I

Mutation	Primary Tissue
Q67H	**Lung**
F68L	**Large intestine**
T17A	Liver
S131N	Skin
R71T	**Pancreas**
L57S	Large intestine
D232N	**Prostate**

Table I: NRMT2 missense mutations found in human cancers. **Bolded** mutations are incorporating residues implicated in the NRMT1-NRMT2 heterotrimer interaction.

Table II

NRMT2 mutation	WT NRMT1	Distance b/w WT residues (Å)	Distance b/w mutated NRMT2 & WT NRMT1 residues (Å)
Gln67His	Ser44	2.1	5.1
Phe68Leu	Ser39	1.0	2.5
Arg71Thr	Gln50	1.4	10.6
Asp232Asn	Pro83	3.2	5.3

Table II. NRMT2 mutations increase distance between corresponding NRMT1 residues previously implicated in interaction (see figure 4).

Figure 12

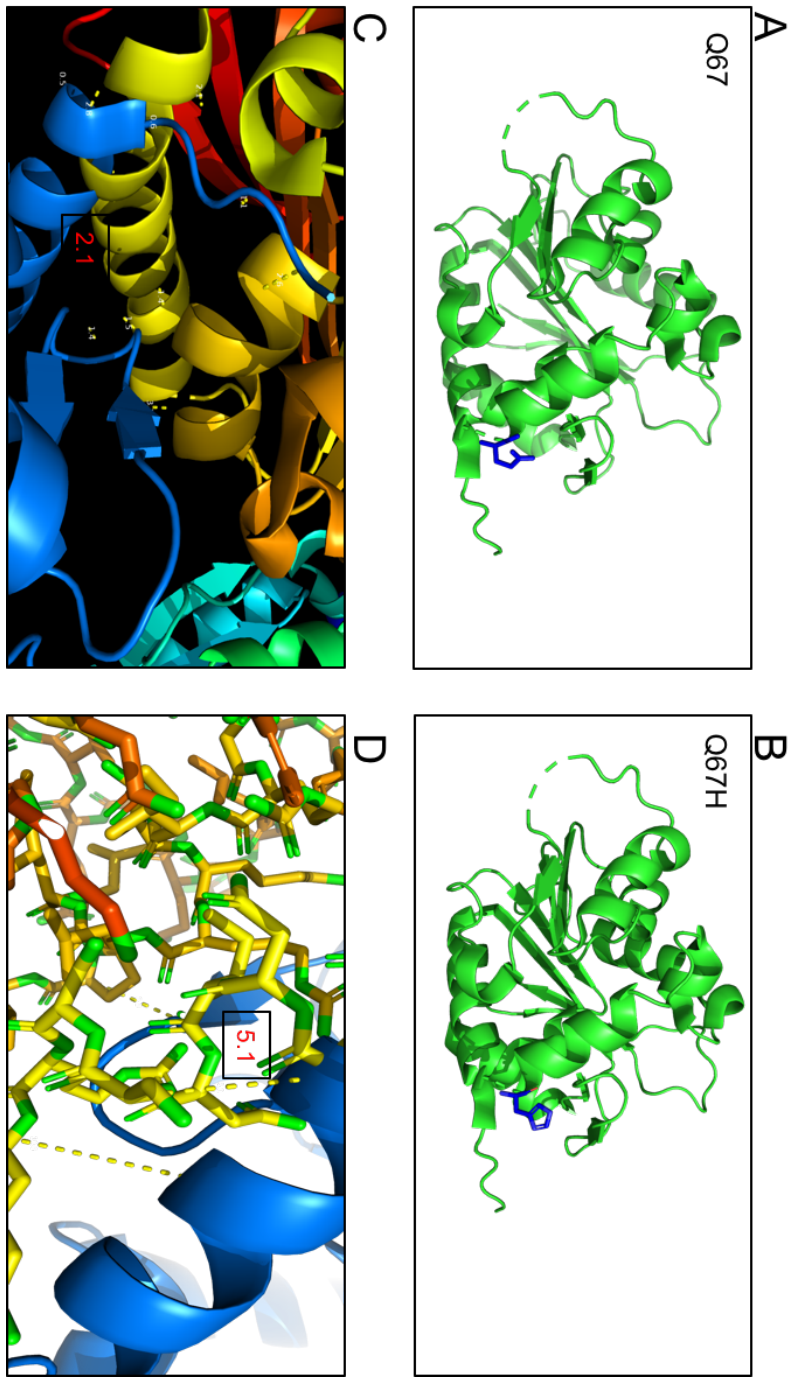

Figure 12. NRMT2 mutations found in cancers. (A) WT NRMT2 possessing glutamine at residue 67 (blue). (B) Q67H mutation (blue) found in lung cancer. (C) Bond length (Å) between NRMT2 D67 and WT NRMT1 S44. (D) The distance measured in (C) is increased to 5.1 Å in the NRMT2 Q67H mutant. Mutational analysis and molecular measurements were produced using the PyMOL Molecular Graphics System, Version 2.0.6 (Schrödinger, LLC). PDB accession numbers are 2EX4 (NRMT1) and 5UBB (NRMT2).

Figure 13

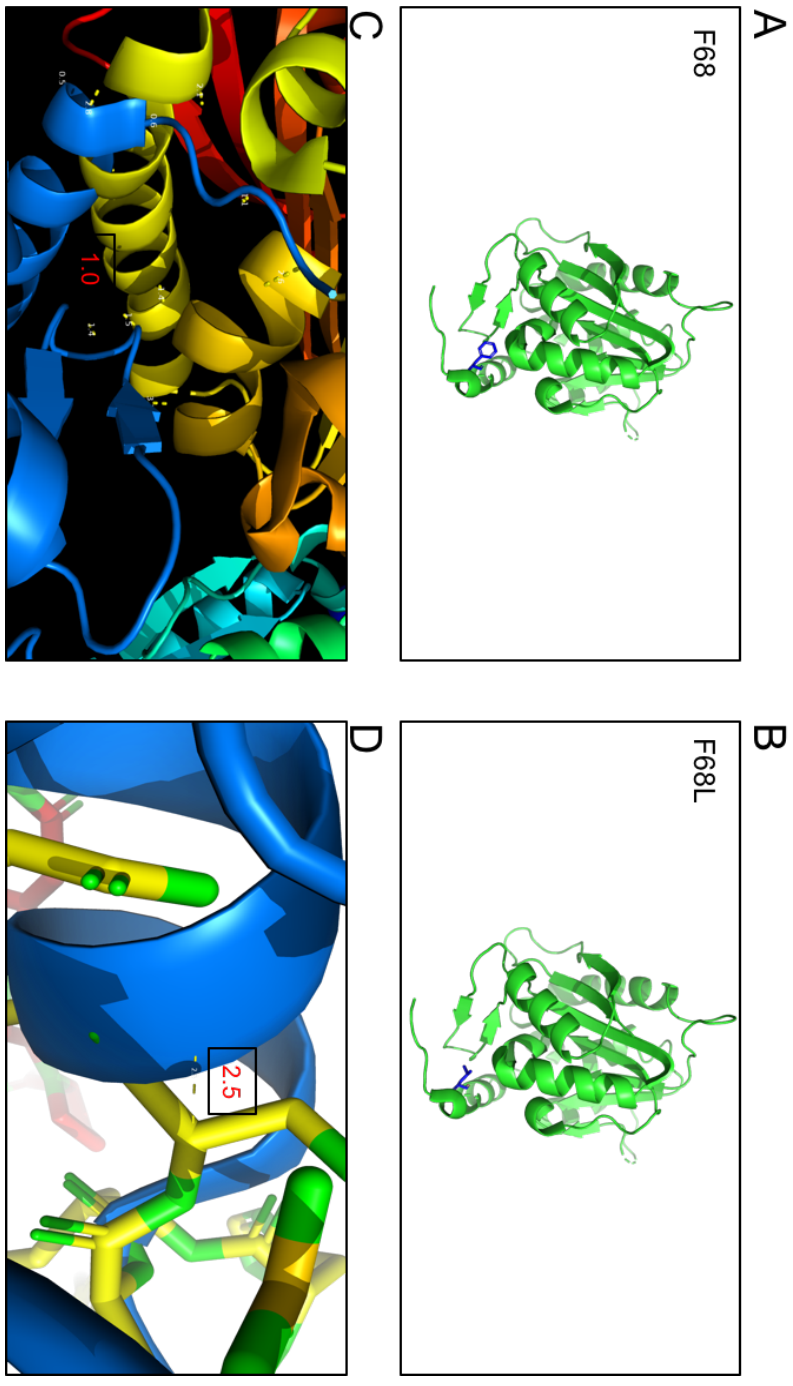

Figure 13. NRMT2 mutations found in cancers. (A) WT NRMT2 possessing phenylalanine at residue 68 (blue). (B) F68L (blue) found in pancreatic cancer. (C) Bond length (Å) between NRMT2 F68 and WT NRMT1 S39. (D) The distance measured in (C) is increased to 2.5 Å in the NRMT2 F68L mutant. Mutational analysis and molecular measurements were produced using the PyMOL Molecular Graphics System, Version 2.0.6 (Schrödinger, LLC). PDB accession numbers are 2EX4 (NRMT1) and 5UBB (NRMT2).

Figure 14

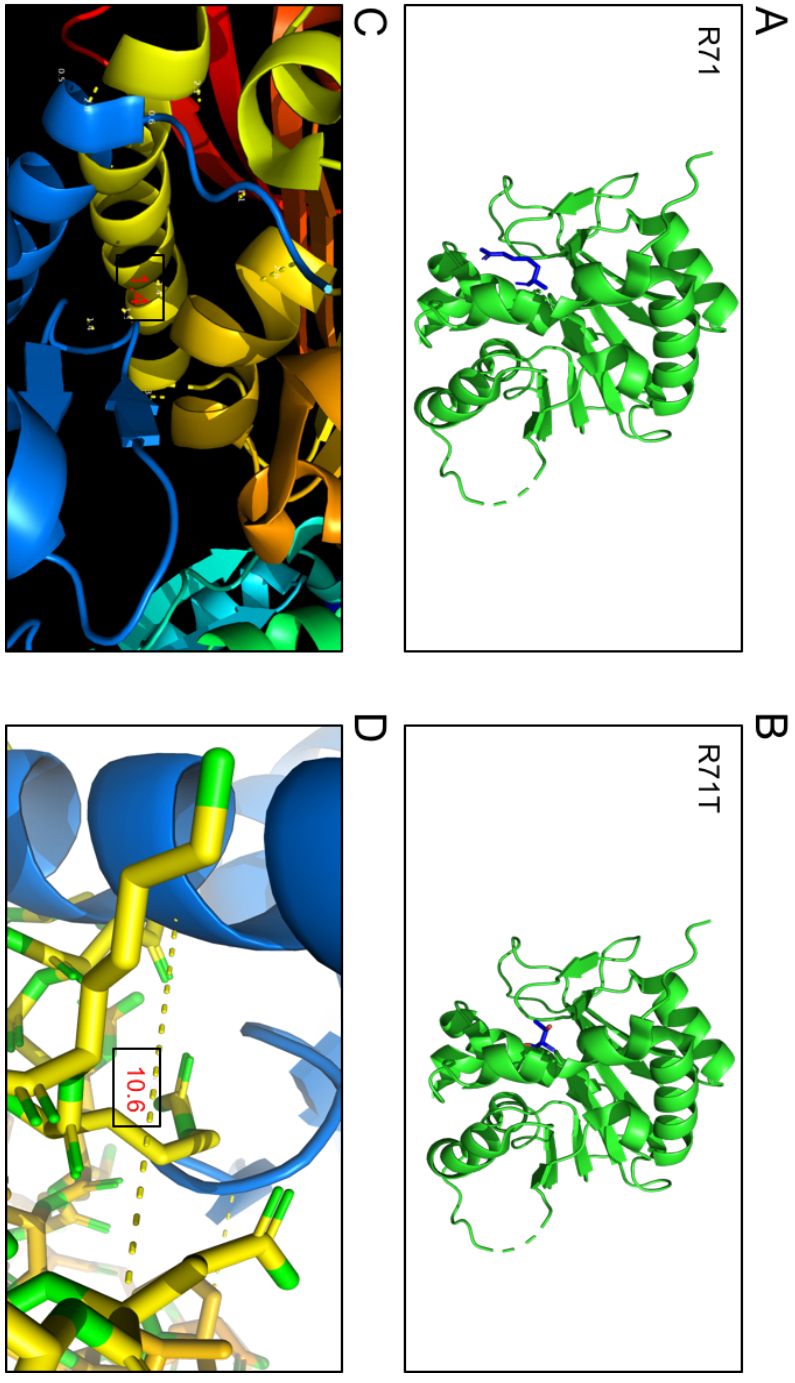

Figure 14. NRMT2 mutations found in cancers. (A) WT NRMT2 possessing arginine at residue 71 (blue). (B) R71T (blue) found in pancreatic cancer. (C) Bond length (Å) between NRMT2 R71 and WT NRMT1 Q50. (D) The distance measured in (C) is increased to 10.6 Å in the NRMT2 R71T mutant. Mutational analysis and molecular measurements were produced using the PyMOL Molecular Graphics System, Version 2.0.6 (Schrödinger, LLC). PDB accession numbers are 2EX4 (NRMT1) and 5UBB (NRMT2).

Figure 15

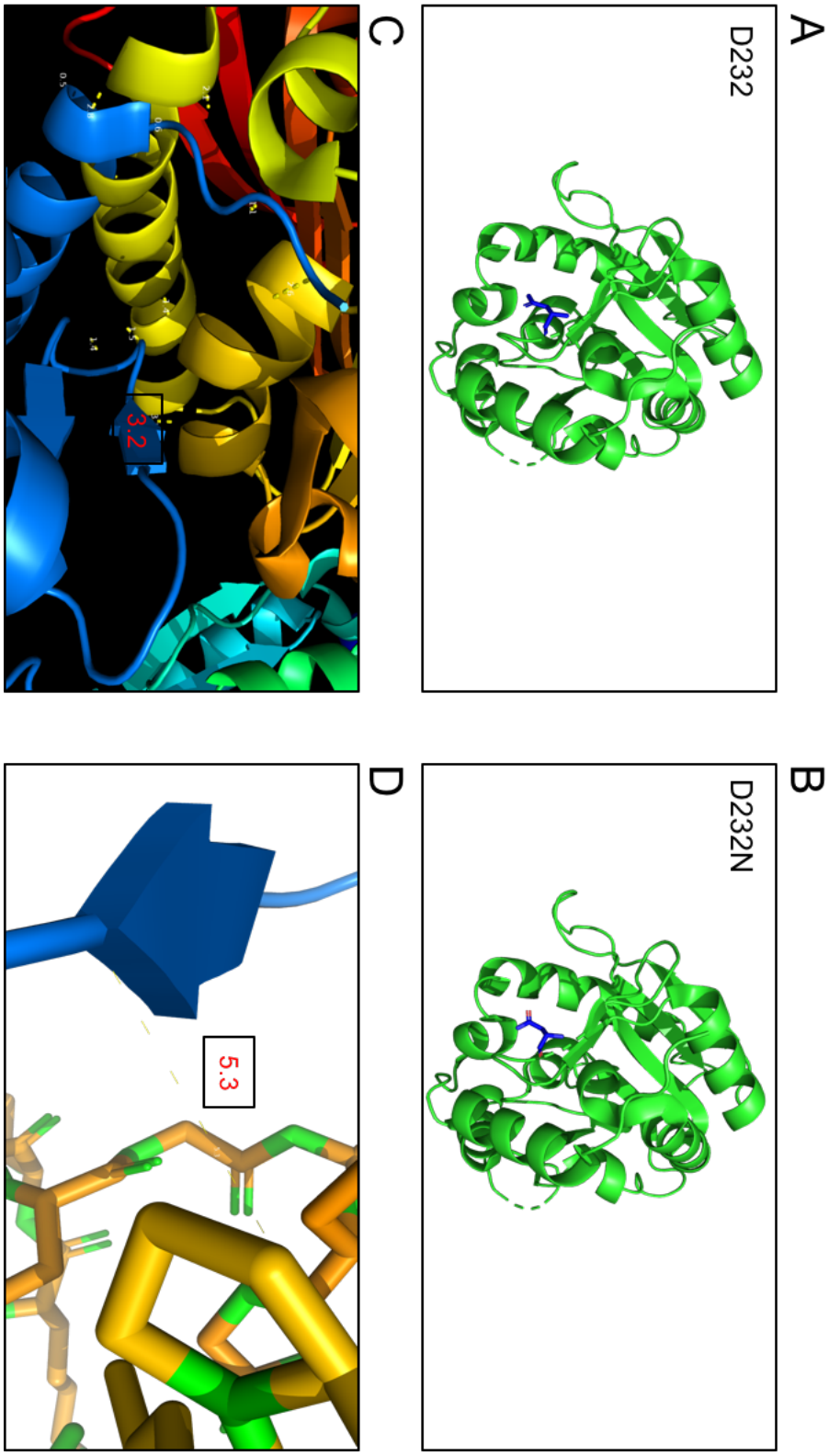

Figure 15. NRMT2 mutations found in cancers. (A) WT NRMT2 possessing aspartic acid at residue 232 (blue). (B) D232N mutation (blue) found in prostate cancer. (C) Bond length (Å) between NRMT2 D232 and WT NRMT1 P83. (D) The distance measured in (C) is increased to 5.3 Å in the NRMT2 D232N mutant. Mutational analysis and molecular measurements were produced using the PyMOL Molecular Graphics System, Version 2.0.6 (Schrödinger, LLC). PDB accession numbers are 2EX4 (NRMT1) and 5UBB (NRMT2).

Missense mutations, including those outside the active site, have been widely implicated in the alteration of protein structure and stability (Ode et al., 2007; Lorch et al., 2000; De Cristofaro et al., 2006). Changes of residues, especially those altering polarity or charge, can direct conformational changes in the native folding of the protein. These include disruption of salt bridges and hydrogen bonds, which facilitate potential interactome alterations. Additionally, single aberrant amino acid substitutions have been shown to disrupt protein-protein interactions and substrate binding. Ung et al have shown a Glu230 to Gln mutation in the cAMP-dependent protein kinase catalytic subunit leaves the enzyme with physical properties similar to that of the wildtype, but with the inability to form a native ternary complex with MgATP and a protein kinase inhibitor (Ung et al., 2006). Protein function alteration may direct or as a result of an alteration of protein stability conveyed by a missense mutation. Of the number of known disease-causing missense mutations, 83% result in a change of protein stability (Wang & Moult, 2001).

I have shown that NRMT1 is structurally dependent upon the presence of NRMT2 to avoid premature degradation (Figure 7). The aforementioned NRMT2 mutations found in human cancers all decrease the proximity of key interacting residues I predict stabilize the NRMT1/NRMT2 complex. With this decrease in stability, likely comes an increase in protein degradation. If the heterotrimer complex is degrading prematurely, it's unlikely that key substrates are being properly trimethylated. As noted, N-terminal trimethylation produces a pH-

independent positive charge on substrates and functions to increase interaction with the positively-charged substrates and negatively-charged phosphate backbone of DNA. The inability of substrates to be trimethylated, facilitated by the early degradation of the NRMT heterotrimer, could cause misregulation of key protein-protein or protein-DNA interactions implicated in the suppression of tumorigenesis, thus acting as a driver mutation for these small subsets of cancers. This would be relatively straightforward to examine experimentally, although a full NRMT2 knockout cell line would need to be initially developed. A number of mutagenesis experiments could be carried out to produce the Q67H, F68L, R71T, and D232N NRMT2 mutants. These could be co-expressed, along with WT NRMT1 in a NRMT2-null cell line and NRMT1 stability could be measured via cycloheximide, similar to Figure 6 in Chapter II.

Computational molecular mapping of disease causing mutations onto known protein structures and free energy perturbation (FEP) calculation are additional *in silico* methods of determining structurally and functionally important sites and the effects of mutations on protein stability (Dimmic et al., 2005; Dixit et al., 2009). FEP takes into account the energies between covalently bonded atoms, as well as the geometry and torsion forces between WT and mutated residues in comparison to their surrounding environment to deduce a comparable value of electrostatic energy and subsequent stability on the entire molecule (Dixit et al., 2009). While these techniques are processor-heavy and require a robust learning curve, they are able to generate large amounts of data that can subsequently be used to develop hypotheses and direct further bench work.

The COSMIC database also lists three NRMT2 missense mutations found in residues not previously implicated in the heterotrimer stability. One of these, S131N, slightly increases the size of the SAM-binding pocket, near which the WT serine is positioned. This marginal increase in size of the SAM-binding motif could have detrimental functional consequences on an enzyme that already has very select and relatively low catalytic abilities. The inability of NRMT2 to stabilize SAM and thus utilize it for monomethylation will be of key interest as the tissue- and developmentally-specific roles of monomethylation are deduced.

Interestingly, the two other missense mutations listed on the COSMIC database, T17A and L57S, are located on the 60 amino acid, free N-terminal tail of the enzyme. As noted in the previous chapters, this tail is the most distinct feature of NRMT2 when compared to NRMT1, and floats freely from the N-terminal end (as such, it does not readily crystalize and is missing from PDB accession 5UBB) (Petkowski et al., 2013). We have shown that removal of the N-terminal tail abolishes all methylation activity of NRMT2 (discussed in Shields et al., 2017). It seems unlikely that the tail functions in NRMT1/NRMT2 trimerization, as my co-immunoprecipitation data show its inclusion seems to disrupt binding (Figure 6). Similar to what was described above, experiments on protein stability and heterotrimer formation in the presence of WT NRMT1 and tailless NRMT2 could provide some insight into this phenomenon.

NRMT1 and NRMT2 share a general consensus sequences for substrates, but I have shown there are some distinct differences (Figure 8), and it is possible this tail regulates these differences. The NRMT2 V224L mutant has

no methyltransferase activity of its own. However, when combined *in vitro* with NRMT1, it reduces the K_M of binding the SPK-RCC1 peptide around 10-fold versus NRMT1 alone, and around 7-fold versus the combination of NRMT1 and WT NRMT2. An additional significant outcome, though less pronounced, is seen when binding the SSK-MYL9 peptide. Though the V224L mutation is not in the N-terminal tail, it is possible the T17A and L57S mutations are increasing or decreasing substrate-binding efficiency in a similar manner. Similar *in vitro* methyltransferase experiments using recombinantly-produced NRMT2 T17A and NRMT2 L57S, alone and combined with WT NRMT1, would give evidence into any changes in binding efficiency conveyed by these mutations. It is also possible that the N-terminal tail is indeed cause for increasing the binding affinity of NRMT2 for particular substrates. Experiments using circular dichroism or isothermal calorimetry would yield information on binding and dissociation of Wildtype, as well as mutant NRMT2, with and without the presence of NRMT1, on any number of selected substrates.

In my initial model, I predicted that the behavior of NRMT1 and NRMT2 would be similar to that of the class I methyltransferases METTL3 and METTL14 (Liu, 2014), where a heterodimeric complex would form with the less catalytically active NRMT2 promoting N-terminal trimethylation via NRMT1 (see Figure 1). Experimentally, I have demonstrated that while NRMT1 and NRMT2 do physically interact, they do so as a heterotrimeric species consisting of a NRMT1 dimer and NRMT2 monomer. Furthermore, I have shown that NRMT1 and NRMT2, individually, have catalytic activity. However, the catalytic activity of

NRMT2 is not necessary for the increased trimethylation by NRMT1. Instead, I have shown the promotion of N-terminal trimethylation to be dependent on the structural presence of NRMT2 within the heterotrimer complex. (Figure 16).

Figure 16

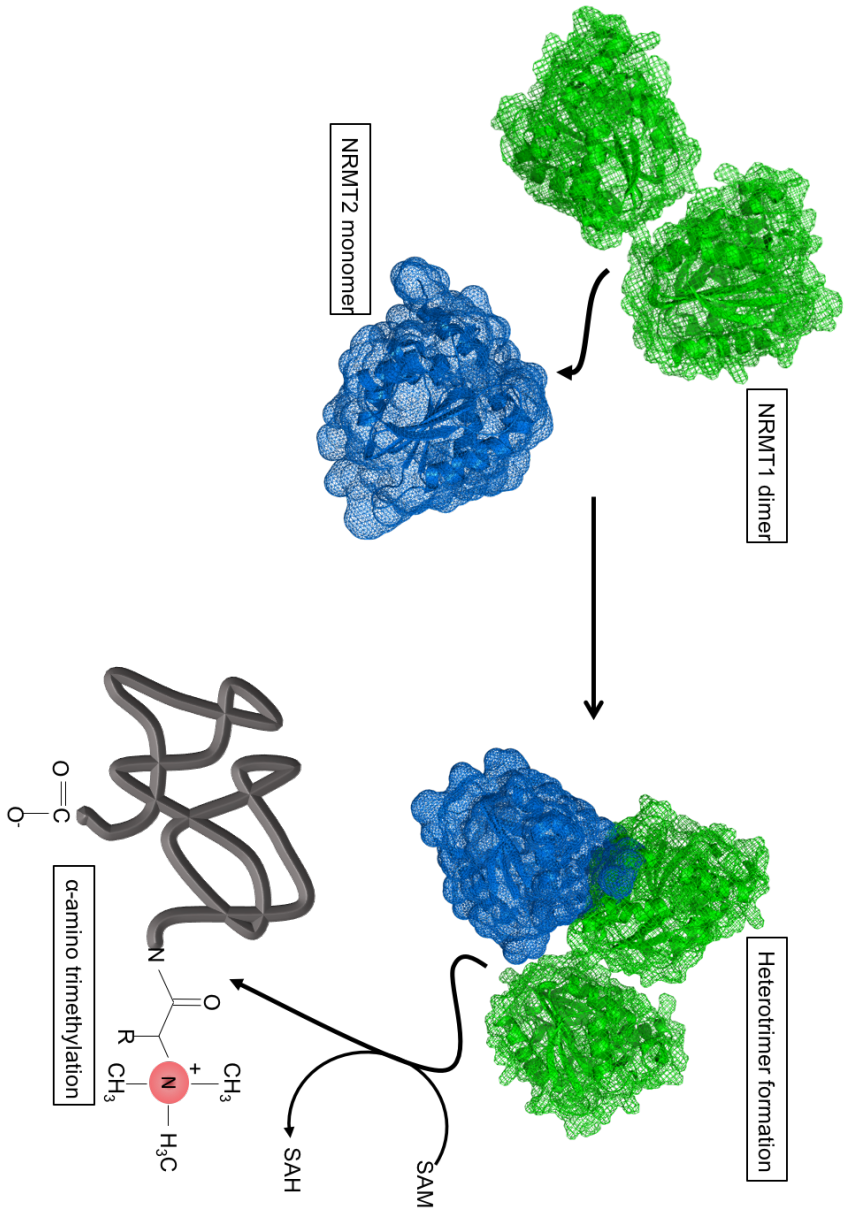
NRMT2 monomer
NRMT1 dimer
Heterotrimer formation
α-amino trimethylation
SAM
SAH

Figure 16. Revised model of NRMT1 and NRMT2 interaction. A NRMT1 homodimer and NRMT2 monomer physically interact to promote stability and N-terminal trimethylation.

The methyltransferome, like other post-translational modifications, adds yet another layer of diversity beyond the central dogma of molecular biology. The many facets of “readers,” “writers,” and “erasers” of methylation will continue to be deduced and only more-so as the combination of computational chemistry, structural biology, and biochemistry gets ever more advanced. The work presented in this dissertation is but a small, albeit integral, part of vast landscape of chemical modifications to macromolecules that no doubt has an impact on health and disease. As the experiments proposed in chapter III are completed, the impact N-terminal methylation has on development, physiology, and the promotion or suppression of pathogenic cell growth will become more illuminated.

REFERENCES

(2008). "Comprehensive genomic characterization defines human glioblastoma genes and core pathways." Nature **455**(7216): 1061-1068.

Albert, M. and K. Helin (2010). "Histone methyltransferases in cancer." Semin Cell Dev Biol **21**(2): 209-220.

Alexandrov, A., I. Chernyakov, W. Gu, S. L. Hiley, T. R. Hughes, E. J. Grayhack and E. M. Phizicky (2006). "Rapid tRNA decay can result from lack of nonessential modifications." Mol Cell **21**(1): 87-96.

Alexandrov, A., M. R. Martzen and E. M. Phizicky (2002). "Two proteins that form a complex are required for 7-methylguanosine modification of yeast tRNA." Rna **8**(10): 1253-1266.

Allfrey, V. G., R. Faulkner and A. E. Mirsky (1964). "ACETYLATION AND METHYLATION OF HISTONES AND THEIR POSSIBLE ROLE IN THE REGULATION OF RNA SYNTHESIS." Proc Natl Acad Sci U S A **51**: 786-794.

Ambler, R. P. and M. W. Rees (1959). "Epsilon-N-Methyl-lysine in bacterial flagellar protein." Nature **184**: 56-57.

Anantharaman, V., E. V. Koonin and L. Aravind (2002). "SPOUT: a class of methyltransferases that includes spoU and trmD RNA methylase superfamilies, and novel superfamilies of predicted prokaryotic RNA methylases." J Mol Microbiol Biotechnol **4**(1): 71-75.

Antonysamy, S., B. Condon, Z. Druzina, J. B. Bonanno, T. Gheyi, F. Zhang, I. MacEwan, A. Zhang, S. Ashok, L. Rodgers, M. Russell and J. Gately Luz (2013). "Structural context of disease-associated mutations and putative mechanism of autoinhibition revealed by X-ray crystallographic analysis of the EZH2-SET domain." PLoS One **8**(12): e84147.

Baldwin, G. S. and P. R. Carnegie (1971). "Specific enzymic methylation of an arginine in the experimental allergic encephalomyelitis protein from human myelin." Science **171**(3971): 579-581.

Bannister, A. J., P. Zegerman, J. F. Partridge, E. A. Miska, J. O. Thomas, R. C. Allshire and T. Kouzarides (2001). "Selective recognition of methylated lysine 9 on histone H3 by the HP1 chromo domain." Nature **410**(6824): 120-124.
Barski, A., S. Cuddapah, K. Cui, T. Y. Roh, D. E. Schones, Z. Wang, G. Wei, I. Chepelev and K. Zhao (2007). "High-resolution profiling of histone methylations in the human genome." Cell **129**(4): 823-837.

Barth, T. K. and A. Imhof (2010). "Fast signals and slow marks: the dynamics of histone modifications." Trends Biochem Sci **35**(11): 618-626.

Beaver, J. E. and M. L. Waters (2016). "Molecular Recognition of Lys and Arg Methylation." ACS Chem Biol **11**(3): 643-653.

Bedford, M. T. (2007). "Arginine methylation at a glance." J Cell Sci **120**(Pt 24): 4243-4246.

Beguelin, W., R. Popovic, M. Teater, Y. Jiang, K. L. Bunting, M. Rosen, H. Shen, S. N. Yang, L. Wang, T. Ezponda, E. Martinez-Garcia, H. Zhang, Y. Zheng, S. K. Verma, M. T. McCabe, H. M. Ott, G. S. Van Aller, R. G. Kruger, Y. Liu, C. F. McHugh, D. W. Scott, Y. R. Chung, N. Kelleher, R. Shaknovich, C. L. Creasy, R. D. Gascoyne, K. K. Wong, L. Cerchietti, R. L. Levine, O. Abdel-Wahab, J. D. Licht, O. Elemento and A. M. Melnick (2013). "EZH2 is required for germinal center formation and somatic EZH2 mutations promote lymphoid transformation." Cancer Cell **23**(5): 677-692.

Bernstein, B. E., E. L. Humphrey, R. L. Erlich, R. Schneider, P. Bouman, J. S. Liu, T. Kouzarides and S. L. Schreiber (2002). "Methylation of histone H3 Lys 4 in coding regions of active genes." Proc Natl Acad Sci U S A **99**(13): 8695-8700.

Bernstein, B. E., T. S. Mikkelsen, X. Xie, M. Kamal, D. J. Huebert, J. Cuff, B. Fry, A. Meissner, M. Wernig, K. Plath, R. Jaenisch, A. Wagschal, R. Feil, S. L. Schreiber and E. S. Lander (2006). "A bivalent chromatin structure marks key developmental genes in embryonic stem cells." Cell **125**(2): 315-326.

Bjork, G. R., K. Jacobsson, K. Nilsson, M. J. Johansson, A. S. Bystrom and O. P. Persson (2001). "A primordial tRNA modification required for the evolution of life?" Embo j **20**(1-2): 231-239.

Bloom, J., V. Amador, F. Bartolini, G. DeMartino and M. Pagano (2003). "Proteasome-mediated degradation of p21 via N-terminal ubiquitinylation." Cell **115**(1): 71-82.

Blus, B. J., K. Wiggins and S. Khorasanizadeh (2011). "Epigenetic virtues of chromodomains." Crit Rev Biochem Mol Biol **46**(6): 507-526.

Boal, A. K., T. L. Grove, M. I. McLaughlin, N. H. Yennawar, S. J. Booker and A. C. Rosenzweig (2011). "Structural basis for methyl transfer by a radical SAM enzyme." Science **332**(6033): 1089-1092.
Bokar, J. A., M. E. Shambaugh, D. Polayes, A. G. Matera and F. M. Rottman (1997). "Purification and cDNA cloning of the AdoMet-binding subunit of the human mRNA (N6-adenosine)-methyltransferase." Rna **3**(11): 1233-1247.

Bostick, M., J. K. Kim, P. O. Esteve, A. Clark, S. Pradhan and S. E. Jacobsen (2007). "UHRF1 plays a role in maintaining DNA methylation in mammalian cells." Science **317**(5845): 1760-1764.

Botuyan, M. V., J. Lee, I. M. Ward, J. E. Kim, J. R. Thompson, J. Chen and G. Mer (2006). "Structural basis for the methylation state-specific recognition of histone H4-K20 by 53BP1 and Crb2 in DNA repair." Cell **127**(7): 1361-1373.

Bourgeois, G., J. Marcoux, J. M. Saliou, S. Cianferani and M. Graille (2017). "Activation mode of the eukaryotic m2G10 tRNA methyltransferase Trm11 by its partner protein Trm112." Nucleic Acids Res **45**(4): 1971-1982.

Bratkowski, M., X. Yang and X. Liu (2017). "Polycomb repressive complex 2 in an autoinhibited state." J Biol Chem **292**(32): 13323-13332.

Briggs, S. D., M. Bryk, B. D. Strahl, W. L. Cheung, J. K. Davie, S. Y. Dent, F. Winston and C. D. Allis (2001). "Histone H3 lysine 4 methylation is mediated by Set1 and required for cell growth and rDNA silencing in Saccharomyces cerevisiae." Genes Dev **15**(24): 3286-3295.

Bromberg, Y. and B. Rost (2009). "Correlating protein function and stability through the analysis of single amino acid substitutions." BMC Bioinformatics **10 Suppl 8**: S8.

Brostoff, S. and E. H. Eylar (1971). "Localization of methylated arginine in the A1 protein from myelin." Proc Natl Acad Sci U S A **68**(4): 765-769.

Brown, J. L. and W. K. Roberts (1976). "Evidence that approximately eighty per cent of the soluble proteins from Ehrlich ascites cells are Nalpha-acetylated." J Biol Chem **251**(4): 1009-1014.

Buhr, N., C. Carapito, C. Schaeffer, E. Kieffer, A. Van Dorsselaer and S. Viville (2008). "Nuclear proteome analysis of undifferentiated mouse embryonic stem and germ cells." Electrophoresis **29**(11): 2381-2390.

Bujnicki, J. M., M. Feder, M. Radlinska and R. M. Blumenthal (2002). "Structure prediction and phylogenetic analysis of a functionally diverse family of proteins homologous to the MT-A70 subunit of the human mRNA:m(6)A methyltransferase." J Mol Evol **55**(4): 431-444.

Byvoet, P., G. R. Shepherd, J. M. Hardin and B. J. Noland (1972). "The distribution and turnover of labeled methyl groups in histone fractions of cultured mammalian cells." Arch Biochem Biophys **148**(2): 558-567.

Caceres, T. B., A. Thakur, O. M. Price, N. Ippolito, J. Li, J. Qu, O. Acevedo and J. M. Hevel (2018). "Phe71 in Type III Trypanosomal Protein Arginine Methyltransferase 7 (TbPRMT7) Restricts the Enzyme to Monomethylation." Biochemistry **57**(8): 1349-1359.

Cai, Q., L. Fu, Z. Wang, N. Gan, X. Dai and Y. Wang (2014). "alpha-N-methylation of damaged DNA-binding protein 2 (DDB2) and its function in nucleotide excision repair." J Biol Chem **289**(23): 16046-16056.

Cai, X., X. Wang, C. Cao, Y. Gao, S. Zhang, Z. Yang, Y. Liu, X. Zhang, W. Zhang and L. Ye (2018). "HBXIP-elevated methyltransferase METTL3 promotes the progression of breast cancer via inhibiting tumor suppressor let-7g." Cancer Lett **415**: 11-19.

Calvo, F., N. Ege, A. Grande-Garcia, S. Hooper, R. P. Jenkins, S. I. Chaudhry, K. Harrington, P. Williamson, E. Moeendarbary, G. Charras and E. Sahai (2013). "Mechanotransduction and YAP-dependent matrix remodelling is required for the generation and maintenance of cancer-associated fibroblasts." Nat Cell Biol **15**(6): 637-646.

Cantara, W. A., P. F. Crain, J. Rozenski, J. A. McCloskey, K. A. Harris, X. Zhang, F. A. Vendeix, D. Fabris and P. F. Agris (2011). "The RNA Modification Database, RNAMDB: 2011 update." Nucleic Acids Res **39**(Database issue): D195-201.

Cao, R. and Y. Zhang (2004). "SUZ12 is required for both the histone methyltransferase activity and the silencing function of the EED-EZH2 complex." Mol Cell **15**(1): 57-67.

Carr, S. M., S. Munro, B. Kessler, U. Oppermann and N. B. La Thangue (2011). "Interplay between lysine methylation and Cdk phosphorylation in growth control by the retinoblastoma protein." Embo j **30**(2): 317-327.

Cermak, V., J. Kosla, J. Plachy, K. Trejbalova, J. Hejnar and M. Dvorak (2010). "The transcription factor EGR1 regulates metastatic potential of v-src transformed sarcoma cells." Cell Mol Life Sci **67**(20): 3557-3568.

Chang, C. N., M. Schwartz and F. N. Chang (1976). "Identification and characterization of a new methylated amino acid in ribosomal protein L33 of Escherichia coli." Biochem Biophys Res Commun **73**(2): 233-239.

Chauhan, C., C. B. Zraly, M. Parilla, M. O. Diaz and A. K. Dingwall (2012). "Histone recognition and nuclear receptor co-activator functions of Drosophila cara mitad, a homolog of the N-terminal portion of mammalian MLL2 and MLL3." Development **139**(11): 1997-2008.

Chen, J., Y. Sun, X. Xu, D. Wang, J. He, H. Zhou, Y. Lu, J. Zeng, F. Du, A. Gong and M. Xu (2017). "YTH domain family 2 orchestrates epithelial-mesenchymal transition/proliferation dichotomy in pancreatic cancer cells." Cell Cycle **16**(23): 2259-2271.

Chen, T., T. L. Muratore, C. E. Schaner-Tooley, J. Shabanowitz, D. F. Hunt and I. G. Macara (2007). "N-terminal alpha-methylation of RCC1 is necessary for stable chromatin association and normal mitosis." Nat Cell Biol **9**(5): 596-603.
Cheng, X. (1995). "Structure and function of DNA methyltransferases." Annu Rev Biophys Biomol Struct **24**: 293-318.

Cheng, X. and R. M. Blumenthal (2008). "Mammalian DNA methyltransferases: a structural perspective." Structure **16**(3): 341-350.

Cheng, X., S. Kumar, J. Posfai, J. W. Pflugrath and R. J. Roberts (1993). "Crystal structure of the HhaI DNA methyltransferase complexed with S-adenosyl-L-methionine." Cell **74**(2): 299-307.

Chi, P., C. D. Allis and G. G. Wang (2010). "Covalent histone modifications--miswritten, misinterpreted and mis-erased in human cancers." Nat Rev Cancer **10**(7): 457-469.

Chinenov, Y. (2002). "A second catalytic domain in the Elp3 histone acetyltransferases: a candidate for histone demethylase activity?" Trends Biochem Sci **27**(3): 115-117.

Cho, H. S., S. Hayami, G. Toyokawa, K. Maejima, Y. Yamane, T. Suzuki, N. Dohmae, M. Kogure, D. Kang, D. E. Neal, B. A. Ponder, H. Yamaue, Y. Nakamura and R. Hamamoto (2012). "RB1 methylation by SMYD2 enhances cell cycle progression through an increase of RB1 phosphorylation." Neoplasia **14**(6): 476-486.

Cho, H. S., J. D. Kelly, S. Hayami, G. Toyokawa, M. Takawa, M. Yoshimatsu, T. Tsunoda, H. I. Field, D. E. Neal, B. A. Ponder, Y. Nakamura and R. Hamamoto (2011). "Enhanced expression of EHMT2 is involved in the proliferation of cancer cells through negative regulation of SIAH1." Neoplasia **13**(8): 676-684.

Cho, H. S., T. Shimazu, G. Toyokawa, Y. Daigo, Y. Maehara, S. Hayami, A. Ito, K. Masuda, N. Ikawa, H. I. Field, E. Tsuchiya, S. Ohnuma, B. A. Ponder, M. Yoshida, Y. Nakamura and R. Hamamoto (2012). "Enhanced HSP70 lysine

methylation promotes proliferation of cancer cells through activation of Aurora kinase B." Nat Commun **3**: 1072.

Cho, H. S., T. Suzuki, N. Dohmae, S. Hayami, M. Unoki, M. Yoshimatsu, G. Toyokawa, M. Takawa, T. Chen, J. K. Kurash, H. I. Field, B. A. Ponder, Y. Nakamura and R. Hamamoto (2011). "Demethylation of RB regulator MYPT1 by histone demethylase LSD1 promotes cell cycle progression in cancer cells." Cancer Res **71**(3): 655-660.

Cho, H. S., G. Toyokawa, Y. Daigo, S. Hayami, K. Masuda, N. Ikawa, Y. Yamane, K. Maejima, T. Tsunoda, H. I. Field, J. D. Kelly, D. E. Neal, B. A. Ponder, Y. Maehara, Y. Nakamura and R. Hamamoto (2012). "The JmjC domain-containing histone demethylase KDM3A is a positive regulator of the G1/S transition in cancer cells via transcriptional regulation of the HOXA1 gene." Int J Cancer **131**(3): E179-189.

Chuikov, S., J. K. Kurash, J. R. Wilson, B. Xiao, N. Justin, G. S. Ivanov, K. McKinney, P. Tempst, C. Prives, S. J. Gamblin, N. A. Barlev and D. Reinberg (2004). "Regulation of p53 activity through lysine methylation." Nature **432**(7015): 353-360.

Ciferri, C., G. C. Lander, A. Maiolica, F. Herzog, R. Aebersold and E. Nogales (2012). "Molecular architecture of human polycomb repressive complex 2." Elife **1**: e00005.

Cihak, A. (1974). "Biological effects of 5-azacytidine in eukaryotes." Oncology **30**(5): 405-422.

Clarke, S. (1993). "Protein methylation." Curr Opin Cell Biol **5**(6): 977-983.
Cleary, S. P., W. R. Jeck, X. Zhao, K. Chen, S. R. Selitsky, G. L. Savich, T. X. Tan, M. C. Wu, G. Getz, M. S. Lawrence, J. S. Parker, J. Li, S. Powers, H. Kim, S. Fischer, M. Guindi, A. Ghanekar and D. Y. Chiang (2013). "Identification of driver genes in hepatocellular carcinoma by exome sequencing." Hepatology **58**(5): 1693-1702.

Cowan, L. A., S. Talwar and A. S. Yang (2010). "Will DNA methylation inhibitors work in solid tumors? A review of the clinical experience with azacitidine and decitabine in solid tumors." Epigenomics **2**(1): 71-86.

Crea, F., E. M. Hurt and W. L. Farrar (2010). "Clinical significance of Polycomb gene expression in brain tumors." Mol Cancer **9**: 265.

Cui, Q., H. Shi, P. Ye, L. Li, Q. Qu, G. Sun, G. Sun, Z. Lu, Y. Huang, C. G. Yang, A. D. Riggs, C. He and Y. Shi (2017). "m(6)A RNA Methylation Regulates the Self-Renewal and Tumorigenesis of Glioblastoma Stem Cells." Cell Rep **18**(11): 2622-2634.

Dai, X., K. Otake, C. You, Q. Cai, Z. Wang, H. Masumoto and Y. Wang (2013). "Identification of novel alpha-n-methylation of CENP-B that regulates its binding to the centromeric DNA." J Proteome Res **12**(9): 4167-4175.

Dapp, M. J., C. L. Clouser, S. Patterson and L. M. Mansky (2009). "5-Azacytidine can induce lethal mutagenesis in human immunodeficiency virus type 1." J Virol **83**(22): 11950-11958.

de Almeida, S. F., A. R. Grosso, F. Koch, R. Fenouil, S. Carvalho, J. Andrade, H. Levezinho, M. Gut, D. Eick, I. Gut, J. C. Andrau, P. Ferrier and M. Carmo-Fonseca (2011). "Splicing enhances recruitment of methyltransferase HYPB/Setd2 and methylation of histone H3 Lys36." Nat Struct Mol Biol **18**(9): 977-983.

de Boer, J., J. O. Andressoo, J. de Wit, J. Huijmans, R. B. Beems, H. van Steeg, G. Weeda, G. T. van der Horst, W. van Leeuwen, A. P. Themmen, M. Meradji and J. H. Hoeijmakers (2002). "Premature aging in mice deficient in DNA repair and transcription." Science **296**(5571): 1276-1279.

De Cristofaro, R., A. Carotti, S. Akhavan, R. Palla, F. Peyvandi, C. Altomare and P. M. Mannucci (2006). "The natural mutation by deletion of Lys9 in the thrombin A-chain affects the pKa value of catalytic residues, the overall enzyme's stability and conformational transitions linked to Na+ binding." Febs j **273**(1): 159-169.

de Laat, W. L., N. G. Jaspers and J. H. Hoeijmakers (1999). "Molecular mechanism of nucleotide excision repair." Genes Dev **13**(7): 768-785.

Debler, E. W., K. Jain, R. A. Warmack, Y. Feng, S. G. Clarke, G. Blobel and P. Stavropoulos (2016). "A glutamate/aspartate switch controls product specificity in a protein arginine methyltransferase." Proc Natl Acad Sci U S A **113**(8): 2068-2073.

Dehe, P. M. and V. Geli (2006). "The multiple faces of Set1." Biochem Cell Biol **84**(4): 536-548.

Diamantopoulos, P. T., M. Michael, O. Benopoulou, E. Bazanis, G. Tzeletas, J. Meletis, G. Vayopoulos and N. A. Viniou (2012). "Antiretroviral activity of 5-azacytidine during treatment of a HTLV-1 positive myelodysplastic syndrome with autoimmune manifestations." Virol J **9**: 1.

Dimmic, M. W., S. Sunyaev and C. D. Bustamante (2005). "Inferring SNP function using evolutionary, structural, and computational methods." Pac Symp Biocomput: 382-384.

Dixit, A., A. Torkamani, N. J. Schork and G. Verkhivker (2009). "Computational modeling of structurally conserved cancer mutations in the RET and MET

kinases: the impact on protein structure, dynamics, and stability." Biophys J **96**(3): 858-874.

Dixon, J. E. and T. A. Woodford (1984). "Rat pituitary N alpha-acetyltransferase." Methods Enzymol **106**: 170-179.

Dixon, M. M., S. Huang, R. G. Matthews and M. Ludwig (1996). "The structure of the C-terminal domain of methionine synthase: presenting S-adenosylmethionine for reductive methylation of B12." Structure **4**(11): 1263-1275.

Dominissini, D., S. Moshitch-Moshkovitz, S. Schwartz, M. Salmon-Divon, L. Ungar, S. Osenberg, K. Cesarkas, J. Jacob-Hirsch, N. Amariglio, M. Kupiec, R. Sorek and G. Rechavi (2012). "Topology of the human and mouse m6A RNA methylomes revealed by m6A-seq." Nature **485**(7397): 201-206.

Doukov, T., J. Seravalli, J. J. Stezowski and S. W. Ragsdale (2000). "Crystal structure of a methyltetrahydrofolate- and corrinoid-dependent methyltransferase." Structure **8**(8): 817-830.

Dubuc, A. M., M. Remke, A. Korshunov, P. A. Northcott, S. H. Zhan, M. Mendez-Lago, M. Kool, D. T. Jones, A. Unterberger, A. S. Morrissy, D. Shih, J. Peacock, V. Ramaswamy, A. Rolider, X. Wang, H. Witt, T. Hielscher, C. Hawkins, R. Vibhakar, S. Croul, J. T. Rutka, W. A. Weiss, S. J. Jones, C. G. Eberhart, M. A. Marra, S. M. Pfister and M. D. Taylor (2013). "Aberrant patterns of H3K4 and H3K27 histone lysine methylation occur across subgroups in medulloblastoma." Acta Neuropathol **125**(3): 373-384.

Ea, C. K. and D. Baltimore (2009). "Regulation of NF-kappaB activity through lysine monomethylation of p65." Proc Natl Acad Sci U S A **106**(45): 18972-18977.

Edmonds, C. G., P. F. Crain, R. Gupta, T. Hashizume, C. H. Hocart, J. A. Kowalak, S. C. Pomerantz, K. O. Stetter and J. A. McCloskey (1991). "Posttranscriptional modification of tRNA in thermophilic archaea (Archaebacteria)." J Bacteriol **173**(10): 3138-3148.

Eisert, R. J. and M. L. Waters (2011). "Tuning HP1alpha chromodomain selectivity for di- and trimethyllysine." Chembiochem **12**(18): 2786-2790.
Esteller, M. (2007). "Cancer epigenomics: DNA methylomes and histone-modification maps." Nat Rev Genet **8**(4): 286-298.

Evans, J. C., D. P. Huddler, M. T. Hilgers, G. Romanchuk, R. G. Matthews and M. L. Ludwig (2004). "Structures of the N-terminal modules imply large domain motions during catalysis by methionine synthase." Proc Natl Acad Sci U S A **101**(11): 3729-3736.

Evans, J. C., D. P. Huddler, J. Jiracek, C. Castro, N. S. Millian, T. A. Garrow and M. L. Ludwig (2002). "Betaine-homocysteine methyltransferase: zinc in a distorted barrel." Structure **10**(9): 1159-1171.

Fang, R., A. J. Barbera, Y. Xu, M. Rutenberg, T. Leonor, Q. Bi, F. Lan, P. Mei, G. C. Yuan, C. Lian, J. Peng, D. Cheng, G. Sui, U. B. Kaiser, Y. Shi and Y. G. Shi (2010). "Human LSD2/KDM1b/AOF1 regulates gene transcription by modulating intragenic H3K4me2 methylation." Mol Cell **39**(2): 222-233.

Feinberg, A. P., R. Ohlsson and S. Henikoff (2006). "The epigenetic progenitor origin of human cancer." Nat Rev Genet **7**(1): 21-33.

Feng, Q., H. Wang, H. H. Ng, H. Erdjument-Bromage, P. Tempst, K. Struhl and Y. Zhang (2002). "Methylation of H3-lysine 79 is mediated by a new family of HMTases without a SET domain." Curr Biol **12**(12): 1052-1058.

Fenwick, M. K. and S. E. Ealick (2018). "Towards the structural characterization of the human methyltransferome." Curr Opin Struct Biol **53**: 12-21.

Filippakopoulos, P. and S. Knapp (2012). "The bromodomain interaction module." FEBS Lett **586**(17): 2692-2704.

Fingerman, I. M., C. L. Wu, B. D. Wilson and S. D. Briggs (2005). "Global loss of Set1-mediated H3 Lys4 trimethylation is associated with silencing defects in Saccharomyces cerevisiae." J Biol Chem **280**(31): 28761-28765.

Foyn, H., P. Van Damme, S. I. Stove, N. Glomnes, R. Evjenth, K. Gevaert and T. Arnesen (2013). "Protein N-terminal acetyltransferases act as N-terminal propionyltransferases in vitro and in vivo." Mol Cell Proteomics **12**(1): 42-54.

Fraga, M. F., E. Ballestar, M. F. Paz, S. Ropero, F. Setien, M. L. Ballestar, D. Heine-Suner, J. C. Cigudosa, M. Urioste, J. Benitez, M. Boix-Chornet, A. Sanchez-Aguilera, C. Ling, E. Carlsson, P. Poulsen, A. Vaag, Z. Stephan, T. D. Spector, Y. Z. Wu, C. Plass and M. Esteller (2005). "Epigenetic differences arise during the lifetime of monozygotic twins." Proc Natl Acad Sci U S A **102**(30): 10604-10609.

Fu, Y., D. Dominissini, G. Rechavi and C. He (2014). "Gene expression regulation mediated through reversible m(6)A RNA methylation." Nat Rev Genet **15**(5): 293-306.

Gardner, K. E., C. D. Allis and B. D. Strahl (2011). "Operating on chromatin, a colorful language where context matters." J Mol Biol **409**(1): 36-46.

Geula, S., S. Moshitch-Moshkovitz, D. Dominissini, A. A. Mansour, N. Kol, M. Salmon-Divon, V. Hershkovitz, E. Peer, N. Mor, Y. S. Manor, M. S. Ben-Haim, E.

Eyal, S. Yunger, Y. Pinto, D. A. Jaitin, S. Viukov, Y. Rais, V. Krupalnik, E. Chomsky, M. Zerbib, I. Maza, Y. Rechavi, R. Massarwa, S. Hanna, I. Amit, E. Y. Levanon, N. Amariglio, N. Stern-Ginossar, N. Novershtern, G. Rechavi and J. H. Hanna (2015). "Stem cells. m6A mRNA methylation facilitates resolution of naive pluripotency toward differentiation." Science **347**(6225): 1002-1006.

Gonatopoulos-Pournatzis, T., S. Dunn, R. Bounds and V. H. Cowling (2011). "RAM/Fam103a1 is required for mRNA cap methylation." Mol Cell **44**(4): 585-596.

Gossage, L., M. Murtaza, A. F. Slatter, C. P. Lichtenstein, A. Warren, B. Haynes, F. Marass, I. Roberts, S. J. Shanahan, A. Claas, A. Dunham, A. P. May, N. Rosenfeld, T. Forshew and T. Eisen (2014). "Clinical and pathological impact of VHL, PBRM1, BAP1, SETD2, KDM6A, and JARID1c in clear cell renal cell carcinoma." Genes Chromosomes Cancer **53**(1): 38-51.

Gowher, H. and A. Jeltsch (2002). "Molecular enzymology of the catalytic domains of the Dnmt3a and Dnmt3b DNA methyltransferases." J Biol Chem **277**(23): 20409-20414.

Grasso, C. S., Y. M. Wu, D. R. Robinson, X. Cao, S. M. Dhanasekaran, A. P. Khan, M. J. Quist, X. Jing, R. J. Lonigro, J. C. Brenner, I. A. Asangani, B. Ateeq, S. Y. Chun, J. Siddiqui, L. Sam, M. Anstett, R. Mehra, J. R. Prensner, N. Palanisamy, G. A. Ryslik, F. Vandin, B. J. Raphael, L. P. Kunju, D. R. Rhodes, K. J. Pienta, A. M. Chinnaiyan and S. A. Tomlins (2012). "The mutational landscape of lethal castration-resistant prostate cancer." Nature **487**(7406): 239-243.

Greer, E. L., T. J. Maures, A. G. Hauswirth, E. M. Green, D. S. Leeman, G. S. Maro, S. Han, M. R. Banko, O. Gozani and A. Brunet (2010). "Members of the H3K4 trimethylation complex regulate lifespan in a germline-dependent manner in C. elegans." Nature **466**(7304): 383-387.

Greer, E. L. and Y. Shi (2012). "Histone methylation: a dynamic mark in health, disease and inheritance." Nat Rev Genet **13**(5): 343-357.

Grimm, S. L. and J. M. Rosen (2003). "The role of C/EBPbeta in mammary gland development and breast cancer." J Mammary Gland Biol Neoplasia **8**(2): 191-204.

Gui, Y., G. Guo, Y. Huang, X. Hu, A. Tang, S. Gao, R. Wu, C. Chen, X. Li, L. Zhou, M. He, Z. Li, X. Sun, W. Jia, J. Chen, S. Yang, F. Zhou, X. Zhao, S. Wan, R. Ye, C. Liang, Z. Liu, P. Huang, C. Liu, H. Jiang, Y. Wang, H. Zheng, L. Sun, X. Liu, Z. Jiang, D. Feng, J. Chen, S. Wu, J. Zou, Z. Zhang, R. Yang, J. Zhao, C. Xu, W. Yin, Z. Guan, J. Ye, H. Zhang, J. Li, K. Kristiansen, M. L. Nickerson, D. Theodorescu, Y. Li, X. Zhang, S. Li, J. Wang, H. Yang, J. Wang and Z. Cai

(2011). "Frequent mutations of chromatin remodeling genes in transitional cell carcinoma of the bladder." Nat Genet **43**(9): 875-878.

Guo, X., L. Wang, J. Li, Z. Ding, J. Xiao, X. Yin, S. He, P. Shi, L. Dong, G. Li, C. Tian, J. Wang, Y. Cong and Y. Xu (2015). "Structural insight into autoinhibition and histone H3-induced activation of DNMT3A." Nature **517**(7536): 640-644.

Guo, Y., N. Nady, C. Qi, A. Allali-Hassani, H. Zhu, P. Pan, M. A. Adams-Cioaba, M. F. Amaya, A. Dong, M. Vedadi, M. Schapira, R. J. Read, C. H. Arrowsmith and J. Min (2009). "Methylation-state-specific recognition of histones by the MBT repeat protein L3MBTL2." Nucleic Acids Res **37**(7): 2204-2210.

Guy, M. P. and E. M. Phizicky (2014). "Two-subunit enzymes involved in eukaryotic post-transcriptional tRNA modification." RNA Biol **11**(12): 1608-1618.

Hagemeier, C. H., M. Krer, R. K. Thauer, E. Warkentin and U. Ermler (2006). "Insight into the mechanism of biological methanol activation based on the crystal structure of the methanol-cobalamin methyltransferase complex." Proc Natl Acad Sci U S A **103**(50): 18917-18922.

Hamamoto, R., Y. Furukawa, M. Morita, Y. Iimura, F. P. Silva, M. Li, R. Yagyu and Y. Nakamura (2004). "SMYD3 encodes a histone methyltransferase involved in the proliferation of cancer cells." Nat Cell Biol **6**(8): 731-740.

Hamamoto, R., F. P. Silva, M. Tsuge, T. Nishidate, T. Katagiri, Y. Nakamura and Y. Furukawa (2006). "Enhanced SMYD3 expression is essential for the growth of breast cancer cells." Cancer Sci **97**(2): 113-118.

Hamamoto, R., G. Toyokawa, M. Nakakido, K. Ueda and Y. Nakamura (2014). "SMYD2-dependent HSP90 methylation promotes cancer cell proliferation by regulating the chaperone complex formation." Cancer Lett **351**(1): 126-133.

Hao, B., G. Zhao, P. T. Kang, J. A. Soares, T. K. Ferguson, J. Gallucci, J. A. Krzycki and M. K. Chan (2004). "Reactivity and chemical synthesis of L-pyrrolysine- the 22(nd) genetically encoded amino acid." Chem Biol **11**(9): 1317-1324.

Hao, Y. and I. G. Macara (2008). "Regulation of chromatin binding by a conformational switch in the tail of the Ran exchange factor RCC1." J Cell Biol **182**(5): 827-836.

Hartsough, E. J., R. D. Meyer, V. Chitalia, Y. Jiang, V. E. Marquez, I. V. Zhdanova, J. Weinberg, C. E. Costello and N. Rahimi (2013). "Lysine methylation promotes VEGFR-2 activation and angiogenesis." Sci Signal **6**(304): ra104.

Hayami, S., J. D. Kelly, H. S. Cho, M. Yoshimatsu, M. Unoki, T. Tsunoda, H. I. Field, D. E. Neal, H. Yamaue, B. A. Ponder, Y. Nakamura and R. Hamamoto (2011). "Overexpression of LSD1 contributes to human carcinogenesis through chromatin regulation in various cancers." Int J Cancer **128**(3): 574-586.

He, B., K. Wang, Y. Liu, B. Xue, V. N. Uversky and A. K. Dunker (2009). "Predicting intrinsic disorder in proteins: an overview." Cell Res **19**(8): 929-949.
He, C. (2010). "Grand challenge commentary: RNA epigenetics?" Nat Chem Biol **6**(12): 863-865.

Heintzman, N. D., G. C. Hon, R. D. Hawkins, P. Kheradpour, A. Stark, L. F. Harp, Z. Ye, L. K. Lee, R. K. Stuart, C. W. Ching, K. A. Ching, J. E. Antosiewicz-Bourget, H. Liu, X. Zhang, R. D. Green, V. V. Lobanenkov, R. Stewart, J. A. Thomson, G. E. Crawford, M. Kellis and B. Ren (2009). "Histone modifications at human enhancers reflect global cell-type-specific gene expression." Nature **459**(7243): 108-112.

Heintzman, N. D., R. K. Stuart, G. Hon, Y. Fu, C. W. Ching, R. D. Hawkins, L. O. Barrera, S. Van Calcar, C. Qu, K. A. Ching, W. Wang, Z. Weng, R. D. Green, G. E. Crawford and B. Ren (2007). "Distinct and predictive chromatin signatures of transcriptional promoters and enhancers in the human genome." Nat Genet **39**(3): 311-318.

Hempel, K. and H. W. Lange (1968). "[Nepsilon-methylated lysine in histones from chicken erythrocytes]." Hoppe Seylers Z Physiol Chem **349**(5): 603-607.
Henry, M. F. and P. A. Silver (1996). "A novel methyltransferase (Hmt1p) modifies poly(A)+-RNA-binding proteins." Mol Cell Biol **16**(7): 3668-3678.

Herz, H. M., A. Garruss and A. Shilatifard (2013). "SET for life: biochemical activities and biological functions of SET domain-containing proteins." Trends Biochem Sci **38**(12): 621-639.

Herz, H. M., M. Mohan, A. S. Garruss, K. Liang, Y. H. Takahashi, K. Mickey, O. Voets, C. P. Verrijzer and A. Shilatifard (2012). "Enhancer-associated H3K4 monomethylation by Trithorax-related, the Drosophila homolog of mammalian Mll3/Mll4." Genes Dev **26**(23): 2604-2620.

Hetzer, M., O. J. Gruss and I. W. Mattaj (2002). "The Ran GTPase as a marker of chromosome position in spindle formation and nuclear envelope assembly." Nat Cell Biol **4**(7): E177-184.

Ho, A. S., K. Kannan, D. M. Roy, L. G. Morris, I. Ganly, N. Katabi, D. Ramaswami, L. A. Walsh, S. Eng, J. T. Huse, J. Zhang, I. Dolgalev, K. Huberman, A. Heguy, A. Viale, M. Drobnjak, M. A. Leversha, C. E. Rice, B. Singh, N. G. Iyer, C. R. Leemans, E. Bloemena, R. L. Ferris, R. R. Seethala, B. E. Gross, Y. Liang, R. Sinha, L. Peng, B. J. Raphael, S. Turcan, Y. Gong, N.

Schultz, S. Kim, S. Chiosea, J. P. Shah, C. Sander, W. Lee and T. A. Chan (2013). "The mutational landscape of adenoid cystic carcinoma." Nat Genet **45**(7): 791-798.

Hodel, M. R., A. H. Corbett and A. E. Hodel (2001). "Dissection of a nuclear localization signal." J Biol Chem **276**(2): 1317-1325.

Holliday, R. and J. E. Pugh (1975). "DNA modification mechanisms and gene activity during development." Science **187**(4173): 226-232.

Huang, J., L. Perez-Burgos, B. J. Placek, R. Sengupta, M. Richter, J. A. Dorsey, S. Kubicek, S. Opravil, T. Jenuwein and S. L. Berger (2006). "Repression of p53 activity by Smyd2-mediated methylation." Nature **444**(7119): 629-632.

Huang, J., R. Sengupta, A. B. Espejo, M. G. Lee, J. A. Dorsey, M. Richter, S. Opravil, R. Shiekhattar, M. T. Bedford, T. Jenuwein and S. L. Berger (2007). "p53 is regulated by the lysine demethylase LSD1." Nature **449**(7158): 105-108.

Huang, Y., J. Komoto, K. Konishi, Y. Takata, H. Ogawa, T. Gomi, M. Fujioka and F. Takusagawa (2000). "Mechanisms for auto-inhibition and forced product release in glycine N-methyltransferase: crystal structures of wild-type, mutant R175K and S-adenosylhomocysteine-bound R175K enzymes." J Mol Biol **298**(1): 149-162.

Ishiyama, S., A. Nishiyama, Y. Saeki, K. Moritsugu, D. Morimoto, L. Yamaguchi, N. Arai, R. Matsumura, T. Kawakami, Y. Mishima, H. Hojo, S. Shimamura, F. Ishikawa, S. Tajima, K. Tanaka, M. Ariyoshi, M. Shirakawa, M. Ikeguchi, A. Kidera, I. Suetake, K. Arita and M. Nakanishi (2017). "Structure of the Dnmt1 Reader Module Complexed with a Unique Two-Mono-Ubiquitin Mark on Histone H3 Reveals the Basis for DNA Methylation Maintenance." Mol Cell **68**(2): 350-360.e357.

Iyer, L. M., D. Zhang and L. Aravind (2016). "Adenine methylation in eukaryotes: Apprehending the complex evolutionary history and functional potential of an epigenetic modification." Bioessays **38**(1): 27-40.

Jacobs, S. A. and S. Khorasanizadeh (2002). "Structure of HP1 chromodomain bound to a lysine 9-methylated histone H3 tail." Science **295**(5562): 2080-2083.
Jaenisch, R. and A. Bird (2003). "Epigenetic regulation of gene expression: how the genome integrates intrinsic and environmental signals." Nat Genet **33 Suppl**: 245-254.

Jaffe, J. D., Y. Wang, H. M. Chan, J. Zhang, R. Huether, G. V. Kryukov, H. E. Bhang, J. E. Taylor, M. Hu, N. P. Englund, F. Yan, Z. Wang, E. Robert McDonald, 3rd, L. Wei, J. Ma, J. Easton, Z. Yu, R. deBeaumount, V. Gibaja, K. Venkatesan, R. Schlegel, W. R. Sellers, N. Keen, J. Liu, G. Caponigro, J.

Barretina, V. G. Cooke, C. Mullighan, S. A. Carr, J. R. Downing, L. A. Garraway and F. Stegmeier (2013). "Global chromatin profiling reveals NSD2 mutations in pediatric acute lymphoblastic leukemia." Nat Genet **45**(11): 1386-1391.
Jain, K., R. A. Warmack, E. W. Debler, A. Hadjikyriacou, P. Stavropoulos and S. G. Clarke (2016). "Protein Arginine Methyltransferase Product Specificity Is Mediated by Distinct Active-site Architectures." J Biol Chem **291**(35): 18299-18308.

Jankowska, A. M., H. Makishima, R. V. Tiu, H. Szpurka, Y. Huang, F. Traina, V. Visconte, Y. Sugimoto, C. Prince, C. O'Keefe, E. D. Hsi, A. List, M. A. Sekeres, A. Rao, M. A. McDevitt and J. P. Maciejewski (2011). "Mutational spectrum analysis of chronic myelomonocytic leukemia includes genes associated with epigenetic regulation: UTX, EZH2, and DNMT3A." Blood **118**(14): 3932-3941.

Jeltsch, A. (2002). "Beyond Watson and Crick: DNA methylation and molecular enzymology of DNA methyltransferases." Chembiochem **3**(4): 274-293.
Jeltsch, A. and R. Z. Jurkowska (2014). "New concepts in DNA methylation." Trends Biochem Sci **39**(7): 310-318.

Jeong, H. J., H. J. Lee, T. A. Vuong, K. S. Choi, D. Choi, S. H. Koo, S. C. Cho, H. Cho and J. S. Kang (2016). "Prmt7 Deficiency Causes Reduced Skeletal Muscle Oxidative Metabolism and Age-Related Obesity." Diabetes **65**(7): 1868-1882.

Jia, D., R. Z. Jurkowska, X. Zhang, A. Jeltsch and X. Cheng (2007). "Structure of Dnmt3a bound to Dnmt3L suggests a model for de novo DNA methylation." Nature **449**(7159): 248-251.

Jia, G., Y. Fu, X. Zhao, Q. Dai, G. Zheng, Y. Yang, C. Yi, T. Lindahl, T. Pan, Y. G. Yang and C. He (2011). "N6-methyladenosine in nuclear RNA is a major substrate of the obesity-associated FTO." Nat Chem Biol **7**(12): 885-887.

Jurkowska, R. Z., N. Anspach, C. Urbanke, D. Jia, R. Reinhardt, W. Nellen, X. Cheng and A. Jeltsch (2008). "Formation of nucleoprotein filaments by mammalian DNA methyltransferase Dnmt3a in complex with regulator Dnmt3L." Nucleic Acids Res **36**(21): 6656-6663.

Jurkowska, R. Z., T. P. Jurkowski and A. Jeltsch (2011). "Structure and function of mammalian DNA methyltransferases." Chembiochem **12**(2): 206-222.

Kandoth, C., M. D. McLellan, F. Vandin, K. Ye, B. Niu, C. Lu, M. Xie, Q. Zhang, J. F. McMichael, M. A. Wyczalkowski, M. D. M. Leiserson, C. A. Miller, J. S. Welch, M. J. Walter, M. C. Wendl, T. J. Ley, R. K. Wilson, B. J. Raphael and L. Ding (2013). "Mutational landscape and significance across 12 major cancer types." Nature **502**(7471): 333-339.

Kareta, M. S., Z. M. Botello, J. J. Ennis, C. Chou and F. Chedin (2006). "Reconstitution and mechanism of the stimulation of de novo methylation by human DNMT3L." J Biol Chem **281**(36): 25893-25902.

Khanna, P. and M. Schuman Jorns (2001). "Characterization of the FAD-containing N-methyltryptophan oxidase from Escherichia coli." Biochemistry **40**(5): 1441-1450.

Khorasanizadeh, S. (2011). "Recognition of methylated histones: new twists and variations." Curr Opin Struct Biol **21**(6): 744-749.

Kim, E., M. Kim, D. H. Woo, Y. Shin, J. Shin, N. Chang, Y. T. Oh, H. Kim, J. Rheey, I. Nakano, C. Lee, K. M. Joo, J. N. Rich, D. H. Nam and J. Lee (2013). "Phosphorylation of EZH2 activates STAT3 signaling via STAT3 methylation and promotes tumorigenicity of glioblastoma stem-like cells." Cancer Cell **23**(6): 839-852.

Kim, J., J. Daniel, A. Espejo, A. Lake, M. Krishna, L. Xia, Y. Zhang and M. T. Bedford (2006). "Tudor, MBT and chromo domains gauge the degree of lysine methylation." EMBO Rep **7**(4): 397-403.

Kim, K., A. D. Skora, Z. Li, Q. Liu, A. J. Tam, R. L. Blosser, L. A. Diaz, Jr., N. Papadopoulos, K. W. Kinzler, B. Vogelstein and S. Zhou (2014). "Eradication of metastatic mouse cancers resistant to immune checkpoint blockade by suppression of myeloid-derived cells." Proc Natl Acad Sci U S A **111**(32): 11774-11779.

Kim, S., L. Benoiton and W. K. Paik (1964). "EPSILON-ALKYLLYSINASE. PURIFICATION AND PROPERTIES OF THE ENZYME." J Biol Chem **239**: 3790-3796.

Kim, S. and W. K. Paik (1965). "Studies on the origin of epsilon-N-methyl-L-lysine in protein." J Biol Chem **240**(12): 4629-4634.

Kimura, Y., Y. Kurata, A. Ishikawa, A. Okayama, M. Kamita and H. Hirano (2013). "N-Terminal methylation of proteasome subunit Rpt1 in yeast." Proteomics **13**(21): 3167-3174.

Kirmizis, A., H. Santos-Rosa, C. J. Penkett, M. A. Singer, R. D. Green and T. Kouzarides (2009). "Distinct transcriptional outputs associated with mono- and dimethylated histone H3 arginine 2." Nat Struct Mol Biol **16**(4): 449-451.

Kleer, C. G., Q. Cao, S. Varambally, R. Shen, I. Ota, S. A. Tomlins, D. Ghosh, R. G. Sewalt, A. P. Otte, D. F. Hayes, M. S. Sabel, D. Livant, S. J. Weiss, M. A. Rubin and A. M. Chinnaiyan (2003). "EZH2 is a marker of aggressive breast

cancer and promotes neoplastic transformation of breast epithelial cells." Proc Natl Acad Sci U S A **100**(20): 11606-11611.

Klein, R. R. and R. L. Houtz (1995). "Cloning and developmental expression of pea ribulose-1,5-bisphosphate carboxylase/oxygenase large subunit N-methyltransferase." Plant Mol Biol **27**(2): 249-261.

Kogure, M., M. Takawa, V. Saloura, K. Sone, L. Piao, K. Ueda, R. Ibrahim, T. Tsunoda, M. Sugiyama, Y. Atomi, Y. Nakamura and R. Hamamoto (2013). "The oncogenic polycomb histone methyltransferase EZH2 methylates lysine 120 on histone H2B and competes ubiquitination." Neoplasia **15**(11): 1251-1261.

Kontaki, H. and I. Talianidis (2010). "Lysine methylation regulates E2F1-induced cell death." Mol Cell **39**(1): 152-160.

Kotake, Y., R. Cao, P. Viatour, J. Sage, Y. Zhang and Y. Xiong (2007). "pRB family proteins are required for H3K27 trimethylation and Polycomb repression complexes binding to and silencing p16INK4alpha tumor suppressor gene." Genes Dev **21**(1): 49-54.

Krause, C. D., Z. H. Yang, Y. S. Kim, J. H. Lee, J. R. Cook and S. Pestka (2007). "Protein arginine methyltransferases: evolution and assessment of their pharmacological and therapeutic potential." Pharmacol Ther **113**(1): 50-87.

Kreso, A. and J. E. Dick (2014). "Evolution of the cancer stem cell model." Cell Stem Cell **14**(3): 275-291.

Krogan, N. J., M. Kim, A. Tong, A. Golshani, G. Cagney, V. Canadien, D. P. Richards, B. K. Beattie, A. Emili, C. Boone, A. Shilatifard, S. Buratowski and J. Greenblatt (2003). "Methylation of histone H3 by Set2 in Saccharomyces cerevisiae is linked to transcriptional elongation by RNA polymerase II." Mol Cell Biol **23**(12): 4207-4218.

Krogh, N., M. D. Jansson, S. J. Hafner, D. Tehler, U. Birkedal, M. Christensen-Dalsgaard, A. H. Lund and H. Nielsen (2016). "Profiling of 2'-O-Me in human rRNA reveals a subset of fractionally modified positions and provides evidence for ribosome heterogeneity." Nucleic Acids Res **44**(16): 7884-7895.

Kuhn, P., S. A. Lesley, Mathews, II, J. M. Canaves, L. S. Brinen, X. Dai, A. M. Deacon, M. A. Elsliger, S. Eshaghi, R. Floyd, A. Godzik, C. Grittini, S. K. Grzechnik, C. Guda, K. O. Hodgson, L. Jaroszewski, C. Karlak, H. E. Klock, E. Koesema, J. M. Kovarik, A. T. Kreusch, D. McMullan, T. M. McPhillips, M. A. Miller, M. Miller, A. Morse, K. Moy, J. Ouyang, A. Robb, K. Rodrigues, T. L. Selby, G. Spraggon, R. C. Stevens, S. S. Taylor, H. van den Bedem, J. Velasquez, J. Vincent, X. Wang, B. West, G. Wolf, J. Wooley and I. A. Wilson

(2002). "Crystal structure of thy1, a thymidylate synthase complementing protein from Thermotoga maritima at 2.25 A resolution." Proteins **49**(1): 142-145.

Kunizaki, M., R. Hamamoto, F. P. Silva, K. Yamaguchi, T. Nagayasu, M. Shibuya, Y. Nakamura and Y. Furukawa (2007). "The lysine 831 of vascular endothelial growth factor receptor 1 is a novel target of methylation by SMYD3." Cancer Res **67**(22): 10759-10765.

Kuzmichev, A., K. Nishioka, H. Erdjument-Bromage, P. Tempst and D. Reinberg (2002). "Histone methyltransferase activity associated with a human multiprotein complex containing the Enhancer of Zeste protein." Genes Dev **16**(22): 2893-2905.

Lachner, M. and T. Jenuwein (2002). "The many faces of histone lysine methylation." Curr Opin Cell Biol **14**(3): 286-298.

Lee, J. M., J. S. Lee, H. Kim, K. Kim, H. Park, J. Y. Kim, S. H. Lee, I. S. Kim, J. Kim, M. Lee, C. H. Chung, S. B. Seo, J. B. Yoon, E. Ko, D. Y. Noh, K. I. Kim, K. K. Kim and S. H. Baek (2012). "EZH2 generates a methyl degron that is recognized by the DCAF1/DDB1/CUL4 E3 ubiquitin ligase complex." Mol Cell **48**(4): 572-586.

Leulliot, N., M. Chaillet, D. Durand, N. Ulryck, K. Blondeau and H. van Tilbeurgh (2008). "Structure of the yeast tRNA m7G methylation complex." Structure **16**(1): 52-61.

Levin, H. L. and J. V. Moran (2011). "Dynamic interactions between transposable elements and their hosts." Nat Rev Genet **12**(9): 615-627.

Levy, D., A. J. Kuo, Y. Chang, U. Schaefer, C. Kitson, P. Cheung, A. Espejo, B. M. Zee, C. L. Liu, S. Tangsombatvisit, R. I. Tennen, A. Y. Kuo, S. Tanjing, R. Cheung, K. F. Chua, P. J. Utz, X. Shi, R. K. Prinjha, K. Lee, B. A. Garcia, M. T. Bedford, A. Tarakhovsky, X. Cheng and O. Gozani (2011). "Lysine methylation of the NF-kappaB subunit RelA by SETD6 couples activity of the histone methyltransferase GLP at chromatin to tonic repression of NF-kappaB signaling." Nat Immunol **12**(1): 29-36.

Li, H., W. Fischle, W. Wang, E. M. Duncan, L. Liang, S. Murakami-Ishibe, C. D. Allis and D. J. Patel (2007). "Structural basis for lower lysine methylation state-specific readout by MBT repeats of L3MBTL1 and an engineered PHD finger." Mol Cell **28**(4): 677-691.

Li, H., S. Ilin, W. Wang, E. M. Duncan, J. Wysocka, C. D. Allis and D. J. Patel (2006). "Molecular basis for site-specific read-out of histone H3K4me3 by the BPTF PHD finger of NURF." Nature **442**(7098): 91-95.

Li, K., G. Li, L. M. Bradbury, A. D. Hanson and S. D. Bruner (2016). "Crystal structure of the homocysteine methyltransferase MmuM from Escherichia coli." Biochem J **473**(3): 277-284.

Li, Q. and S. K. Sarna (2009). "Nuclear myosin II regulates the assembly of preinitiation complex for ICAM-1 gene transcription." Gastroenterology **137**(3): 1051-1060, 1060.e1051-1053.

Lim, K., H. Zhang, A. Tempczyk, W. Krajewski, N. Bonander, J. Toedt, A. Howard, E. Eisenstein and O. Herzberg (2003). "Structure of the YibK methyltransferase from Haemophilus influenzae (HI0766): a cofactor bound at a site formed by a knot." Proteins **51**(1): 56-67.

Lin, W. J., J. D. Gary, M. C. Yang, S. Clarke and H. R. Herschman (1996). "The mammalian immediate-early TIS21 protein and the leukemia-associated BTG1 protein interact with a protein-arginine N-methyltransferase." J Biol Chem **271**(25): 15034-15044.

Lindberg, J., I. G. Mills, D. Klevebring, W. Liu, M. Neiman, J. Xu, P. Wikstrom, P. Wiklund, F. Wiklund, L. Egevad and H. Gronberg (2013). "The mitochondrial and autosomal mutation landscapes of prostate cancer." Eur Urol **63**(4): 702-708.
Liss, M. and L. M. Edelstein (1967). "Evidence for the enzymatic methylation of crystalline ovalbumin preparations." Biochem Biophys Res Commun **26**(4): 497-504.

Liu, J., Y. Yue, D. Han, X. Wang, Y. Fu, L. Zhang, G. Jia, M. Yu, Z. Lu, X. Deng, Q. Dai, W. Chen and C. He (2014). "A METTL3-METTL14 complex mediates mammalian nuclear RNA N6-adenosine methylation." Nat Chem Biol **10**(2): 93-95.

Liu, N., Q. Dai, G. Zheng, C. He, M. Parisien and T. Pan (2015). "N(6)-methyladenosine-dependent RNA structural switches regulate RNA-protein interactions." Nature **518**(7540): 560-564.

Lorch, M., J. M. Mason, R. B. Sessions and A. R. Clarke (2000). "Effects of mutations on the thermodynamics of a protein folding reaction: implications for the mechanism of formation of the intermediate and transition states." Biochemistry **39**(12): 3480-3485.

Lu, T., M. W. Jackson, B. Wang, M. Yang, M. R. Chance, M. Miyagi, A. V. Gudkov and G. R. Stark (2010). "Regulation of NF-kappaB by NSD1/FBXL11-dependent reversible lysine methylation of p65." Proc Natl Acad Sci U S A **107**(1): 46-51.

Lu, T., M. Yang, D. B. Huang, H. Wei, G. H. Ozer, G. Ghosh and G. R. Stark (2013). "Role of lysine methylation of NF-kappaB in differential gene regulation." Proc Natl Acad Sci U S A **110**(33): 13510-13515.

Luco, R. F., M. Allo, I. E. Schor, A. R. Kornblihtt and T. Misteli (2011). "Epigenetics in alternative pre-mRNA splicing." Cell **144**(1): 16-26.
Ma, J. C. and D. A. Dougherty (1997). "The Cationminus signpi Interaction." Chem Rev **97**(5): 1303-1324.

Marino, G., U. Eckhard and C. M. Overall (2015). "Protein Termini and Their Modifications Revealed by Positional Proteomics." ACS Chem Biol **10**(8): 1754-1764.

Martin, C., R. Cao and Y. Zhang (2006). "Substrate preferences of the EZH2 histone methyltransferase complex." J Biol Chem **281**(13): 8365-8370.
Martin, J. L. and F. M. McMillan (2002). "SAM (dependent) I AM: the S-adenosylmethionine-dependent methyltransferase fold." Curr Opin Struct Biol **12**(6): 783-793.

Maurer-Stroh, S., N. J. Dickens, L. Hughes-Davies, T. Kouzarides, F. Eisenhaber and C. P. Ponting (2003). "The Tudor domain 'Royal Family': Tudor, plant Agenet, Chromo, PWWP and MBT domains." Trends Biochem Sci **28**(2): 69-74.

Mazur, P. K., N. Reynoird, P. Khatri, P. W. Jansen, A. W. Wilkinson, S. Liu, O. Barbash, G. S. Van Aller, M. Huddleston, D. Dhanak, P. J. Tummino, R. G. Kruger, B. A. Garcia, A. J. Butte, M. Vermeulen, J. Sage and O. Gozani (2014). "SMYD3 links lysine methylation of MAP3K2 to Ras-driven cancer." Nature **510**(7504): 283-287.

Mazzone, R., C. Zwergel, A. Mai and S. Valente (2017). "Epi-drugs in combination with immunotherapy: a new avenue to improve anticancer efficacy." Clin Epigenetics **9**: 59.

Metzger, E., M. Wissmann, N. Yin, J. M. Muller, R. Schneider, A. H. Peters, T. Gunther, R. Buettner and R. Schule (2005). "LSD1 demethylates repressive histone marks to promote androgen-receptor-dependent transcription." Nature **437**(7057): 436-439.

Meyer, K. D., Y. Saletore, P. Zumbo, O. Elemento, C. E. Mason and S. R. Jaffrey (2012). "Comprehensive analysis of mRNA methylation reveals enrichment in 3' UTRs and near stop codons." Cell **149**(7): 1635-1646.

Michel, G., V. Sauve, R. Larocque, Y. Li, A. Matte and M. Cygler (2002). "The structure of the RlmB 23S rRNA methyltransferase reveals a new methyltransferase fold with a unique knot." Structure **10**(10): 1303-1315.

Miller, T., N. J. Krogan, J. Dover, H. Erdjument-Bromage, P. Tempst, M. Johnston, J. F. Greenblatt and A. Shilatifard (2001). "COMPASS: a complex of proteins associated with a trithorax-related SET domain protein." Proc Natl Acad Sci U S A **98**(23): 12902-12907.

Mohan, M., H. M. Herz, E. R. Smith, Y. Zhang, J. Jackson, M. P. Washburn, L. Florens, J. C. Eissenberg and A. Shilatifard (2011). "The COMPASS family of H3K4 methylases in Drosophila." Mol Cell Biol **31**(21): 4310-4318.

Montfort, W. R., K. M. Perry, E. B. Fauman, J. S. Finer-Moore, G. F. Maley, L. Hardy, F. Maley and R. M. Stroud (1990). "Structure, multiple site binding, and segmental accommodation in thymidylate synthase on binding dUMP and an anti-folate." Biochemistry **29**(30): 6964-6977.

Moore, M. H., J. M. Gulbis, E. J. Dodson, B. Demple and P. C. Moody (1994). "Crystal structure of a suicidal DNA repair protein: the Ada O6-methylguanine-DNA methyltransferase from E. coli." Embo j **13**(7): 1495-1501.

Morin, R. D., N. A. Johnson, T. M. Severson, A. J. Mungall, J. An, R. Goya, J. E. Paul, M. Boyle, B. W. Woolcock, F. Kuchenbauer, D. Yap, R. K. Humphries, O. L. Griffith, S. Shah, H. Zhu, M. Kimbara, P. Shashkin, J. F. Charlot, M. Tcherpakov, R. Corbett, A. Tam, R. Varhol, D. Smailus, M. Moksa, Y. Zhao, A. Delaney, H. Qian, I. Birol, J. Schein, R. Moore, R. Holt, D. E. Horsman, J. M. Connors, S. Jones, S. Aparicio, M. Hirst, R. D. Gascoyne and M. A. Marra (2010). "Somatic mutations altering EZH2 (Tyr641) in follicular and diffuse large B-cell lymphomas of germinal-center origin." Nat Genet **42**(2): 181-185.

Morin, R. D., M. Mendez-Lago, A. J. Mungall, R. Goya, K. L. Mungall, R. D. Corbett, N. A. Johnson, T. M. Severson, R. Chiu, M. Field, S. Jackman, M. Krzywinski, D. W. Scott, D. L. Trinh, J. Tamura-Wells, S. Li, M. R. Firme, S. Rogic, M. Griffith, S. Chan, O. Yakovenko, I. M. Meyer, E. Y. Zhao, D. Smailus, M. Moksa, S. Chittaranjan, L. Rimsza, A. Brooks-Wilson, J. J. Spinelli, S. Ben-Neriah, B. Meissner, B. Woolcock, M. Boyle, H. McDonald, A. Tam, Y. Zhao, A. Delaney, T. Zeng, K. Tse, Y. Butterfield, I. Birol, R. Holt, J. Schein, D. E. Horsman, R. Moore, S. J. Jones, J. M. Connors, M. Hirst, R. D. Gascoyne and M. A. Marra (2011). "Frequent mutation of histone-modifying genes in non-Hodgkin lymphoma." Nature **476**(7360): 298-303.

Moritz, L. E. and R. C. Trievel (2017). "Structure, mechanism, and regulation of polycomb repressive complex 2." J Biol Chem.

Moser, J., M. Volker, H. Kool, S. Alekseev, H. Vrieling, A. Yasui, A. A. van Zeeland and L. H. Mullenders (2005). "The UV-damaged DNA binding protein mediates efficient targeting of the nucleotide excision repair complex to UV-induced photo lesions." DNA Repair (Amst) **4**(5): 571-582.

Musselman, C. A. and T. G. Kutateladze (2011). "Handpicking epigenetic marks with PHD fingers." Nucleic Acids Res **39**(21): 9061-9071.

Musselman, C. A., M. E. Lalonde, J. Cote and T. G. Kutateladze (2012). "Perceiving the epigenetic landscape through histone readers." Nat Struct Mol Biol **19**(12): 1218-1227.

Nemergut, M. E., C. A. Mizzen, T. Stukenberg, C. D. Allis and I. G. Macara (2001). "Chromatin docking and exchange activity enhancement of RCC1 by histones H2A and H2B." Science **292**(5521): 1540-1543.

Niedzialkowska, E., O. Gasiorowska, K. B. Handing, K. A. Majorek, P. J. Porebski, I. G. Shabalin, E. Zasadzinska, M. Cymborowski and W. Minor (2016). "Protein purification and crystallization artifacts: The tale usually not told." Protein Sci **25**(3): 720-733.

Nielsen, P. R., D. Nietlispach, H. R. Mott, J. Callaghan, A. Bannister, T. Kouzarides, A. G. Murzin, N. V. Murzina and E. D. Laue (2002). "Structure of the HP1 chromodomain bound to histone H3 methylated at lysine 9." Nature **416**(6876): 103-107.

Ode, H., S. Matsuyama, M. Hata, S. Neya, J. Kakizawa, W. Sugiura and T. Hoshino (2007). "Computational characterization of structural role of the non-active site mutation M36I of human immunodeficiency virus type 1 protease." J Mol Biol **370**(3): 598-607.

Ooi, S. K., C. Qiu, E. Bernstein, K. Li, D. Jia, Z. Yang, H. Erdjument-Bromage, P. Tempst, S. P. Lin, C. D. Allis, X. Cheng and T. H. Bestor (2007). "DNMT3L connects unmethylated lysine 4 of histone H3 to de novo methylation of DNA." Nature **448**(7154): 714-717.

Ouderkirk, J. L. and M. Krendel (2014). "Non-muscle myosins in tumor progression, cancer cell invasion, and metastasis." Cytoskeleton (Hoboken) **71**(8): 447-463.

Ozanick, S., A. Krecic, J. Andersland and J. T. Anderson (2005). "The bipartite structure of the tRNA m1A58 methyltransferase from S. cerevisiae is conserved in humans." Rna **11**(8): 1281-1290.

Paik, W. K. and S. Kim (1968). "Protein methylase I. Purification and properties of the enzyme." J Biol Chem **243**(9): 2108-2114.

Paik, W. K. and S. Kim (1970). "Solubilization and partial purification of protein methylase 3 from calf thymus nuclei." J Biol Chem **245**(22): 6010-6015.

Paik, W. K. and S. Kim (1973). "Enzymatic demethylation of calf thymus histones." Biochem Biophys Res Commun **51**(3): 781-788.

Paik, W. K. and S. Kim (1974). "Epsilon-alkyllysinase. New assay method, purification, and biological significance." Arch Biochem Biophys **165**(1): 369-378.
Pan, Y., P. Ma, Y. Liu, W. Li and Y. Shu (2018). "Multiple functions of m(6)A RNA methylation in cancer." J Hematol Oncol **11**(1): 48.

Pang, C. N., E. Gasteiger and M. R. Wilkins (2010). "Identification of arginine- and lysine-methylation in the proteome of Saccharomyces cerevisiae and its functional implications." BMC Genomics **11**: 92.

Pascual, J., M. Martinez-Yamout, H. J. Dyson and P. E. Wright (2000). "Structure of the PHD zinc finger from human Williams-Beuren syndrome transcription factor." J Mol Biol **304**(5): 723-729.

Pasini, D., A. P. Bracken, M. R. Jensen, E. Lazzerini Denchi and K. Helin (2004). "Suz12 is essential for mouse development and for EZH2 histone methyltransferase activity." Embo j **23**(20): 4061-4071.

Patel, D. J. and Z. Wang (2013). "Readout of epigenetic modifications." Annu Rev Biochem **82**: 81-118.

Pejchal, R. and M. L. Ludwig (2005). "Cobalamin-independent methionine synthase (MetE): a face-to-face double barrel that evolved by gene duplication." PLoS Biol **3**(2): e31.

Pena, P. V., F. Davrazou, X. Shi, K. L. Walter, V. V. Verkhusha, O. Gozani, R. Zhao and T. G. Kutateladze (2006). "Molecular mechanism of histone H3K4me3 recognition by plant homeodomain of ING2." Nature **442**(7098): 100-103.

Peters, J. (2014). "The role of genomic imprinting in biology and disease: an expanding view." Nat Rev Genet **15**(8): 517-530.

Petkowski, J. J., L. A. Bonsignore, J. G. Tooley, D. W. Wilkey, M. L. Merchant, I. G. Macara and C. E. Schaner Tooley (2013). "NRMT2 is an N-terminal monomethylase that primes for its homologue NRMT1." Biochem J **456**(3): 453-462.

Petkowski, J. J., C. E. Schaner Tooley, L. C. Anderson, I. A. Shumilin, J. L. Balsbaugh, J. Shabanowitz, D. F. Hunt, W. Minor and I. G. Macara (2012). "Substrate specificity of mammalian N-terminal alpha-amino methyltransferase NRMT." Biochemistry **51**(30): 5942-5950.

Petrossian, T. C. and S. G. Clarke (2011). "Uncovering the human methyltransferasome." Mol Cell Proteomics **10**(1): M110.000976.

Piao, L., D. Kang, T. Suzuki, A. Masuda, N. Dohmae, Y. Nakamura and R. Hamamoto (2014). "The histone methyltransferase SMYD2 methylates PARP1 and promotes poly(ADP-ribosyl)ation activity in cancer cells." Neoplasia **16**(3): 257-264, 264.e252.

Ping, X. L., B. F. Sun, L. Wang, W. Xiao, X. Yang, W. J. Wang, S. Adhikari, Y. Shi, Y. Lv, Y. S. Chen, X. Zhao, A. Li, Y. Yang, U. Dahal, X. M. Lou, X. Liu, J. Huang, W. P. Yuan, X. F. Zhu, T. Cheng, Y. L. Zhao, X. Wang, J. M. Rendtlew Danielsen, F. Liu and Y. G. Yang (2014). "Mammalian WTAP is a regulatory subunit of the RNA N6-methyladenosine methyltransferase." Cell Res **24**(2): 177-189.

Pless, O., E. Kowenz-Leutz, M. Knoblich, J. Lausen, M. Beyermann, M. J. Walsh and A. Leutz (2008). "G9a-mediated lysine methylation alters the function of CCAAT/enhancer-binding protein-beta." J Biol Chem **283**(39): 26357-26363.

Qiu, C., K. Sawada, X. Zhang and X. Cheng (2002). "The PWWP domain of mammalian DNA methyltransferase Dnmt3b defines a new family of DNA-binding folds." Nat Struct Biol **9**(3): 217-224.

Rhodes, D. R., M. G. Sanda, A. P. Otte, A. M. Chinnaiyan and M. A. Rubin (2003). "Multiplex biomarker approach for determining risk of prostate-specific antigen-defined recurrence of prostate cancer." J Natl Cancer Inst **95**(9): 661-668.

Richardson, S. L., Y. Mao, G. Zhang, P. Hanjra, D. L. Peterson and R. Huang (2015). "Kinetic mechanism of protein N-terminal methyltransferase 1." J Biol Chem **290**(18): 11601-11610.

Riggs, A. D. (1975). "X inactivation, differentiation, and DNA methylation." Cytogenet Cell Genet **14**(1): 9-25.

Riggs, A. D. and Z. Xiong (2004). "Methylation and epigenetic fidelity." Proc Natl Acad Sci U S A **101**(1): 4-5.

Roguev, A., D. Schaft, A. Shevchenko, W. W. Pijnappel, M. Wilm, R. Aasland and A. F. Stewart (2001). "The Saccharomyces cerevisiae Set1 complex includes an Ash2 homologue and methylates histone 3 lysine 4." Embo j **20**(24): 7137-7148.

Rosenfeld, J. A., Z. Wang, D. E. Schones, K. Zhao, R. DeSalle and M. Q. Zhang (2009). "Determination of enriched histone modifications in non-genic portions of the human genome." BMC Genomics **10**: 143.

Saddic, L. A., L. E. West, A. Aslanian, J. R. Yates, 3rd, S. M. Rubin, O. Gozani and J. Sage (2010). "Methylation of the retinoblastoma tumor suppressor by SMYD2." J Biol Chem **285**(48): 37733-37740.

Sanchez, R. and M. M. Zhou (2011). "The PHD finger: a versatile epigenome reader." Trends Biochem Sci **36**(7): 364-372.

Santos-Rosa, H., R. Schneider, A. J. Bannister, J. Sherriff, B. E. Bernstein, N. C. Emre, S. L. Schreiber, J. Mellor and T. Kouzarides (2002). "Active genes are tri-methylated at K4 of histone H3." Nature **419**(6905): 407-411.

Saramaki, O. R., T. L. Tammela, P. M. Martikainen, R. L. Vessella and T. Visakorpi (2006). "The gene for polycomb group protein enhancer of zeste homolog 2 (EZH2) is amplified in late-stage prostate cancer." Genes Chromosomes Cancer **45**(7): 639-645.

Schneider, J., A. Wood, J. S. Lee, R. Schuster, J. Dueker, C. Maguire, S. K. Swanson, L. Florens, M. P. Washburn and A. Shilatifard (2005). "Molecular regulation of histone H3 trimethylation by COMPASS and the regulation of gene expression." Mol Cell **19**(6): 849-856.

Schubert, H. L., R. M. Blumenthal and X. Cheng (2003). "Many paths to methyltransfer: a chronicle of convergence." Trends Biochem Sci **28**(6): 329-335.
Schubert, H. L., K. S. Wilson, E. Raux, S. C. Woodcock and M. J. Warren (1998). "The X-ray structure of a cobalamin biosynthetic enzyme, cobalt-precorrin-4 methyltransferase." Nat Struct Biol **5**(7): 585-592.

Schultz, J., F. Milpetz, P. Bork and C. P. Ponting (1998). "SMART, a simple modular architecture research tool: identification of signaling domains." Proc Natl Acad Sci U S A **95**(11): 5857-5864.

Schwartz, S., M. R. Mumbach, M. Jovanovic, T. Wang, K. Maciag, G. G. Bushkin, P. Mertins, D. Ter-Ovanesyan, N. Habib, D. Cacchiarelli, N. E. Sanjana, E. Freinkman, M. E. Pacold, R. Satija, T. S. Mikkelsen, N. Hacohen, F. Zhang, S. A. Carr, E. S. Lander and A. Regev (2014). "Perturbation of m6A writers reveals two distinct classes of mRNA methylation at internal and 5' sites." Cell Rep **8**(1): 284-296.

Sedkov, Y., E. Cho, S. Petruk, L. Cherbas, S. T. Smith, R. S. Jones, P. Cherbas, E. Canaani, J. B. Jaynes and A. Mazo (2003). "Methylation at lysine 4 of histone H3 in ecdysone-dependent development of Drosophila." Nature **426**(6962): 78-83.

Shahid, T., J. Soroka, E. Kong, L. Malivert, M. J. McIlwraith, T. Pape, S. C. West and X. Zhang (2014). "Structure and mechanism of action of the BRCA2 breast cancer tumor suppressor." Nat Struct Mol Biol **21**(11): 962-968.

Shao, Z., F. Raible, R. Mollaaghababa, J. R. Guyon, C. T. Wu, W. Bender and R. E. Kingston (1999). "Stabilization of chromatin structure by PRC1, a Polycomb complex." Cell **98**(1): 37-46.

Shao, Z., W. Yan, J. Peng, X. Zuo, Y. Zou, F. Li, D. Gong, R. Ma, J. Wu, Y. Shi, Z. Zhang, M. Teng, X. Li and Q. Gong (2014). "Crystal structure of tRNA m1G9 methyltransferase Trm10: insight into the catalytic mechanism and recognition of tRNA substrate." Nucleic Acids Res **42**(1): 509-525.

Sharif, J., M. Muto, S. Takebayashi, I. Suetake, A. Iwamatsu, T. A. Endo, J. Shinga, Y. Mizutani-Koseki, T. Toyoda, K. Okamura, S. Tajima, K. Mitsuya, M. Okano and H. Koseki (2007). "The SRA protein Np95 mediates epigenetic inheritance by recruiting Dnmt1 to methylated DNA." Nature **450**(7171): 908-912.

Shen, E. C., M. F. Henry, V. H. Weiss, S. R. Valentini, P. A. Silver and M. S. Lee (1998). "Arginine methylation facilitates the nuclear export of hnRNP proteins." Genes Dev **12**(5): 679-691.

Shi, X., T. Hong, K. L. Walter, M. Ewalt, E. Michishita, T. Hung, D. Carney, P. Pena, F. Lan, M. R. Kaadige, N. Lacoste, C. Cayrou, F. Davrazou, A. Saha, B. R. Cairns, D. E. Ayer, T. G. Kutateladze, Y. Shi, J. Cote, K. F. Chua and O. Gozani (2006). "ING2 PHD domain links histone H3 lysine 4 methylation to active gene repression." Nature **442**(7098): 96-99.

Shi, X., I. Kachirskaia, H. Yamaguchi, L. E. West, H. Wen, E. W. Wang, S. Dutta, E. Appella and O. Gozani (2007). "Modulation of p53 function by SET8-mediated methylation at lysine 382." Mol Cell **27**(4): 636-646.

Shi, Y., F. Lan, C. Matson, P. Mulligan, J. R. Whetstine, P. A. Cole, R. A. Casero and Y. Shi (2004). "Histone demethylation mediated by the nuclear amine oxidase homolog LSD1." Cell **119**(7): 941-953.

Shilatifard, A. (2012). "The COMPASS family of histone H3K4 methylases: mechanisms of regulation in development and disease pathogenesis." Annu Rev Biochem **81**: 65-95.

Shimazu, T., J. Barjau, Y. Sohtome, M. Sodeoka and Y. Shinkai (2014). "Selenium-based S-adenosylmethionine analog reveals the mammalian seven-beta-strand methyltransferase METTL10 to be an EF1A1 lysine methyltransferase." PLoS One **9**(8): e105394.

Siebold, A. P., R. Banerjee, F. Tie, D. L. Kiss, J. Moskowitz and P. J. Harte (2010). "Polycomb Repressive Complex 2 and Trithorax modulate Drosophila longevity and stress resistance." Proc Natl Acad Sci U S A **107**(1): 169-174.

Sims, R. J., 3rd, S. Millhouse, C. F. Chen, B. A. Lewis, H. Erdjument-Bromage, P. Tempst, J. L. Manley and D. Reinberg (2007). "Recognition of trimethylated histone H3 lysine 4 facilitates the recruitment of transcription postinitiation factors and pre-mRNA splicing." Mol Cell **28**(4): 665-676.

Sledz, P. and M. Jinek (2016). "Structural insights into the molecular mechanism of the m(6)A writer complex." Elife **5**.

Sloan, K. E., A. S. Warda, S. Sharma, K. D. Entian, D. L. J. Lafontaine and M. T. Bohnsack (2017). "Tuning the ribosome: The influence of rRNA modification on eukaryotic ribosome biogenesis and function." RNA Biol **14**(9): 1138-1152.

Smith, B. C. and J. M. Denu (2009). "Chemical mechanisms of histone lysine and arginine modifications." Biochim Biophys Acta **1789**(1): 45-57.

Snouwaert, J. N., L. C. Gowen, A. M. Latour, A. R. Mohn, A. Xiao, L. DiBiase and B. H. Koller (1999). "BRCA1 deficient embryonic stem cells display a decreased homologous recombination frequency and an increased frequency of non-homologous recombination that is corrected by expression of a brca1 transgene." Oncogene **18**(55): 7900-7907.

Sone, K., L. Piao, M. Nakakido, K. Ueda, T. Jenuwein, Y. Nakamura and R. Hamamoto (2014). "Critical role of lysine 134 methylation on histone H2AX for gamma-H2AX production and DNA repair." Nat Commun **5**: 5691.

Song, J., O. Rechkoblit, T. H. Bestor and D. J. Patel (2011). "Structure of DNMT1-DNA complex reveals a role for autoinhibition in maintenance DNA methylation." Science **331**(6020): 1036-1040.

Song, J., M. Teplova, S. Ishibe-Murakami and D. J. Patel (2012). "Structure-based mechanistic insights into DNMT1-mediated maintenance DNA methylation." Science **335**(6069): 709-712.

Sparmann, A. and M. van Lohuizen (2006). "Polycomb silencers control cell fate, development and cancer." Nat Rev Cancer **6**(11): 846-856.

Stark, G. R., Y. Wang and T. Lu (2011). "Lysine methylation of promoter-bound transcription factors and relevance to cancer." Cell Res **21**(3): 375-380.

Steger, D. J., M. I. Lefterova, L. Ying, A. J. Stonestrom, M. Schupp, D. Zhuo, A. L. Vakoc, J. E. Kim, J. Chen, M. A. Lazar, G. A. Blobel and C. R. Vakoc (2008). "DOT1L/KMT4 recruitment and H3K79 methylation are ubiquitously coupled with gene transcription in mammalian cells." Mol Cell Biol **28**(8): 2825-2839.

Stock, A., S. Clarke, C. Clarke and J. Stock (1987). "N-terminal methylation of proteins: structure, function and specificity." FEBS Lett **220**(1): 8-14.
Strahl, B. D. and C. D. Allis (2000). "The language of covalent histone modifications." Nature **403**(6765): 41-45.

Strahl, B. D., R. Ohba, R. G. Cook and C. D. Allis (1999). "Methylation of histone H3 at lysine 4 is highly conserved and correlates with transcriptionally active nuclei in Tetrahymena." Proc Natl Acad Sci U S A **96**(26): 14967-14972.

Syeda, F., R. L. Fagan, M. Wean, G. V. Avvakumov, J. R. Walker, S. Xue, S. Dhe-Paganon and C. Brenner (2011). "The replication focus targeting sequence (RFTS) domain is a DNA-competitive inhibitor of Dnmt1." J Biol Chem **286**(17): 15344-15351.

Takawa, M., H. S. Cho, S. Hayami, G. Toyokawa, M. Kogure, Y. Yamane, Y. Iwai, K. Maejima, K. Ueda, A. Masuda, N. Dohmae, H. I. Field, T. Tsunoda, T. Kobayashi, T. Akasu, M. Sugiyama, S. Ohnuma, Y. Atomi, B. A. Ponder, Y. Nakamura and R. Hamamoto (2012). "Histone lysine methyltransferase SETD8 promotes carcinogenesis by deregulating PCNA expression." Cancer Res **72**(13): 3217-3227.

Takeshita, K., I. Suetake, E. Yamashita, M. Suga, H. Narita, A. Nakagawa and S. Tajima (2011). "Structural insight into maintenance methylation by mouse DNA methyltransferase 1 (Dnmt1)." Proc Natl Acad Sci U S A **108**(22): 9055-9059.

Tamaru, H., X. Zhang, D. McMillen, P. B. Singh, J. Nakayama, S. I. Grewal, C. D. Allis, X. Cheng and E. U. Selker (2003). "Trimethylated lysine 9 of histone H3 is a mark for DNA methylation in Neurospora crassa." Nat Genet **34**(1): 75-79.
Taverna, S. D., H. Li, A. J. Ruthenburg, C. D. Allis and D. J. Patel (2007). "How chromatin-binding modules interpret histone modifications: lessons from professional pocket pickers." Nat Struct Mol Biol **14**(11): 1025-1040.

Teng, S., A. K. Srivastava, C. E. Schwartz, E. Alexov and L. Wang (2010). "Structural assessment of the effects of amino acid substitutions on protein stability and protein protein interaction." Int J Comput Biol Drug Des **3**(4): 334-349.

Tooley, C. E., J. J. Petkowski, T. L. Muratore-Schroeder, J. L. Balsbaugh, J. Shabanowitz, M. Sabat, W. Minor, D. F. Hunt and I. G. Macara (2010). "NRMT is an alpha-N-methyltransferase that methylates RCC1 and retinoblastoma protein." Nature **466**(7310): 1125-1128.

Toyokawa, G., H. S. Cho, Y. Iwai, M. Yoshimatsu, M. Takawa, S. Hayami, K. Maejima, N. Shimizu, H. Tanaka, T. Tsunoda, H. I. Field, J. D. Kelly, D. E. Neal, B. A. Ponder, Y. Maehara, Y. Nakamura and R. Hamamoto (2011). "The histone demethylase JMJD2B plays an essential role in human carcinogenesis through positive regulation of cyclin-dependent kinase 6." Cancer Prev Res (Phila) **4**(12): 2051-2061.

Trievel, R. C., B. M. Beach, L. M. Dirk, R. L. Houtz and J. H. Hurley (2002). "Structure and catalytic mechanism of a SET domain protein methyltransferase." Cell **111**(1): 91-103.

Tsukada, Y., J. Fang, H. Erdjument-Bromage, M. E. Warren, C. H. Borchers, P. Tempst and Y. Zhang (2006). "Histone demethylation by a family of JmjC domain-containing proteins." Nature **439**(7078): 811-816.

Tsunasawa, S., J. W. Stewart and F. Sherman (1985). "Amino-terminal processing of mutant forms of yeast iso-1-cytochrome c. The specificities of methionine aminopeptidase and acetyltransferase." J Biol Chem **260**(9): 5382-5391.

Tumes, D. J., A. Onodera, A. Suzuki, K. Shinoda, Y. Endo, C. Iwamura, H. Hosokawa, H. Koseki, K. Tokoyoda, Y. Suzuki, S. Motohashi and T. Nakayama (2013). "The polycomb protein Ezh2 regulates differentiation and plasticity of CD4(+) T helper type 1 and type 2 cells." Immunity **39**(5): 819-832.

Ung, M. U., B. Lu and J. A. McCammon (2006). "E230Q mutation of the catalytic subunit of cAMP-dependent protein kinase affects local structure and the binding of peptide inhibitor." Biopolymers **81**(6): 428-439.

Uversky, V. N., C. J. Oldfield and A. K. Dunker (2008). "Intrinsically disordered proteins in human diseases: introducing the D2 concept." Annu Rev Biophys **37**: 215-246.

Vakoc, C. R., S. A. Mandat, B. A. Olenchock and G. A. Blobel (2005). "Histone H3 lysine 9 methylation and HP1gamma are associated with transcription elongation through mammalian chromatin." Mol Cell **19**(3): 381-391.

Varambally, S., S. M. Dhanasekaran, M. Zhou, T. R. Barrette, C. Kumar-Sinha, M. G. Sanda, D. Ghosh, K. J. Pienta, R. G. Sewalt, A. P. Otte, M. A. Rubin and A. M. Chinnaiyan (2002). "The polycomb group protein EZH2 is involved in progression of prostate cancer." Nature **419**(6907): 624-629.

Varshney, D., A. P. Petit, J. A. Bueren-Calabuig, C. Jansen, D. A. Fletcher, M. Peggie, S. Weidlich, P. Scullion, A. V. Pisliakov and V. H. Cowling (2016). "Molecular basis of RNA guanine-7 methyltransferase (RNMT) activation by RAM." Nucleic Acids Res **44**(21): 10423-10436.

Vavouri, T., J. I. Semple, R. Garcia-Verdugo and B. Lehner (2009). "Intrinsic protein disorder and interaction promiscuity are widely associated with dosage sensitivity." Cell **138**(1): 198-208.

Voigts-Hoffmann, F., M. Hengesbach, A. Y. Kobitski, A. van Aerschot, P. Herdewijn, G. U. Nienhaus and M. Helm (2007). "A methyl group controls

conformational equilibrium in human mitochondrial tRNA(Lys)." J Am Chem Soc **129**(44): 13382-13383.

Vu, L. P., B. F. Pickering, Y. Cheng, S. Zaccara, D. Nguyen, G. Minuesa, T. Chou, A. Chow, Y. Saletore, M. MacKay, J. Schulman, C. Famulare, M. Patel, V. M. Klimek, F. E. Garrett-Bakelman, A. Melnick, M. Carroll, C. E. Mason, S. R. Jaffrey and M. G. Kharas (2017). "The N(6)-methyladenosine (m(6)A)-forming enzyme METTL3 controls myeloid differentiation of normal hematopoietic and leukemia cells." Nat Med **23**(11): 1369-1376.

Wang, G. G. and C. D. Allis (2009). ""Misinterpretation" of a histone mark is linked to aberrant stem cells and cancer development." Cell Cycle **8**(13): 1982-1983.

Wang, P., K. A. Doxtader and Y. Nam (2016). "Structural Basis for Cooperative Function of Mettl3 and Mettl14 Methyltransferases." Mol Cell **63**(2): 306-317.

Wang, X., J. Feng, Y. Xue, Z. Guan, D. Zhang, Z. Liu, Z. Gong, Q. Wang, J. Huang, C. Tang, T. Zou and P. Yin (2016). "Structural basis of N(6)-adenosine methylation by the METTL3-METTL14 complex." Nature **534**(7608): 575-578.

Wang, X. X., L. Fu, X. Li, X. Wu, Z. Zhu, L. Fu and J. T. Dong (2011). "Somatic mutations of the mixed-lineage leukemia 3 (MLL3) gene in primary breast cancers." Pathol Oncol Res **17**(2): 429-433.

Wang, Y., Y. Li, J. I. Toth, M. D. Petroski, Z. Zhang and J. C. Zhao (2014). "N6-methyladenosine modification destabilizes developmental regulators in embryonic stem cells." Nat Cell Biol **16**(2): 191-198.

Wang, Z. and J. Moult (2001). "SNPs, protein structure, and disease." Hum Mutat **17**(4): 263-270.

Webb, K. J., R. S. Lipson, Q. Al-Hadid, J. P. Whitelegge and S. G. Clarke (2010). "Identification of protein N-terminal methyltransferases in yeast and humans." Biochemistry **49**(25): 5225-5235.

Weiss, V. H., A. E. McBride, M. A. Soriano, D. J. Filman, P. A. Silver and J. M. Hogle (2000). "The structure and oligomerization of the yeast arginine methyltransferase, Hmt1." Nat Struct Biol **7**(12): 1165-1171.

Wittmann-Liebold, B. and R. Pannenbecker (1976). "Primary structure of protein L33 from the large subunit of the Escherichia coli ribosome." FEBS Lett **68**(1): 115-118.

Wu, H., H. Zeng, A. Dong, F. Li, H. He, G. Senisterra, A. Seitova, S. Duan, P. J. Brown, M. Vedadi, C. H. Arrowsmith and M. Schapira (2013). "Structure of the

catalytic domain of EZH2 reveals conformational plasticity in cofactor and substrate binding sites and explains oncogenic mutations." PLoS One **8**(12): e83737.

Xu, C., C. Bian, W. Yang, M. Galka, H. Ouyang, C. Chen, W. Qiu, H. Liu, A. E. Jones, F. MacKenzie, P. Pan, S. S. Li, H. Wang and J. Min (2010). "Binding of different histone marks differentially regulates the activity and specificity of polycomb repressive complex 2 (PRC2)." Proc Natl Acad Sci U S A **107**(45): 19266-19271.

Yan, J., S. A. Chen, A. Local, T. Liu, Y. Qiu, K. M. Dorighi, S. Preissl, C. M. Rivera, C. Wang, Z. Ye, K. Ge, M. Hu, J. Wysocka and B. Ren (2018). "Histone H3 lysine 4 monomethylation modulates long-range chromatin interactions at enhancers." Cell Res **28**(2): 204-220.

Yang, J., J. Huang, M. Dasgupta, N. Sears, M. Miyagi, B. Wang, M. R. Chance, X. Chen, Y. Du, Y. Wang, L. An, Q. Wang, T. Lu, X. Zhang, Z. Wang and G. R. Stark (2010). "Reversible methylation of promoter-bound STAT3 by histone-modifying enzymes." Proc Natl Acad Sci U S A **107**(50): 21499-21504.

Yang, J., K. Kulkarni, I. Manolaridis, Z. Zhang, R. B. Dodd, C. Mas-Droux and D. Barford (2011). "Mechanism of isoprenylcysteine carboxyl methylation from the crystal structure of the integral membrane methyltransferase ICMT." Mol Cell **44**(6): 997-1004.

Yang, Y., B. Chen, G. Tan, M. Vihinen and B. Shen (2013). "Structure-based prediction of the effects of a missense variant on protein stability." Amino Acids **44**(3): 847-855.

Yao, Q., L. Zhang, X. Wan, J. Chen, L. Hu, X. Ding, L. Li, J. Karar, H. Peng, S. Chen, N. Huang, F. J. Rauscher, 3rd and F. Shao (2014). "Structure and specificity of the bacterial cysteine methyltransferase effector NleE suggests a novel substrate in human DNA repair pathway." PLoS Pathog **10**(11): e1004522.

Yap, D. B., J. Chu, T. Berg, M. Schapira, S. W. Cheng, A. Moradian, R. D. Morin, A. J. Mungall, B. Meissner, M. Boyle, V. E. Marquez, M. A. Marra, R. D. Gascoyne, R. K. Humphries, C. H. Arrowsmith, G. B. Morin and S. A. Aparicio (2011). "Somatic mutations at EZH2 Y641 act dominantly through a mechanism of selectively altered PRC2 catalytic activity, to increase H3K27 trimethylation." Blood **117**(8): 2451-2459.

Yin, S., J. Yang, B. Lin, W. Deng, Y. Zhang, X. Yi, Y. Shi, Y. Tao, J. Cai, C. I. Wu, G. Zhao, L. D. Hurst, J. Zhang, L. Hu and X. Kong (2014). "Exome sequencing identifies frequent mutation of MLL2 in non-small cell lung carcinoma from Chinese patients." Sci Rep **4**: 6036.

Yu, J., J. Yu, D. R. Rhodes, S. A. Tomlins, X. Cao, G. Chen, R. Mehra, X. Wang, D. Ghosh, R. B. Shah, S. Varambally, K. J. Pienta and A. M. Chinnaiyan (2007). "A polycomb repression signature in metastatic prostate cancer predicts cancer outcome." Cancer Res **67**(22): 10657-10663.

Yuan, S., H. Tang, J. Xing, X. Fan, X. Cai, Q. Li, P. Han, Y. Luo, Z. Zhang, B. Jiang, Y. Dou, M. Gorospe and W. Wang (2014). "Methylation by NSun2 represses the levels and function of microRNA 125b." Mol Cell Biol **34**(19): 3630-3641.

Zhang, C., X. Luo, L. Liu, S. Guo, W. Zhao, A. Mu, Z. Liu, N. Wang, H. Zhou and T. Zhang (2013). "Myocardin-related transcription factor A is up-regulated by 17beta-estradiol and promotes migration of MCF-7 breast cancer cells via transactivation of MYL9 and CYR61." Acta Biochim Biophys Sin (Shanghai) **45**(11): 921-927.

Zhang, X., H. Tamaru, S. I. Khan, J. R. Horton, L. J. Keefe, E. U. Selker and X. Cheng (2002). "Structure of the Neurospora SET domain protein DIM-5, a histone H3 lysine methyltransferase." Cell **111**(1): 117-127.

Zhang, X., K. Tanaka, J. Yan, J. Li, D. Peng, Y. Jiang, Z. Yang, M. C. Barton, H. Wen and X. Shi (2013). "Regulation of estrogen receptor alpha by histone methyltransferase SMYD2-mediated protein methylation." Proc Natl Acad Sci U S A **110**(43): 17284-17289.

Zhang, X., L. Zhou and X. Cheng (2000). "Crystal structure of the conserved core of protein arginine methyltransferase PRMT3." Embo j **19**(14): 3509-3519.

Zhang, Y., R. Jurkowska, S. Soeroes, A. Rajavelu, A. Dhayalan, I. Bock, P. Rathert, O. Brandt, R. Reinhardt, W. Fischle and A. Jeltsch (2010). "Chromatin methylation activity of Dnmt3a and Dnmt3a/3L is guided by interaction of the ADD domain with the histone H3 tail." Nucleic Acids Res **38**(13): 4246-4253.

Zhang, Z. M., S. Liu, K. Lin, Y. Luo, J. J. Perry, Y. Wang and J. Song (2015). "Crystal Structure of Human DNA Methyltransferase 1." J Mol Biol **427**(15): 2520-2531.

Zheng, G., J. A. Dahl, Y. Niu, P. Fedorcsak, C. M. Huang, C. J. Li, C. B. Vagbo, Y. Shi, W. L. Wang, S. H. Song, Z. Lu, R. P. Bosmans, Q. Dai, Y. J. Hao, X. Yang, W. M. Zhao, W. M. Tong, X. J. Wang, F. Bogdan, K. Furu, Y. Fu, G. Jia, X. Zhao, J. Liu, H. E. Krokan, A. Klungland, Y. G. Yang and C. He (2013). "ALKBH5 is a mammalian RNA demethylase that impacts RNA metabolism and mouse fertility." Mol Cell **49**(1): 18-29.

Zhuang, J., J. Zhang, H. Willers, H. Wang, J. H. Chung, D. C. van Gent, D. E. Hallahan, S. N. Powell and F. Xia (2006). "Checkpoint kinase 2-mediated

phosphorylation of BRCA1 regulates the fidelity of nonhomologous end-joining." Cancer Res **66**(3): 1401-1408.

CURRICULM VITAE

Jon Faughn
62 Days Park #3
Buffalo, NY 14201
(270) 210-3363
jon.faughn@louisville.edu
jon.faughn@gmail.com

Education

In progress Ph.D. in Biochemistry and Molecular Genetics, University of Louisville, Louisville, KY

2015 M.S. in Biochemistry and Molecular Genetics, University of Louisville, Louisville, KY

2011 M.S. in Molecular and Cell Biology, Western Kentucky University, Bowling Green, KY

2006 B.S. in Biology and Chemistry, Western Kentucky University, Bowling Green, KY

Research Experience

Current Graduate Student
Department of Biochemistry and Molecular Genetics
University of Louisville, Louisville KY

2012/2013 Research Assistant
Department of Medicine
University of Louisville, Louisville KY

2011/2012 Research Associate
CONRAD
Eastern Virginia Medical School, Norfolk, VA

2009/2011 Graduate Student and Research Assistant
Department of Biology
Western Kentucky University, Bowling Green, KY

Honors and Awards

2010 Outstanding Research Award
NISBRE National Meeting
Bethesda, MD

Teaching Activities

2014 Teaching Assistant (Intro to Biochemical Methods)
Department of Biochemistry and Molecular Genetics
University of Louisville, Louisville, KY

2011 Teaching Assistant (Intro to Molecular and Cell Biology)
Department of Biology
Western Kentucky University, Bowling Green, KY

2011 Teaching Assistant (Cells, Metabolism, and Genes: An intro to biological concepts)
Department of Biology
Western Kentucky University, Bowling Green, KY

2010 Primary Instructor (Biotechnology Certification Program)
Department of Biology
Western Kentucky University, Bowling Green, KY

Publications/Presentations

1. Faughn JD, Dean William L., Shaner Tooley Christine E. "The N-terminal methyltransferase homologs NRMT1 and NRMT2 exhibit novel regulation of activity through heterotrimer formation." *Protein Science* 2018

2. "The N-terminal Methyltransferase NRMT1 and NRMT2 interact and are Codependent on each other for Activity and Stability". Poster Presentation- Sixth Biochemistry and Molecular Genetics Colloquium, Research! Louisville

3. Yaddanapudi K, Putty K, Rendon BE, Lamont GJ, **Faughn JD**, Satoskar A, Lasnik A, Eaton JW, Mitchell RA. Control of tumor-associated macrophage alternative activation by macrophage migration inhibitory factor. *J Immunol*. 2013 Mar 15;190(6):2984-93.

4. Pope WH, Bowman CA, Russell DA, Jacobs-Sera D, Asai DJ, Cresawn SG, Jacobs WR, Hendrix RW, Lawrence JG, Hatfull GF (**Faughn J (collaborating author)**); Science Education Alliance Phage Hunters Advancing Genomics and Evolutionary Science; Phage Hunters Integrating Research and Education; Mycobacterial Genetics Course.

Whole genome comparison of a large collection of mycobacteriophages reveals a continuum of phage genetic diversity. Elife. 2015 Apr 28;4:e06416

5. “Vaccination with Embryonic Stem Cells Protects against Lung Cancer” and “Control of tumor-associated macrophage activation by macrophage migration inhibitory factor.” Poster Presentations- James Graham Brown Cancer Center Annual Retreat

6. “Protein kinase C regulation of pulmonary myofibroblasts” Poster Presentation- NISBRE Regional Meeting, New Orleans, LA

7. “Regulation of endothelial nitric oxide synthase translocation in pulmonary myofibroblasts” Poster Presentation- Kentucky Academy of Science, Western Kentucky University

8. “eNOS translocation in pulmonary myofibroblasts” Poster Presentation- NISBRE National Meeting, Bethesda, MD

Affiliations

Current Science Policy and Outreach Program, University of Louisville, Louisville, KY